Escola de Camins
Escola Tècnica Superior d'Enginyeria de Camins, Canals i Ports
UPC BARCELONATECH

MASTER THESIS

Master

Structural and Construction Engineering

Title

Nonlinear dynamic analysis of a seismically retrofitted reinforced concrete building: Selection criteria for natural records and reliability analysis of results.

Author

Paola Carolina Pérez Batista

Tutor

Luca Pelá & Alessandra Aprile

Intensification

Technology and Construction

Date

May 2016

Escola de Camins
Escola Tècnica Superior d'Enginyeria de Camins, Canals i Ports
UPC BARCELONATECH

MASTER THESIS

Master

Structural and Construction Engineering

Title

Nonlinear dynamic analysis of a seismically retrofitted reinforced concrete building: Selection criteria for natural records and reliability analysis of results.

Author

Paola Carolina Pérez Batista

Tutor

Luca Pelá & Alessandra Aprile

Intensification

Technology and Construction

Date

May 2016

Abstract.

To perform a design or assessment considering earthquakes, Nonlinear Dynamic Analysis (NDA) is the only approach that attempts to fully represent the seismic response of buildings without any the major simplifying assumptions such as ignoring nonlinearity and /or dynamic effects (Chambers & Trevor, 2004). Moreover NDA has gained its place for current and foreseeable future of seismic assessment of existing structures (Fardis, 2009). At present time for nonlinear dynamic analysis, according to Eurocode 8 and NTC08, at least 7 recordings should be used in order to consider the mean structural response of the structure. However, the probability of collapse associated to this average is unknown.

On the other hand natural recordings are becoming popular for NDA in order to acquire unbiased results (Iervolino, Maddaloni, & Cosenza, 2008). Nevertheless, the primary difficulty using this type of recordings is the lacking of an unified criteria in the selection of the ground motion parameter (Ye et al 2013). In summary, even though there is a clear need of nonlinear dynamic analysis, there are uncertainties regarding to its application. Therefore, this situation creates a necessity to investigate methods for earthquake selection and their respectively reliability verification.

As a consequence, this investigation describes the structural behavior of a single case study and its reliability index while the number of observations "ground motions recordings" is increased and the parameter for earthquake selection is changed. Furthermore it is also analyzed (with a minor emphasis) the displacement behavior varying the type of earthquake (near field/far field). The selected case study is from a town in the north of Italy, called Ferrara. This case study is a retrofitted reinforced concrete multistory building from 1970s that nowadays serves as municipal police offices.

In this case via the proposed methodology, different sets with 7 and 30 recordings were arranged by earthquake parameter and modeled using MIDAS/GEN developed by MIDAS Information Technology, Co., Ltd. Korea. In addition a 50_recording set was assembled to take as one of the references. Regarding to the average structural response, the maximum displacement was observed due to a pounding problem. Finally a probabilistic analysis was performed by distribution fitting in order to estimate the reliability values.

From the presentation of results it is described the differences among results due to set dimension and earthquake parameter variation. Furthermore, a pseudo-comparison among far field and near field earthquakes is discussed. As a final point, it is illustrated how different are the displacements obtained from average and the reliable displacements prescribed by current codes.

Acknowledgements

"When a project becomes reality it should not only be attributed to our own efforts. Behind every achieved goal there are always people who support us and who were the first ones to believe in "the dream" before it came true."

Therefore I dedicate this project to:

God for giving me the strength to move forward in the most difficult moments.

To Ministerio de Educación, Ciencia y Tecnología de la República Dominicana, for allowing me the opportunity to go one step further in my career.

To my tutors, Luca Pelá for considering me to realize this project and Alessandra Aprile, for her generous encouragements, supervision, suggestions and unlimited patience. Thanks to both of you for helping me to face this challenge with confidence. Therefore my utmost gratitude.

To my parents Marcelina Batista and Florentino Perez for having supported throughout this period and distance regardless fatigue or effort required.

To my brothers and Ariel Diogenes who have always given me the motivation of being a good example for them and have given me their unconditional support.

To the rest of my family who sent me all their support despite of the distance.

To my best friend Patricia Calderón Rodríguez who always provided words of encouragement at the right times, strengthening the aspiration to fulfill this goal.

To Gioribel Rivas Rodríguez for helping me to find the balance.

To my colleges from UPC, especially to Jhomar Jara del Rosario, for all their support and caring inside and more important outside the classroom.

- ***Paola Carolina Pérez Batista.***

TABLE OF CONTENTS.

List of equations.

List of figures.

List of graphics.

List of tables.

1. INTRODUCTION

A brief overview of the thesis is presented in this chapter. Motivations of the investigation are stated along with the initial hypotheses. Moreover herein it is specified: intended objectives, research's contents and its limitations. Finally an outline of the thesis is listed.

1.1. Background

Prior to modern seismic codes' introduction in the mid-1970s most of the structures were designed and built without adequate detailing and reinforcement for seismic protection (Pampanin & Christopoulos, 2002). Besides most earthquakes related deaths are caused by the collapse of structures (Ammon, 2011). Furthermore Italy has medium-high seismic hazard, very high vulnerability and an extremely high exposure due to population density and its historical heritage (Italian Department of Civil Protection, 2012).

From this situation a well acknowledged necessity to rehabilitate existing structures throughout structural improvements has rapidly increased in recent years. This structural enhancing called seismic retrofitting aims to decrease building´s vulnerability against ground motions or soil failures due to earthquakes. It has several different approaches such as: strategies, techniques and planned material. Likewise any regular design the selection of analysis type (linear/nonlinear, static/dynamic) is an essential part of retrofitting planning among its strategies.

Even though it is still considered that excessive sophistication in structural analysis is not warranted since ground motions cannot be accurately predicted due to large uncertainties and randomness (Reitherman, 1998), Nonlinear Dynamic Analysis has gained its place for current and foreseeable future of seismic assessment of existing structures (Fardis, 2009) after the availability of reliable numerically stable computer codes. Current codes (Eurocode 8, NTC08) prescribes that at least seven recordings should be matched in order to consider mean response. However the procedure for a non-linear analysis is still not quite clear. In particular, the ground motion records selection phase which believed as a bit of black art (Powell, 2006).

It is important to highlight that mentioned codes give to the designer the freedom of choosing the type of accelerogram from the available information. Nevertheless authors (Masi, Vona, & Mucciarelli, 2011) explain that generating synthetic ground motion records, in other words forcing accelerogram to converge to a building code spectrum, for vulnerabilities studies and damage scenarios is not appropriate at all. As a consequence, natural accelerograms are becoming the most attractive option to get unbiased estimations of the seismic demand (Iervolino, Maddaloni, & Cosenza, 2008).

In summary there is a clear need of seismic assessment/retrofitting and nonlinear dynamic analysis has earned its position to be applied in this field. However, NDA procedure is not as clear as its need of implementation. Being more specific there is uncertainty respecting to ground motion selection criteria and average results reliability. This produces a necessity to investigate methods for earthquake selection and its reliability verification.

1.2 Research motivations

So far Nonlinear Dynamic Analysis (NDA) is the only approach that attempts to fully represent the seismic response of buildings without any the major simplifying assumptions such as ignoring nonlinearity and /or dynamic effects (Chambers & Trevor, 2004). At present time for NDA, according to Eurocode 8 and NTC08, at least 7 recordings should be used in order to consider the mean structural response of the structure. However the probability of collapse associated to this average is unknown. This indicates that project's reliability is also unknown and cannot be compared with current prescriptions from EN-1990. Therefore by failing to conduct such verification it is possible that projects have a probability of collapse major than current codes stipulation.

In addition natural earthquakes are becoming popular for nonlinear dynamic analysis in order to acquire unbiased results(Iervolino et al., 2008). Nevertheless there is no clear criteria for its selection. As a result some concerns come to the surface such as: what would happen if the parameter for the selection is changed? Does the average response of the building experience any variation? Is there a difference between near and far field in terms of displacement response?

Consequently a case study from Ferrara, Italy was selected. This case study is a retrofitted reinforced concrete multistory building from 1970s that nowadays serves as municipal police offices. Different sets were arranged by earthquake parameter and modeled using MIDAS/GEN developed by MIDAS Information Technology, Co., Ltd. Korea. The average structural response observed was maximum displacement due to a pounding problem. Finally a probabilistic analysis was performed by distribution fitting in order to estimate reliability values.

1.3 Research hypotheses

From research motivations two different studies of the average structural response have been developed varying the parameter to select far field earthquakes. The first study was conducted with a set according to current code prescriptions. Whereas the second investigation was performed using a set with at least a 90% of confidence. Moreover a third set was arranged for the investigation of near field average structural response. However for this latter study, the variation of selection parameter could not be performed since there is a very limited availability of near field seismic events.

Under these circumstances it is anticipated to perceive structural response variances among ground motion sets due to earthquake parameter variation. Similarly in general terms for all sets it is thought that reliability values will increase enlarging the number of the considered recordings. Regarding to average response of code sets it is expected to obtain a lower reliability than current EN-1990 prescriptions since 7 recordings is a small statistical sample. Conversely, for average response from sets with a 90% confidence it is predicted to satisfy project´s reliability requirements. Finally it is expected to find substantial divergences among far field and near field average responses.

1.4 Research objectives

General objective.

Determine the average maximum displacement behavior and its reliability index while the number of observations (ground motions recordings) is increased, the parameter for earthquake selection is changed, and the type of earthquake varies (far/near field).

Specifics objectives for far and near field analysis.

- Identify 3 earthquake parameters for the ground motion selection process.
- Define feasible databases for ground motion search.
- Assemble a ground motion set per earthquake parameter according to current codes prescriptions (at least 7 recordings for average response).
- Arrange a ground motion set per earthquake parameter with 90% of confidence as minimum.
- Contrast average maximum displacement behavior according to earthquake parameter.
- Analyze the average response behavior of code-prescribed and 90%-confidence sets.
- Determine the reliability of code-prescribed and 90%-confidence sets.
- Compare all-sets reliability results with EN-1990 prescriptions.

1.5 Research contents

The Research contents are outlined into 3 main subdivisions:

- **The first section** of the thesis is focused on ground motion selection. In particular it describes the scale factor and deviation factor procedures which allowed the arrangement of sets.
- **Second section** covers the modeling stage of the case study which was executed using MIDAS software. This subdivision pays special attention to maximum displacement behavior while the number of observations is increased. Moreover comparison among results are analyzed by earthquake parameter classification.
- **Third section** details the statistical procedure in order to find distribution functions and the reliability index. This final part concentrates on reliability's determination and its subsequent comparison with the current code prescriptions in order to distinguish whether failure rate of the project is on the safe side or not.

1.6 Outline of the thesis

This thesis is organized into the following chapters:

Chapter I. Introduction describes the background and current situation. Moreover it defines the research motivation, identifies general objectives and specific ones. It also presents research content and an outline of the thesis.

Chapter II. Literature Review firstly presents a brief background where it is explained when, where and why earthquakes occurs, and how are measured and located. Secondly a contextual framework describes the Italian seismic risk and vulnerability. Thirdly a brief review of retrofitting techniques is presented with an especial mention to Buckling Restrained Axial Damper (BRAD) which is the retrofitting proposed solution of the case study. Then a shortly description of Nonlinear Dynamic Analysis (NDA) is detailed expressing how it has gained its actual position on seismic assessment.

Likewise a wide review of ground motion selection techniques is explicated along with the definitions and applications of earthquake parameters. Furthermore the statistical procedure and reliability index analysis are presented in order to explain its meaning and importance in terms of security factor. Finally a brief description REXEL and SeismoSignal software is shown.

Chapter III. Methodology Framework in general terms presents the delineation of each phase from the investigation detailing how it was conducted. This section specifies the investigation type, its variables and dimensions and how sampling was performed. Moreover a step by step methodology is outlined from the subdivision previously explained in research content aiming to improve investigation process organization and it subsequence understanding.

Chapter IV. Building case this section corresponds to the case study description. It presents: geographical location, actual use, geometrical characteristics, soil type, and material properties, among others. Also the seismic vulnerability and its retrofit proposal from previous studies are presented. From these descriptions it is aimed to obtain a 3D virtual model representation as close as possible to the current building situation.

Chapter V. Analysis of results concerns to the outcomes obtained from the methodology framework application. In the first section of the chapter an outline describes the main blocks of the chapter:

- First block displays ground motion results from scale factor and events analysis. It also presents the comparison among target spectrum and the average spectrum obtained per each earthquake parameter.
- Second block describes modeling stage results. Herein displacement behavior is described and discussed by set size dimension (7, 30, or 50). Moreover average displacements are compared according to earthquake parameter selection.
- Finally third stage comprises the statistical results starting with reliability and failure results for the case study. Then results from the fitting distribution analysis are explained along with it reliability value.

Chapter VI. Conclusions and Recommendations this section presents the general observations and conclusions from general and specific objectives. In the same way innovative aspects of the research are highlighted and the future developments recommendations for further research are stated.

Chapter VII. References this section presents the bibliography of the reviewed literature according to the style from the American Psychological Association 6th edition.

2. LITERATURE REVIEW

This chapter presents a summary of the consulted documentation and investigations. First three sections are related to earthquake genesis, seismic risk and retrofit. Then a brief reference of non-linear dynamic analysis is detailed, followed by the explanation of the performed statistical analysis. Finally a short description of used software is shown.

2.1 Tectonics plates & Earthquakes.

2.1.1 Tectonic Plates.

According to (National Oceanic and Atmospheric Administration, 2013) Earth's tectonic plates are in constant motion producing numerous ways of interactions. From these phenomena 3 different types of plate boundaries have been established: **divergent boundary,** two tectonic plates move away from each other, **convergent boundary** when two plates come together and **transform plate boundary** when two plates sliding past each other (see figure 2.1).

The effects of these interactions are confirmed in the map below (figure 2.2) where the Earth's solid surface is displayed with many of the features caused by plate tectonics along their boundaries. Oceanic ridges are the asthenospheric as spreading centers creating new oceanic crust. Continental belts occurring where plates are pressing against each other and subduction zones appear as deep oceanic trenches. (Louie, 2011)

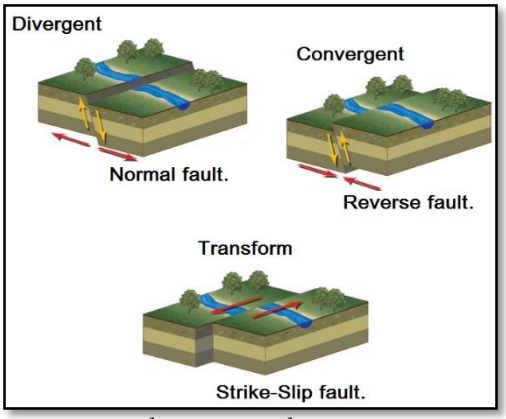

Figure 2.1 Boundaries types; srh.noaa.gov

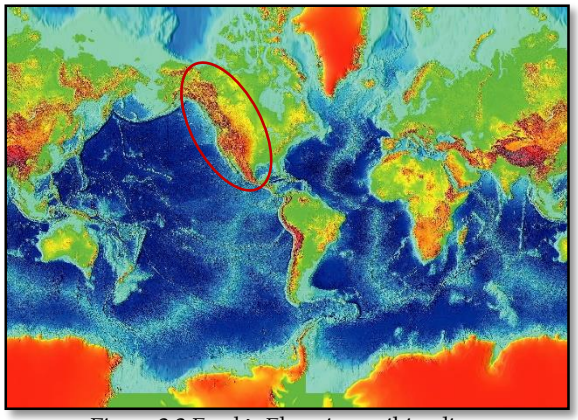
Figure 2.2 Earth's Elevation; wikipedia.org

Nevertheless previous topographies are not the only phenomena observed throughout plate tectonics boundaries. When two plates grinds against each other releasing some form of energy stored in Earth's crust, a passage of seismic waves produces a shaking of the ground called Earthquake. Figure 2.3, depicts major earthquakes occurring mainly in belts (margins of tectonic plates), so nowadays plate's boundaries definition is throughout lines of earthquakes.

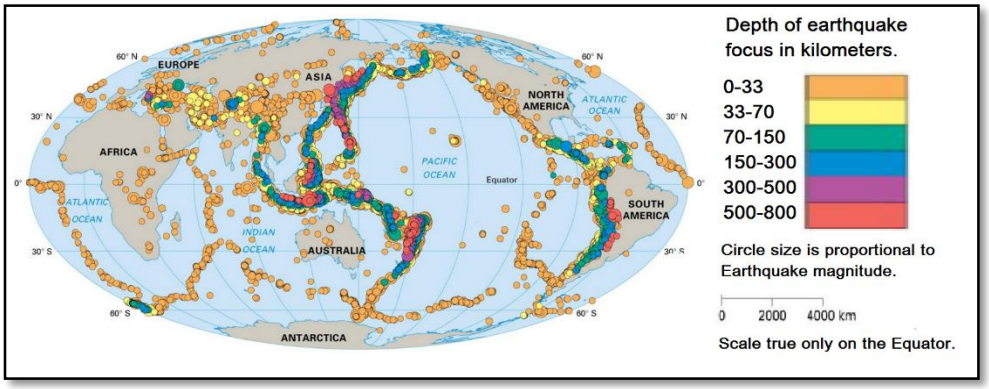

Figure 2.3 Earthquakes around the globe; Britannica.com

Furthermore plate tectonic boundaries have been observed under the subjection of different inter-plate stresses. From these pressures, normal, reverse and strike-slip faults have been identified with their seismic activity. As a result earthquakes along these faults can be classified according to similarities and discrepancies detected in terms of frequency, energy released and depth. Therefore each type has its own special hazard (Louie, 2011). A brief description of faulting types along with their boundaries are described below. They are also illustrated in figure 2.1.

At **divergent boundaries** –normal fault- earthquakes present low depth. Normally are located in superposition with the spreading axis showing an extensional mechanism. Also this type of earthquakes tend to be smaller than magnitude 8. An example of this type of boundary is Juan de Fuca spreading ridge, offshore the Pacific Northwest.

Convergent boundaries –reverse fault- perform a compressional environment hosting Earth´s largest quakes with some events on subduction zones in Alaska and Chile having exceeded magnitude 9. Their setting ranging is very wide from the very near surface to several hundred kilometers depth. This is a consequence from the coldness of the subducting plate which allows brittle failure down to as much 700 kilometers.

From **transform boundaries** –strike-slip fault- the plates slide past each other producing less sinking or lifting than compressional or extensional environment. Earthquakes in this zone can reach a profundity as deep as 25 kilometers. San Andreas Fault in California is an example from this category.

All known faults are assumed to have been the seat of one or more earthquakes in the past. However the majority of geological faults are now aseismic. Hence nowadays it is often no clear whether in a particular event the total energy issues from a single fault plane. Consequently actual faulting associate a fault with a particular earthquake may be complex.(Bolt, 2015)

Actual seismic faulting -Earthquakes belts.

The most important earthquake belt is the Circum-Pacific Belt also called "Pacific Ring of Fire" due to its association with volcanic activity. Even though its seismic activity is far away from uniform due to a number of branches at various points the Pacific Belt releases the 80% of the current energy. At the present time it affects many populated coastal regions from the western coast of America and the Pacific Ocean.

A second belt, known as the Alpide belt generates the 15% of the energy released from world total. It passes through Mediterranean region eastward, Asia and joins the Circum Pacific-belt in East Indies. There are also striking connected belts of seismic activity, mainly along ocean ridges –including those in the Arctic Ocean, and the Western Indian Ocean –and along the rift valleys of East Africa.

Earthquake location, measure and prediction.

From a single seismogram it is impossible to determine an Earthquake location because from a seismogram is only obtained the distance without the direction. Thus the position of an earthquake is obtained by triangulation of 3 different seismograms presented in figure 2.4. First the radio of each a station is obtained individually by looking the amount of time between P and S waves on its seismogram. As shown in figure 2.4, the more distance the more time between each waves. Then each station is represented with it radio in a map and the intersection of those three circles is the epicenter. (UpSeis, 2007)

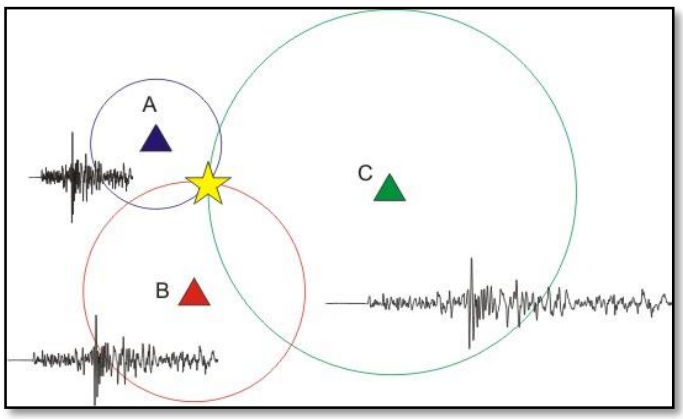

Figure 2.4 Earthquake triangulation; earthquakes.bgs.uk

The size of an earthquake depends on the amount of slip of the fault and its size. However these measures cannot be obtained since faults are several kilometers deep beneath the earth's surface. Eventually, in 1935 Charles Richter introduced a quantitative evaluation of earthquake intensity called magnitude. This index is based on kinetic energy released from hypocenter which is represented on seismogram records. Its main contribution to the scientist community is that provides a precise assessment of the size since its independence from caused damage.

Respecting to earthquake prediction it is unlikely that scientist community will ever be able to predict earthquakes. Many different ways have been tried, but none of them have been successful. Nevertheless on any particular fault, scientists know there will be another earthquake sometime in the future, but they have no way of telling when it will happen. (Wald, 2012)

Earthquake recordings and its components.

Earthquakes are recorded by seismographs and its recording are called seismogram shown in figure 2.5. The seismograph has a base that sets firmly in the ground, and a heavy weight that hangs free. When an earthquake causes the ground to shake, the base of the seismograph shakes too, but the hanging weight does not. Instead the spring or string that it is hanging from absorbs all the movement. The difference in position between the shaking part of the seismograph and the motionless part is what is recorded.

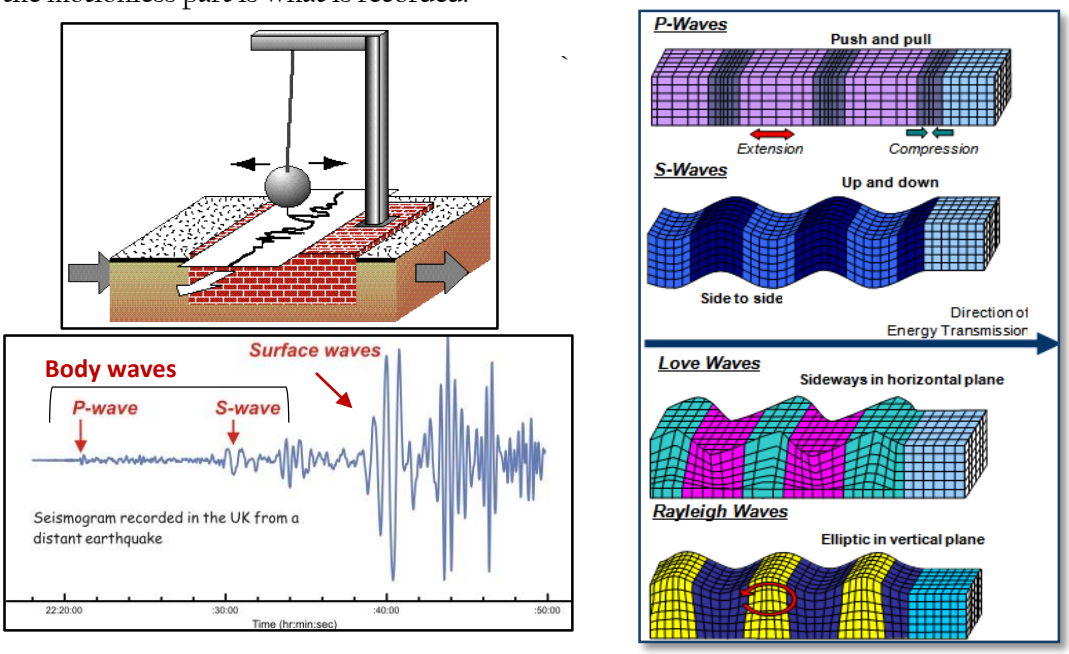

Figure 2.5 Seismograph, Seismogram and Seismic waves; colorado.edu, bgs.ac.uk, nwbobcatscience.weebly.com

As figure 2.5 shows, a seismogram is made by different types of waves. The first one is **Primary waves** also known as compressional wave because of the pushing and pulling they do, is the fastest kind of seismic wave and can move through rocks and fluids, like water or the liquid layers on earth. Then **Secondary waves** arrive which can move only through solid rock. Thanks to this property seismologist consider that Earth's outer core is liquid. S waves moves rock up and down or side-to-side perpendicular to the direction that the wave is traveling. (Wald, 2012)

Finally **Surface waves** are found, they are identified because can travel only through the crust and have a lower frequency than body waves. Though they arrive after P and S waves, it is surface waves that are almost responsible for the damage and destruction associated with earthquakes. Additionally there are 2 types of surface waves: **Love wave** is the fastest surface wave and moves

the ground side to side, but only produces horizontal motion and **Rayleigh wave** which rolls along the ground, which means it moves the ground up and down, and side to side in the same direction that the wave is moving. Most of the shaking felt from an earthquake is due to the latter wave.(UpSeis, 2007; Wald, 2012)

Earthquake recordings classification.

"It is widely proven that in the field area near a seismic source the characteristics of the seismic ground motion (near field) could be meaningfully different from those far from the source (far field), not only in terms of intensity but also in terms of nature and typology. Nevertheless, structures are usually designed on the base of accelerations derived from ordinary probabilistic seismic hazard analyses (PSHA) under the hypothesis of far field conditions. Resulting in a lack of safety levels if the structure is located close to an earthquake source" (Grimaz & Malisan, 2014)

From section earthquake location, measure and prediction, figure 2.5 depicts how from a single event notable differences can be found between recordings. According to (Grimaz & Malisan, 2014) the seismic motion spreads from the source depending on several different factors such as distance from the source, radiation pattern, site effects, etc. As a consequence, to acquire a better understanding of recording´s influence on structural response by its characteristics a classification method has been developed. This cataloguing mainly takes into account distance, but other parameters have been taken into account in a minor proportion.

Ground motions close to a ruptured fault can be significantly different than those observed further away from the seismic source. Depending on fault dimension and mechanism, the area within some ten kilometers from a seismic source could be subjected to specific ground motion effects (Abrahamson & Somerville, 996; Bozorgnia, Niazi, & Campbell, 1995; Housner & Trifunac, 1967). Bibliographic studies on seismic ground motion effects close to the seismic source evidence that researchers use different names in order to address this zone in which these effects are observed, near fault, near source, **near field** or epicentral area (Grimaz & Malisan, 2014). By contrast to refer seismic ground motion recorded far away from source **"far field"** is the distinctive used term.

Furthermore ITACA (Strumento, Nazionale, & Paolucci, 2005), describes **"free-field"** as a ground motion record obtained at a sufficient distance from structures that can alter in significantly the response in a sufficiently wide field of frequencies, approximately between 0 and 20 Hz. The placement of the instrument (v. Housing) must be such as to minimize the effect of interaction with the host structure or neighboring structures.

2.2 Seismic vulnerability, exposure and risk in Italy.

2.2.1 Seismic vulnerability

"Most earthquake related deaths are caused by the collapse of structures and construction practices play a tremendous role in the death toll of an earthquake. In southern Italy in 1909 more than 100,000 people perished in an earthquake that struck the region." (Ammon, 2011)

Seismic vulnerability is defined as the potential of a building to be damaged under a specific seismic action. In order to prevent collapse actual standards such as Eurocode 8 for seismic zones states that buildings must not be damage by low-intensity earthquakes, must not be structurally damaged by medium-intensity earthquakes and must not collapse in the event of severe earthquakes despite suffering serious damage.

Nevertheless when an earthquakes pushes a building backwards and forwards, it starts to sway and deform. So if the structure is flexible and capable to undergo with large deformations, despite of suffering great damage, it will not collapse. In consequence a building can tolerate damage to its load-bearing elements (columns, walls and beams) and/or non-structural parts that do not affect its instability (chimneys, cornices, partitions). This level of damage is determined by: the structure of the building, its age, materials, location, vicinity to other buildings and non-structural elements. (Italian Department of Civil Protection, 2012)

In order to assess buildings vulnerability, it is required to discriminate among before and after an earthquake. At before case assessments become complex, a method should be used. Conversely, to evaluate a building after an earthquake, it is enough to examine and correlate, shown in figure 2.6. For building assessment throughout Italy, statistical methods must be used that adopt standard data regarding their characteristics. ISTAT census data regarding homes are available for Italy and used in the application of statistical methods.

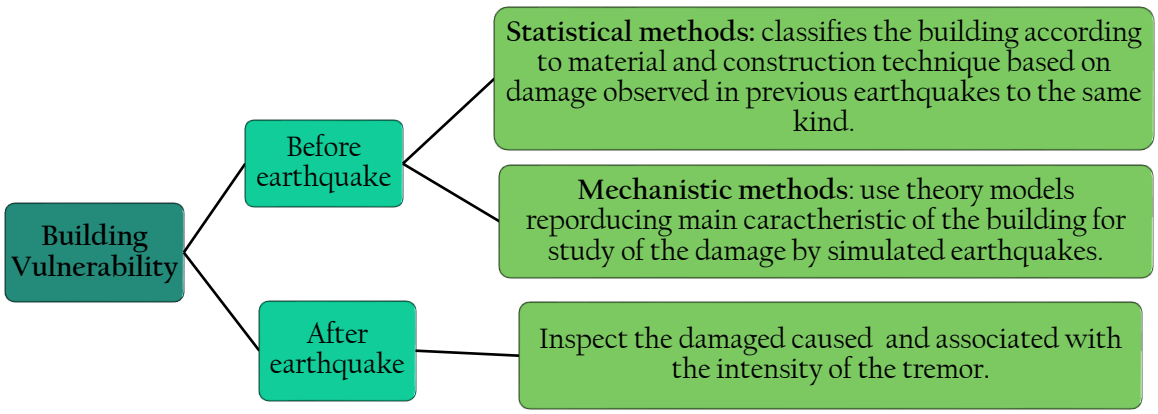

Figure 2.6 Building vulnerability assessment procedure.

2.2.2 Italian seismic exposure.

"The first objective for a general earthquake protection programme is safeguarding human life. For this reason it is very important to assess the number of people involved, dead and/or injured". (Italian Department of Civil Protection, 2012)".

Seismic exposure can be defined as the number of asset with the condition of being affected, damage to cultural heritage in economic terms or the loss of human lives. It is generally estimated taking into account the amount of persons involved, from the projected number of damaged buildings. This estimations have a certain margin for error, especially for more severe earthquakes. Several parameters are considered to obtain a reliable estimation, among these are:

- The number of people living in the buildings.
- The time of the earthquake.
- The possibilities of escape and/or protection.
- How people were affected (dead or injured).
- The possibility of dying even after aid has been given.

From parameters above, it is important to note exposure estimations are rather complex due to the amount and type of variable involved. For instance, the number of people in a building is a variable that not only changes from cities to countryside it also changes along time from daytime to night-time. However, reference to the kind of buildings and relative inhabitants may provide a global estimate acceptable for violent earthquakes that affect large areas.

2.2.3 Seismic risk in Italy.

"Italy is one of the countries facing the greatest seismic risk in the Mediterranean, due to its special geographical location, being in the convergence zone between the African plate and the Eurasian. (Bertaccini, 2014)"

According to (INFP, 2006) in general terms, **seismic hazard** defines the expected seismic ground motion which may result in destruction and losses at a geographical site. There are two major approaches which are worldwide used for seismic hazard assessment: deterministic and probabilistic.

The **deterministic approach** takes into account a single, particular earthquake, the event that is expected to produce the strongest level of shaking at the site. Consequently the outputs (macroseismic intensity, peak ground acceleration, peak ground velocity, peak ground displacement, response spectra) may be used directly in engineering applications.

In contrast to previous methodology the **probabilistic approach**, initiated with the pioneering work of (Cornell, 1968) , the seismic hazard is estimated in terms of a ground motion parameter – macroseismic intensity, peak ground acceleration – and its annual probability of exceedance (or return period) at a site. This method produces regional seismic probability maps, displaying contours of maximum ground motion (macroseismic intensity, PGA) of equal – specified – return period, shown in figure 2.7.

Furthermore the (Italian Department of Civil Protection, 2012) describes seismic hazard in terms of **seismicity** which is an index that specifies frequency and force of earthquakes and represents a physical characteristic of an area. They explained that if we know the frequency and energy of characteristic earthquakes from a certain area a probability can be proposed to a seismic event of a given magnitude occurring in a certain interval of time, allowing to calculate the seismic hazard. Hence from previous statement it is inferred that Italian Seismic hazard has been determined from a probabilistic approach.

Nevertheless the consequences of an Earthquake not only depends in the frequency and energy of an earthquake in a certain interval of time (seismic hazard), it is also influenced by vulnerability and exposure of the zone. Therefore the **seismic risk** is the measurement of the damage expected in a given interval of time, based on seismicity, resistance of buildings, anthropisation nature and quality and quantity of assets exposed.

Italy has a medium-high seismic hazard (due to the frequency and intensity of phenomena), very high vulnerability (due to the fragility of building, infrastructural, industrial, production and service assets) and an extremely high exposure (due to population density and its historical, artistic and monumental heritage that is one of its kind in the world). The Italian peninsula therefore has a high seismic risk, in terms of victims, damage to buildings and direct and indirect costs expected after an earthquake.

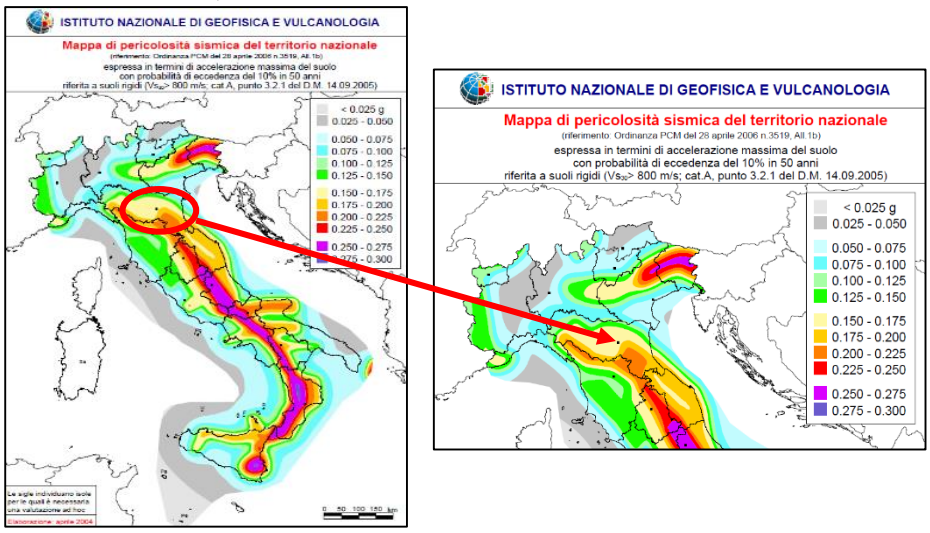

Figure 2.7 Italian Seismic hazard defined in PGA (m/s²); ingv.it

2.3 Seismic retrofit and control system.

2.3.1 Seismic retrofit definition and motivation.

"Unfortunately many existing structures that were built according to past design codes & standards are often found vulnerable to earthquake damage. This fact becomes more obvious every time when there is a major earthquake and the same patterns of damage are observed. (Sahin, 2014)"

Seismic assessment or retrofit is the modification of existing structures that aims to decrease the vulnerability against ground motions or soil failures due to earthquakes. These procedures can be also applicable to other natural hazards like tropical cyclones, tornadoes and severe winds, whereas it is predominantly concerned to seismic hazard reduction.

Prior modern seismic codes introduction most of the structures were designed and built without adequate detailing and reinforcement for seismic response. As a consequence structures with an elevate cost of new construction or historical/cultural importance have been "retrofitted" by governmental agencies and major industries. However this situation is not exclusive to large and important structures. According to (Arya & Agarwal, 2002) the need for seismic retrofitting in existing buildings/structures can arise due to one or more of the following reasons:

- Buildings not designed to codes.
- Upgrading of code based seismic forces.
- Upgrading of seismic zone.
- Deterioration of strength on aging of the structure.
- Modification of the existing structures affecting its strength adversely.
- Change of the use of the building increasing the floor loads.

From above it can be inferred that a considerable amount of existing structures require a seismic assessment. For that reason functioning research work have been developed in order to regularize retrofitting and as a result technical guidelines have been published and some procedures were added in seismic codes. Some current examples are: the Seismic Evaluation and Retrofit of Existing Buildings (ASCE-SEI 41-13), Assessment and Improvement of the Structural Performance of Buildings in Earthquake (NZSEE) and FEMA retrofit guidelines.

2.3.2 Seismic retrofit performance objectives & strategies.

"Regardless of the technical solution adopted the efficiency of a retrofit strategy strongly depends on a proper assessment of the internal hierarchy of the beam-column joints as well as of the expected sequence of events within a beam-column system (shear hinges in the joints or plastic hinges in beam and column elements). The effects of the expected damage mechanism on the local and the global response should also be adequately considered. (Pampanin, Bolognini, & Pavese, 2006)"

In the beginning retrofitting expected to achieve public safety. Nevertheless with engineering limitations by economic and political considerations. As a result, 4 levels of performance objectives (shown in figure 2.8) have been established:

- **Public safety only.** The goal is to protect human life, ensuring that the structure will not collapse upon its occupants or passersby, and that the structure can be safely exited. Under severe seismic conditions the structure may be a total economic write-off, requiring tear-down and replacement.
- **Structure survivability.** The goal is that the structure, while remaining safe for exit, may require extensive repair (but not replacement) before it is generally useful or considered safe for occupation. This is typically the lowest level of retrofit applied to bridges.
- **Structure functionality**. Primary structure undamaged and the structure is undiminished in utility for its primary application. A high level of retrofit, this ensures that any required repairs are only "cosmetic" for instance, minor cracks in plaster, drywall and stucco. This is the minimum acceptable level of retrofit for hospitals.
- **Structure unaffected.** This level of retrofit is preferred for historic structures of high cultural significance.

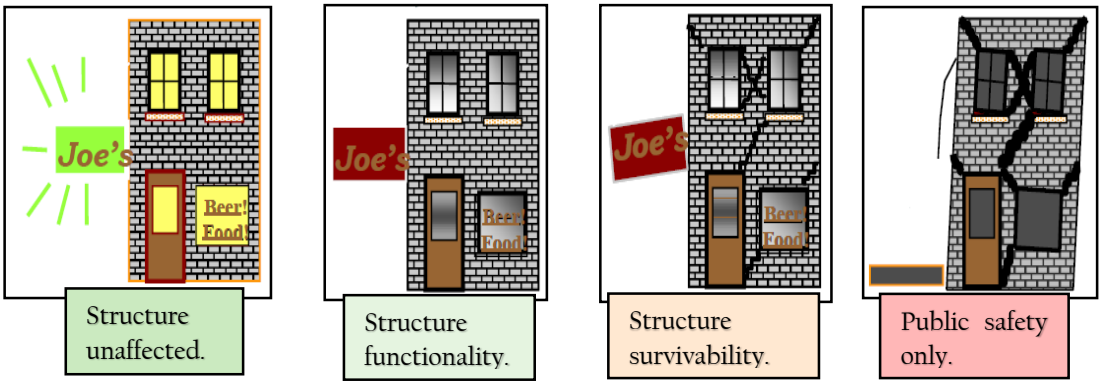

Figure 2.8 Performance according to EN-1998 (from PhD. Jesús Bairán Lecture).

From guidelines, seismic provisions and availability of advanced materials some seismic retrofitting strategies have been established in the past few decades. As shown in table No.2.1, the rehabilitation can be approach from several points of view such as insufficient resistance or over-demanding seismic loading. Moreover not all the strategies are mutually exclusive which enables a combination, if necessary. However, final decision will directly depend on designer judgement and previous experiences.

Increasing global capacity.	This is typically done by the addition of cross braces or new structural walls.
Reduction of the seismic demand	By means of supplementary damping and/or use base isolation systems. (Filiatrault & Cherry, 1988)
Increasing the local capacity of structural elements.	This strategy recognizes the inherent capacity within the existing structures, and therefore adopt a more cost-effective approach to selectively upgrade local capacity (deformation/ductility, strength or stiffness) of individual structural components.
Selective weakening retrofit.	This is a counter intuitive strategy to change the inelastic mechanism of the structure, while recognizing the inherent capacity within the existing structure.(Kam & Pampanin, 2008)
Allowing sliding connections	Such as passageway bridges to accommodate additional movement between seismically independent structures.

Table 2.1 Principals retrofitting strategies.

2.3.3 Seismic retrofitting dilemma.

"Unlike seismic design of new buildings, which is still (mainly) force-based, seismic assessment or retrofitting of existing ones is nowadays fully displacement-based. The underlying reason is practical… (Fardis, 2009)"

Force-based approaches entail capacity demand comparison in terms of internal forces, with seismic force demands computed from a design response spectrum incorporating a global behavior of force reduction factor, q or R. For an existing building to be entitled a q-factor larger than q-factor attributed to overstrength alone (q=1.5 in Eurocode 8) the structure as a whole should meet all the rules pertaining one discrete ductility classes with a higher q value. As the building most likely violates these rules in one way or another, the force capacity of some members considered to contribute to earthquake resistance will be less than the force demand. In this way any old concrete building, possibly except low-rise ones with large walls, will be assessed as seismically inadequate and will need retrofitting.

Moreover, if it is decided to retrofit the building and the designer wants to use the higher q value from one of the discrete ductility classes in a code for new buildings, every single member considered lateral force-resistant should be retrofitted. As a result this approach might cause a considerable increment of retrofitting costs leading to demolition or "do-nothing" alternatives as less expensive alternatives.

A solution for previous dilemma produced by the prescriptive rules of current force-based seismic design codes for new buildings, is to asses and retrofit each earthquake resistant member from its own capacity and peculiarities instead of reducing the overall elastic seismic forces through the q-factor concept. This is an advantageous amendment because for a member seismic performance its deformation is more important than its force. After all structures collapse not because of the seismic lateral loads, but due to gravity loads acting through the lateral displacement induced by earthquakes (P-Δ) effects. (Fardis, 2009)

The leading objective of displacement-based analysis for seismic assessment or retrofitting is the calculation of deformation demands in structural members. Recent developed codes or standards for displacement-based seismic assessment and retrofitting of building (ASCE 2007, CEN2005a) provide as options: Linear static analysis, Modal response spectrum analysis, Nonlinear Static or "pushover" analysis and Nonlinear Dynamic Analysis. In order to make an adequate selection the capacity of model simplification and analysis restrictions should be evaluated.

A feasible example is the linear analysis for displacement-based assessment and retrofitting where member inelastic deformation demands (e.g. chord-rotations) may be derived essentially employing the equal-displacement rule at member level. Nevertheless, this interpretation is only valid when estimated chord-rotation ductility demands fulfill some restrictive conditions comprise upper limits on the absolute magnitude of these demands, as well as on their difference between stories or at opposite's sides of the building. When linear-elastic analysis requirements are not accomplished a nonlinear analysis should be performed.

So, nonlinear analysis, being always applicable is the reference method for displacement-based seismic assessment and retrofitting. Note that, in seismic assessment all information necessary for the calculation of the yield moment, the secant stiffness to the yield-point, and all other member properties needed as an input to nonlinear analysis, are readily available. This represents the foremost benefit in contrast to its use in design of new structures where reinforcement is not known a-priori and several cycles of design –analysis are needed. However, it must be considered that the information needed for the seismic assessment of existing structures are not always known with a good level of reliability. Fortunately in our case, we had a very detailed technical documentation concerning to the original structural design.

2.3.4 Seismic control -Buckling Restrained Axial Damper (BRAD).

Seismic protection devices are equipment that provides an improvement of the structural response to the seismic action. Such modifications can be done by seismic isolation, energy dissipation or creating temporary restraints via rigid connections. The first two ways which are often combined emerged 30 years ago as an alternative to conventional methods admitting even serious damage to the structure provided it does not collapse(J.M Kelly, Skinner, & Heine, 1972; J.M. Kelly, 1973). On the other hand, seismic isolation and energy dissipation can avoid any damage to the structure, if desired.

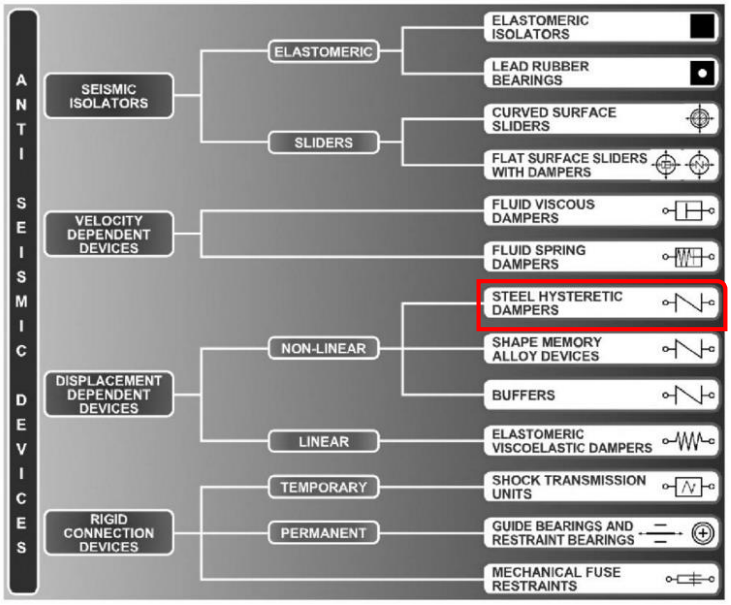

Figure 2.9 Anti-Seismic devices manufactured in Italy

Figure 2.9 illustrates the seismic protection devices manufactured in Italy, as classified according to the European Standard. The first time of seismic isolation was in the 1970, the Somplago Viaduct on the Udine-Tarvisio motorway; this was also the first isolated bridge in Europe. Thanks to the good response 10 years later with Friuli earthquake, new seismic devices were developed and applied in hundreds of bridges. By 1992 Italy became the country with the largest number of seismically isolated bridges (over 150 bridges and over 100 km).

The application of seismic isolation/energy dissipation for buildings started a few years later than bridges. Nevertheless it has a quite slow increasing due to a lack of specific code and very king approvals procedures. It was not until 2003 with the new Italian seismic code publication (and its later update in 2005) that included specific chapters about seismic isolation of building and bridges where the use of anti-seismic devices in buildings started to become more common.

In many cases where the isolation is not possible or too expensive seismic retrofit or RD framed building, has been carried out introducing dissipative bracings. Therefore braces have been extensively used as effective tool for seismic members for low-rise and high-rise building, but conventional braces sustain buckling under compressive forces. As a solution for this limitation, several studies have recommended the use of buckling restrained braces.

This design method started becoming increasingly popular keeping columns and beams of buildings in elastic regions as much as possible by using buckling-restrained braces as hysteretic dampers and allowing this hysteretic to absorb the energy to producing a damping effect, shown in figure 2.9. According to this method the buckling restrained braces plasticize to provide hysteresis damping when medium earthquakes occurs thereby keeping columns and beams in elastic regions when large earthquakes occurs. (Mazzolani & Tremblay, 2000)

Previous proposal scheme has several benefits from a damage and economical point of view, since it reduces plastic strains of lateral-force resistant elements keeping them undamaged. This represents a considerable decrease of repair and replacement costs from the whole building and just leaving a required inspection of braces after the earthquake event.

An example in Italian context is illustrated in figure 2.10 where an example of buckling restrained axial dampers installed in the School "Cappuccini" in Ramacca is shown. Moreover dissipative bracings with buckling restrained axial dampers also have been used to increase ductility and hyper-staticity of a new pre-cast building. It represents the first application of buckling restrained braces in Italy and Europe. (Phocas, Brebbia, & Komodromos, 2009)

Figure 2.10 Buckling restrained axial dampers installed in the School "Cappuccini" in Ramacca.

2.4 Non-linear Dynamic Analysis.

"The response of buildings to earthquakes is a complex, three dimensional, nonlinear, dynamic problem. (Chambers & Trevor, 2004)"

Nonlinear dynamic analysis was developed as a method in the 1970s for research, code-calibration or special applications. Since then, with the availability of several reliable and numerically stable computer codes with nonlinear dynamic analysis capabilities, it has gained its place in engineering practices for the evaluation of structural designs carried out using other approaches

The main practical application of nonlinear dynamic analysis, currently and in the foreseeable future, is for seismic assessment of existing structures. This has been particularly noted since the primary use of non-linear method within the framework of EN-1998 is to evaluate the seismic performance of new designs, or to asses existing or retrofitted buildings. (eurocodes.us, 2013) Professionals practicing seismic assessment of existing structures are fewer and more specialized than in every-day design. So they often master nonlinear dynamic analysis and its special software tools.

Unlike the static version, the dynamic version of non-linear analysis does not require an a priori and approximate determination of the global non-linear seismic demand (cf. the target displacement in pushover analysis). Global displacement demands are determined in the course of the analysis of the response. Moreover, unlike modal response spectrum analysis, which provides only best estimates of the peak response (through statistical means, such as the SRSS and the CQC rules), peak response quantities determined by non-linear dynamic analysis are exact, within the framework of the reliability and representativeness of the non-linear modelling of the structure. The only drawbacks of the approach are its sophistication and the relative sensitivity of its outcome to the choice of input ground motions.

2.5 Ground motion selection.

"Due to latest improvements in structural analysis and computational facilities nonlinear time history analysis has become the most important tool in performance-based seismic studies (Y. M. Fahjan, 2008). Nevertheless, it still requires a large computation capacity and time which cause a reduction of feasible analyses amount. Hence an adequate criteria to select earthquakes is a vital requirement to determine structural response with greater confidence."

2.5.1 The necessity of Earthquake parameters.

The seismic demand on structures due to ground motion excitation is highly uncertain due to the inherently random nature of the fault rupture process, seismic wave propagation and local site effects, as well as the variation in the seismic response of structures subjected to ground motion excitations of similar intensity. (Bradley, Cubrinovski, Macrae, & Zealand, n.d.) As a result of complexity and randomness on earthquake motion, it has been a difficult task to accurately evaluate the applicability of various existing intensity indices (Ye, Ma, Miao, Guan, & Zhuge, 2013) Hence is vitally important to choose an appropriate and comprehensive earthquake intensity index to achieve an accurate correlation with the structural performance (Ye et al., 2013). The latter indicates that in such seismic response analysis it is significant to employ a ground motion IM which is efficient (Shome, 1999) in predicting these seismic demands.

It is know that the uncertainties associated with the estimation of seismic demand are highly dependent on the variable(s) adopted to define earthquake. (Giovenale, Cornell, & Esteva, 2004) For this reason, selecting and scaling accelerogram is a helpful tool (for both engineering design and assessment) as it enables to determine the structural response with greater confidence, but using fewer analyses than if unscaled accelerogram are employed. The objective of selecting and scaling accelerogram is to provide ground motions capable of producing the same damage level as the mean or another target percentile damage level generated by a large suit of ground motion corresponding to design magnitude, source to site distance and site classification. (Hancock, 2006)

Nowadays there is a large and wide database of investigations regarding to the effects of different seismic input on structural response deal with the variability of the input in terms of several parameters. According to Liu, 1958 earthquake intensities can be classified into 2 major categories: (1) intensities in relation to the ground motion parameters which are directly obtained from ground motions records (PGA,PGV), (2) intensities in relation to the structural seismic response such as Peak Spectrum Acceleration (PSA) and Peak Spectrum Velocity (PSV). Figure 2.11 depicts most common used parameters.

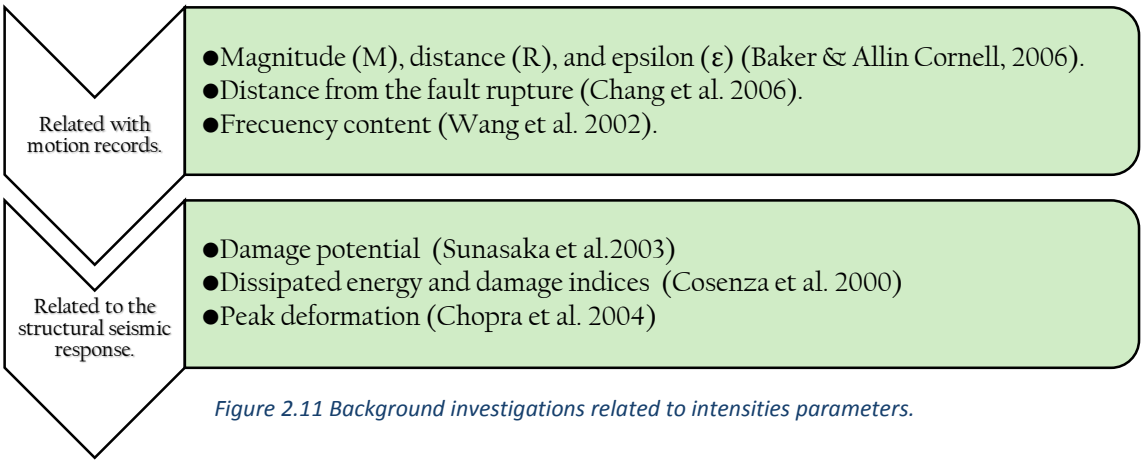

Figure 2.11 Background investigations related to intensities parameters.

2.5.2 Useful earthquake parameters and its current applications.

Peak ground acceleration mostly called PGA is defined as the largest peak acceleration amplitude recorded on an accelerogram at a site during a particular earthquake. According to ITACA, it indicates the maximum value registered of a ground motion from 3 seismic instruments components. It is also considered the simplest strong-motion parameter and therefore more than 120 equations have been derived to predict it (Douglas, 2003).

Nowadays PGA has been adopted in many structural design codes and standards provisions worldwide, some examples are Eurocode 8 (1998) and China code GB50011-2001. Although PGA motion it is only useful for analysis of short period ($T \leq 3$), is still often used as a parameter to describe strong (Douglas, 2003). This popularity is due a historical reason, in the beginning of seismic design most of the structure were low-rise and short fundamental period (Ye et al., 2013).

Radio, also called site-to-source distance, refers to the distance between the epicenter (the point on the earth´s surface directly above the source or focus of the earthquake) and measuring station. Even though distance´s influence on structural response has been discussed for a long time ago, a formal concept has not been reached. This resulted from seismic waves travel variability which brought to surface that has a dependency on more than distance, for instance soil´s homogeneity.

Magnitude -according to British geological survey- is defined as the measure of earthquake size. It is determined from the logarithm of the maximum displacement or amplitude of the earthquake signal as seen on the seismogram, with a correction for the distance between the focus and the seismometer. Since the measure can be made from primary (P), secondary (S), or surface waves several different scales exist, all of which are logarithmical because of the large range of earthquakes energies. Its main application is as a measure of the energy released in the earthquake source. Moreover is commonly used to classify different events from the same area or region. (USGS, 2014)

The **intensity** is a number (written as a Roman numeral) describing the severity of an earthquake in terms of its effects on the earth's surface and on humans and their structures. Several scales exist, but the ones most commonly used are the Modified Mercalli scale and the Rossi-Forel scale. There are many intensities for an earthquake, depending on where you are, unlike the magnitude, which is one number for each earthquake. (USGS, 2014)

Proposed by Chilean engineer Arturo Arias in 1970, **Arias Intensity (IA)** is a measure of the ground motion's strength expressed in velocity (m/s) dimension, see equation 2.1. It determines the intensity of shaking by measuring the acceleration of transient seismic waves (Peter J. Stafford, Berrill, & Pettinga, 2009).

$$I_a = \frac{\pi}{2g}\int_0^{T_d} a(t)^2 dt \ \ (m/s)$$

Td= Significant time
g= gravity
a(t)²= acceleration at t time

Equation 2.1
Arias Intensity

Alternatively ITACA (Strumento et al., 2005) defines Arias Intensity as an integral parameter obtained as a cumulative measure of the seismic movement during a significant time. Where significant time (Td) is the duration of signal above threshold, it can be defined by 2 ways: overpassing a value (most of the time 0.05g) or based on 5% of Arias Intensity.

Although Arias Intensity current applications could be extensive, it has not been included in any standard or national code owing to the fact that is quite recent and its calculation is not as simple as other parameter. Nevertheless there are several studies like (P J Stafford, 2012) where the application of Arias Intensity is recommended as lower bound in the hazard integration.

Housner Intensity (I_h) also called response spectrum intensity, is the area under the (PSV) pseudo-velocity response spectrum over the period range 0.1 to 2.5 sec, defined in equation 2.2. This index also depends on period and damping (which is 5% most of the time) of the structure. Housner intensity is related to the potential damage expected effect of the earthquake in question since most the structures have a fundamental period of vibration in the range between 0.1 and 2.5 seconds. (Strumento et al., 2005)

$$SI\ (\xi) = \int_{0.1}^{2.5} PSV(T,\xi)^2 dT \ \ (cm)$$

T= period of structure.
ξ= damping.
PSV= pseudo-velocity response.

Equation 2.2
Housner Intensity

According to (Martinez-rueda et al., 2008) Arias Intensity and Housner Intensity are two good examples of instrumental intensities that have received the attention of researchers, both to describe their correlation with ductility demand. Dimensionally speaking Housner Intensity is a displacement commonly expressed in cm.

2.5.3 Natural recordings.

The assessment of the structural response via dynamic analysis requires some characterization of seismic input which should reflect the hazard as well as the near-surface geology at the site (Iervolino, Maddaloni, & Cosenza, 2008) As a consequence Eurocode 8, part 1, outlines the requirements for the seismic input for dynamic analysis in section 3.2.3 where specifies:

"The seismic motion may be represented in terms of ground acceleration time-histories and depending on the nature of the application and on the information actually available, the description of the seismic motion may be made by using artificial accelerogram and recorded or simulated accelerogram."

In this previous cite is important to note that when Eurocode specifies the outline for dynamic analysis input gives to the designer the freedom of choosing the type of accelerogram from the available information. The authors Masi, Vona, & Mucciarelli, 2011 explain that generating synthetic ground motion records in other words forcing accelerogram to converge to a building code spectrum for vulnerabilities studies and damage scenarios is not the way to go. This happens independently from the way the accelerogram is generated, from either random white noise (SIMQKE) or physical parameters (BELFAGOR). It is also explained that there is a significant difference between natural and synthetic accelerogram. All the techniques chosen to generate synthetic accelerogram provide more conservative results (higher number of cases exceeding the drift values leading to collapse) when compared with natural recordings.

Furthermore Y. Fahjan & Ozdemir, 2008 presented in their conclusions that for real earthquake records the average nonlinear response of the scaled time histories has compatible behavior. Although with the RSP Match program compatible behavior was also observed, convergence was not guaranteed for many records and the program requested a lot of parameters. Finally while using SIMQKE and TARSCTH programs unrealistic nonlinear behavior were observed for the valid period range.

From the reason exposed above, among all the possible options to define the seismic input for structural analysis, natural recording are emerging as the most attractive (Pelà, Aprile, & Benedetti, 2013). Easily accessible waveform databases are available and evidence shows that only a relatively limited number of criteria has to be considered in selection and scaling to get an unbiased estimation of seismic demand. (Iervolino et al., 2008)

2.5.4 Required parameters for natural earthquake database search.

It is essential to be familiar with database searching parameters before any ground motion records search. This will represent a shrink in time search and more important a higher probability to obtain records more reliable with our target. In the table 2.2 and figure 2.12 below the parameters used for the natural ground motion search are detailed. It is noteworthy that any of these distance metrics fortuitously predicting a future source hypocentral distance is a very unlikely situation. Consequently, in general these parameters should not be used for this purpose.

Hypocentral dist.	Between site and the Earth´s point where an earthquake rupture starts.
Epicentral dist.	Between the point directly above hypocentral at Earth´s surface and site.
Focal depth	Refers to the depth of an earthquake hypocenter.
$R_{Joyner-Boore}$ distance	Denotes from site to the vertical projection Earth´s fault surface.
Rrup distance	The nearest distance to the rupture surface, in general not a hypocentral dist.
Vs_{30m} (velocity)	Shear wave velocity average over the top 30 meters of soil.

Table 2.2 Definition of earthquakes parameters.

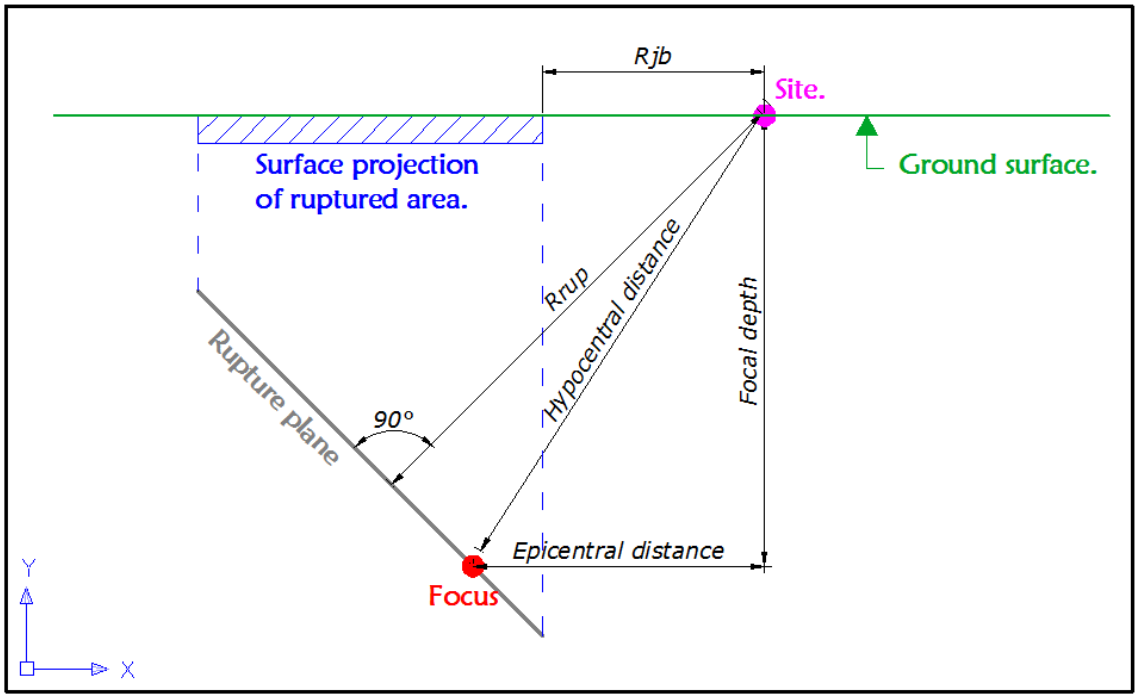

Figure 2.12 Earthquake's parameter description.

It is worth noting that more parameters were available to define previous database search. However it was observed that obtained results are reduced when more parameters are specified. Hence only above mentioned parameters were used in order to extend the amount of possible results.

2.5.5 Current natural recording databases.

European Strong Motion Site: This platform provides an interactive, fully relational database and databank with more than 3,000 uniformly processed and formatted European strong-motion records and associated earthquake-, station and waveform-parameters. More than 2,000 acceleration time histories are archived in the databank as uncorrected and corrected record together with the corresponding elastic response spectra.

The user can search the database and databank interactively and download selected strong-motion records and associated parameters. Information about European organizations involved in strong-motion recordings are also available. These records are all released to the public domain by a number of different individuals, organizations and agencies and may be downloaded from this site as digital record. Their contribution to this database and databank is acknowledged.

The SIMBAD database (Selected Input Motions for displacement-Based Assessment and Design) was created by assembling records from different worldwide strong ground motion databases, with the main objective of providing records of engineering relevance for the most frequent design conditions in Italy.

SIMBAD data selection, on its 3rd release, consists of 467 three-component accelerogram, selected according to the following criteria: a) shallow crustal earthquakes worldwide with moment magnitude MW ranging from 5 to 7.3 and epicenter distance R_{epi} approximately less than 30 km. This ensures to provide strong ground motion records of engineering relevance for most of the design conditions of interest in Italy that can be used without introducing scaling factors.

SIMBAD database has good quality at long periods, expect for a few exceptions, only records for which the high-pass cut-off frequency used by the data provider is below 0.15 Hz. Therefore, most records are from digital instruments, while from analog instruments only those records with a good signal to noise ratios at long periods, typically from large magnitude earthquakes, were retained. Moreover it has availability of VS30 measurements (preferable) or definition of the Eurocode 8 (CEN, 2004) site class based on quantitative criteria.

PEER ground motion database, includes a very large set of ground motions recorded in worldwide shallow crustal earthquakes in active tectonic regimes. The database has one of the most comprehensive sets of meta-data, including different distance measure, various site characterizations, earthquake source data, etc, shown in figure 2.13. The current version of the database is similar to the NGA-West2 database, which was used to develop the 2014 NGA-West2 ground motion models (GMMs). (Ancheta, Darragh, & Stewart, 2013).

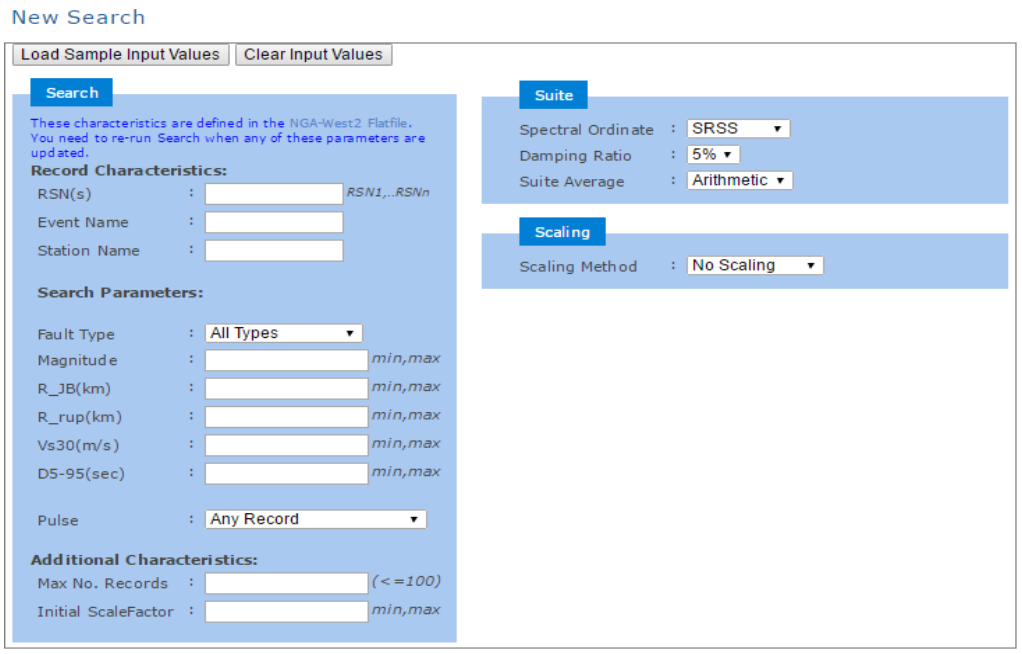

Figure 2.13 PEER database environment search.

2.5.6 Record selection procedure according to Eurocode 8.

Once the reference spectrum has been defined, EC8—Part 1 allows the use of any form of accelerogram for structural assessment; i.e., real, artificial or obtained by simulation of seismic source, propagation and site effects. To comply with Part 1 the set of accelerogram, regardless its type, should basically match the following criteria:

(a) A minimum of 3 accelerogram should be used;
(b) The mean of the zero period spectral response acceleration values (calculated from the individual time histories) should not be smaller than the value of ag S for the site in question (S is the soil factor);
(c) In the range of periods between 0.2 T1 and 2 T1, where T1 is the fundamental period of the structure in the direction where the accelerogram will be applied, no value of the mean 5% damping elastic spectrum, calculated from all time histories, should be ‹90% of the corresponding value of the 5% damping elastic response spectrum.

Furthermore Eurocode 8 prescriptions request for matching of the average response at least seven recordings (each of which includes both horizontal components of a recorded motion if spatial analysis is concerned) to consider mean response. **Little if it any, prescriptions are given about the features of the signal.** Therefore, the code requirements seem to have been developed having spectrum-compatibilities in mind. On the other hand, real accelerogram are becoming the most attractive option to get unbiased estimations of the seismic demand. (Iervolino et al., 2008)

2.6 Statistical Analysis & Reliability Index.

2.6.1 General terms of statistical analysis.

Actions, mechanical properties and dimensions are generally described by random variable (continuous most of the time). Nevertheless, as previously mentioned random variable can be used to evaluate others phenomenon as structural response. An aleatory variable X, maximum displacement for example can take any value along a defined interval with a known or predicted probability.

As a rule, while studying any variable just a limited number of observations is available. This number generates a (N) dimension aleatory campaign x_1, x_2, x_3... x_n taken from a population. **"Population"** refers to the total set of observations that can be made. Also can be defined as every element, individual or units that meet a selection criteria for a group to be studied, and from which a representative sample is taken for detailed information. In order to get this detailed information in a manner that allows to make decisions the statistical methods are used.

From the total sample amount available a **set** is created. Normally sets are prepared with specific criteria under a certain time. The objective of statistical methods is to make decisions regarding to population´s properties using obtained information from one or more random variable.

Sampling is a process that aims the selection of a subset of representative individuals within a statistical population. Therefore, once the sample is established to determine population properties, sample characteristics are estimated. In practical application the 3 more common fundamental characteristic's sample used are mean value, variance and asymmetry coefficient.

Mean value (m): a calculated central value of a set of numbers. Strictly speaking represents the fundamental measure of the central tendency defined as equation 2.3.

$$m = \frac{\sum x_i}{n}$$, where the sum concerns to every n value of x_i. Equation 2.3 Median Value

Variance (S^2): used to indicate how widely individuals in a group vary. If individual observations vary greatly from the group mean, the variance is big; and vice versa. Variance is determined according to equation 2.4.

$$s^2 = \frac{\sum (x_i - m)^2}{n-1}$$ Equation 2.4 Variance

Median value: is the middle number in a sorted list.

$$\tilde{x} \equiv \begin{cases} Y_{(N+1)/2} & \text{if } N \text{ is odd} \\ \frac{1}{2}\left(Y_{N/2} + Y_{1+N/2}\right) & \text{if } N \text{ is even} \end{cases}$$

Histograms.

A histogram is a graphical representation, similar to a bar chart in structure, which organizes a group of data points into user-specified ranges. The histogram condenses a data series into an easily interpreted visual by taking many data points and grouping them into logical ranges or bins. Another definition for histogram is the approach to graph distributions value for a bunch of tiny equal –size non overlapping intervals. These intervals are called bins. Moreover histograms are commonly used in statistics to demonstrate how many of a certain type of variable occurs within a specific range.

Probability Density Function and Cumulative Function.

Most often, the equation used to describe a continuous probability distribution called a **probability density function.** Sometimes, it is referred to as a **density function (PDF)**. For a continuous probability distribution, the density function has the following properties:

- Since the continuous random variable is defined over a continuous range of values (called the **domain** of the variable), the graph of the density function will also be continuous over that range.
- The area bounded by the curve of the density function and the x-axis is equal to 1, when computed over the domain of the variable.
- The probability that a random variable assumes a value between a and b is equal to the area under the density function bounded by a and b.

For example, consider the probability density function shown in the graph below. Suppose we wanted to know the probability that the random variable X was less than or equal to a. The probability that X is less than or equal to a is equal to the area under the curve bounded by a and minus infinity - as indicated by the shaded area in figure 2.14.

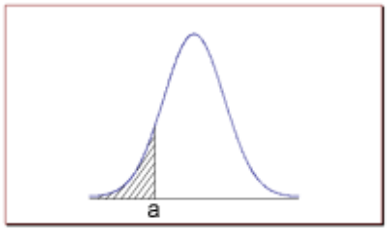

Figure 2.14 Cumulative probability of a value minor than a.

Note: The shaded area in the graph represents the probability that the random variable X is less than or equal to a. This is a cumulative curve. However, the probability that X is exactly equal to a would be zero. A continuous random variable can take on an infinite number of values. The probability that it will equal a specific value (such as a) is always zero. (startrek.com, 2008)

2.6.2 Probability Distribution.

A probability distribution is a table or an equation that links each outcome of a statistical experiment with its probability of occurrence. It has some prerequisites which derives from continuous variable such as:

- A **variable** is a symbol (A, B, x, y, etc.) that can take on any of a specified set of values.
- When the value of a variable is the outcome of a statistical experiment, that variable is a **random variable**.

There is a long and wide catalogue of probability distribution providing that exists a lot of diverse phenomena and each one has its particularities. Hence herein are detailed the distribution that resulted with the higher fitting probability according to chi test.

Log-logarithmic distribution

In probability and statistics, the '''log-logistic distribution''' (known as the '''Fisk distribution''' in economics) is a continuous probability distribution for a non-negative random variable. It is used in survival analysis as a parametric model for events whose rate increases initially and decreases later, for example mortality rate from cancer following diagnosis or treatment. It has also been used in hydrology to model stream flow and precipitation, and in economics as a simple model of the distribution of wealth or income distribution income. (Bennet Steve, 1983)

The log-logistic distribution is the probability distribution of a random variable whose logarithm has a logistic distribution, displayed in figure 2.15. It is similar in shape to the log-normal distribution but has Heavy-tailed distribution heavier tails. Unlike the log-normal, its cumulative distribution function can be written in closed form expression closed form.

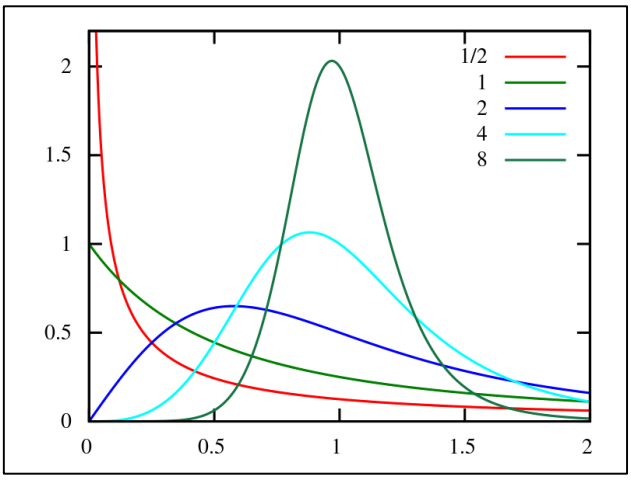

Figure 2.15 Log-logarithmic Function; alpha= 1and beta as shown in legend.

Gamma distribution.

In probability theory and statistics the gamma distribution is a two-parameter family of continuous probability distribution. The common exponential distribution and chi-squared distribution are special cases of the gamma distribution. These are 3 different parametrizations in common use:

1. With a shape parameter k and a scale parameter θ.
2. With a shape parameter $\alpha = k$ and an inverse scale parameter $\beta = 1/\theta$, called a rate parameter.
3. With a shape parameter k and a mean parameter $\mu = k/\beta$.

In each of these three forms, both parameters are positive real numbers. Moreover figure 2.16 presents density and cumulative functions varying scale and shape parameter. The gamma probability density function is useful in reliability models of lifetimes. The gamma distribution is more flexible than the exponential distribution in that the probability of a product surviving an additional period may depend on its current age. The exponential and χ^2 functions are special cases of the gamma function. (MATLAB, 2016)

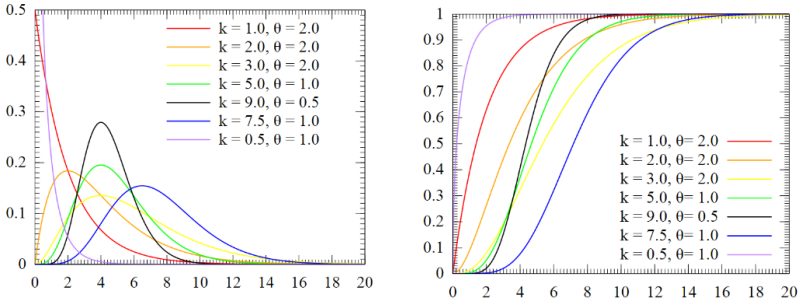

Figure 2.16 Density and Cumulative functions of Gamma distribution; wikipedia.org

2.6.3 Statistical hypothesis Testing.

A statistical hypothesis is an assumption about a population parameter. This assumption may or may not be true. There are two types of statistical hypotheses. The first one is the **null hypothesis,** denoted by H_0, is usually the hypothesis that sample observations result purely from chance. The second one is the **alternative hypothesis**, denoted by H_1 or H_a, is the hypothesis that sample observations are influenced by some non-random cause.

All hypothesis tests are conducted the same way. The researcher states a hypothesis to be tested, formulates an analysis plan, analyzes sample data according to the plan, and accepts or rejects the null hypothesis, based on results of the analysis. **State the hypotheses: e**very hypothesis test requires the analyst to state a null hypothesis and an alternative hypothesis. The hypotheses are stated in such a way that they are mutually exclusive. That is, if one is true, the other must be false; and vice versa.

Formulate an analysis plan. The analysis plan describes how to use sample data to accept or reject the null hypothesis. It should specify the following elements: **significance level.** Often, researchers choose significance levels equal to 0.01, 0.05, or 0.10 and **Test method: t**ypically, the test method involves a test statistic and a sampling distribution. Computed from sample data, the test statistic might be a statistic parameter, ex .mean value. Given a test statistic and its sampling distribution, a researcher can assess probabilities associated with the test statistic. If the test statistical probability is less than the significance level, the null hypothesis is rejected.

Chi-squared goodness of test

The chi-square goodness of fit test is appropriate when the following conditions are met: the sampling method is simple random sampling and the expected value of the number of sample observations in each level of the variable is at least 5. This approach consists of four steps: (1) state the hypotheses, (2) formulate an analysis plan, (3) analyze sample data, and (4) interpret results. Every hypothesis test requires the analyst to state a null hypothesis (H_0) and an alternative hypothesis (H_a). For a chi-square goodness of fit test, the hypotheses take the following form. H_0: The data are consistent with a specified distribution and H_a: The data are not consistent with a specified distribution.

Typically, the null hypothesis (H_0) specifies the proportion of observations at each level of the categorical variable. The alternative hypothesis (H_a) is that at least one of the specified proportions is not true. Finally there is the results interpretation: If the sample findings are unlikely, given the null hypothesis, the researcher rejects the null hypothesis. Typically, this involves comparing the P-value to the significance level, and rejecting the null hypothesis when the P-value is less than the significance level.

2.6.4 Reliability index and failure rate.

A standard reliability measure can be chosen to be generalized reliability index, It is defined where Pf is the probability of failure and is the inverse of the Gaussian function, see equation 2.5.

$$P_s = \phi^{-1}(P_f) . \qquad \text{(Equation2.5)}$$

Where P_f is failure probability and ϕ^{-1} is the inverse of Gaussian distribution.

Another equivalent reliability measure is the probability of the complement of the adverse event where: Ps = 1 – Pf. In this case the probability of failure Pf should be calculated on the basis of the standardized joint distribution type of the basic variables and the standardized distributional formalism of dealing with both model uncertainty and statistical uncertainty. However in special situations other than the standardized distribution types can be relevant for the reliability evaluation. In such cases the distributional assumptions must be tested on a suitable representative set of observation data. (Gulvanessian, Calgaro, & Holicky, 2010)

2.7 Description of used software.

2.7.1 REXEL

To enable record selection according to both approaches of EC8 and NIBC, a specific software tool was developed. Figure 2.17 presents its MATHWORKS-MATLAB_ graphic user interface (GUI) and a FORTRAN engine, based on the software developed for the studies of Iervolino, Galasso, & Cosenza, 2010. In particular, the computer program was developed to search for combinations of seven accelerogram compatible in the average with the reference spectra according to code criteria discussed above. It is also possible to reflect in selection the characteristics of the source (if available) and site, in terms of magnitude (M), epicenter distance (R), and EC8 soil site classification. In fact, REXEL 2.31 beta, freely available on the internet at the website of the Italian consortium of earthquake engineering laboratories.

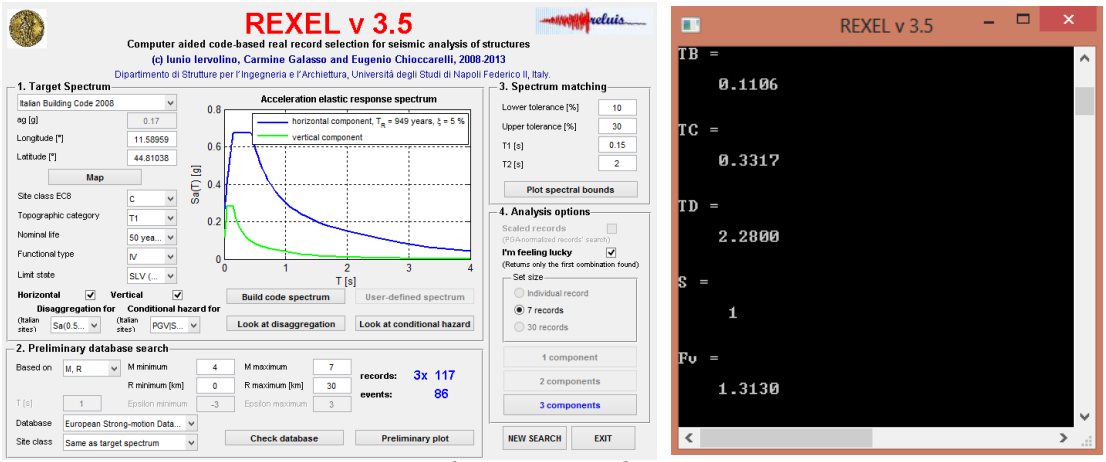

Figure 2.17 Rexel environment and its FORTRAN engine.

The procedure implemented for record selection deploys in four basic steps:

1. Definition of the design (reference) horizontal and/or vertical spectra the set of records has to match on average; the spectra can be built according to EC8, NIBC, or user-defined;
2. List and plot of the records contained in the ESD and embedded in REXEL which fall into the magnitude and distance bins specified by the user for a specific site class;
3. Assigning the period range where the average spectrum of the set has to be compatible with the reference spectrum, and specification of tolerances in compatibility;
4. Running the search for combinations of seven records which include one, two of all three components of motion and that, on average, match the design spectrum with parameters specified in step 3.

2.7.2 SEISMOSIGNAL. (From seismosignal webpage)

Seismosignal is an easy and efficient way to process strong-motion data, featuring a user-friendly visual interface and being capable of deriving a number of strong-motion parameters often required by engineer seismologists and earthquake engineers, see figure 2.18.

Seismosignal calculates: elastic and constant-ductility inelastic response spectra, Fourier and Power spectra, Arias (Ia) and characteristic (Ic) intensities, Cumulative Absolute Velocity (CAV) and much more. Seismosignal also enables the filtering of unwanted frequency content of the given signal. Three different digital filter types are available, all of which capable of carrying out highpass, lowpass, bandpass and bandstop filtering.

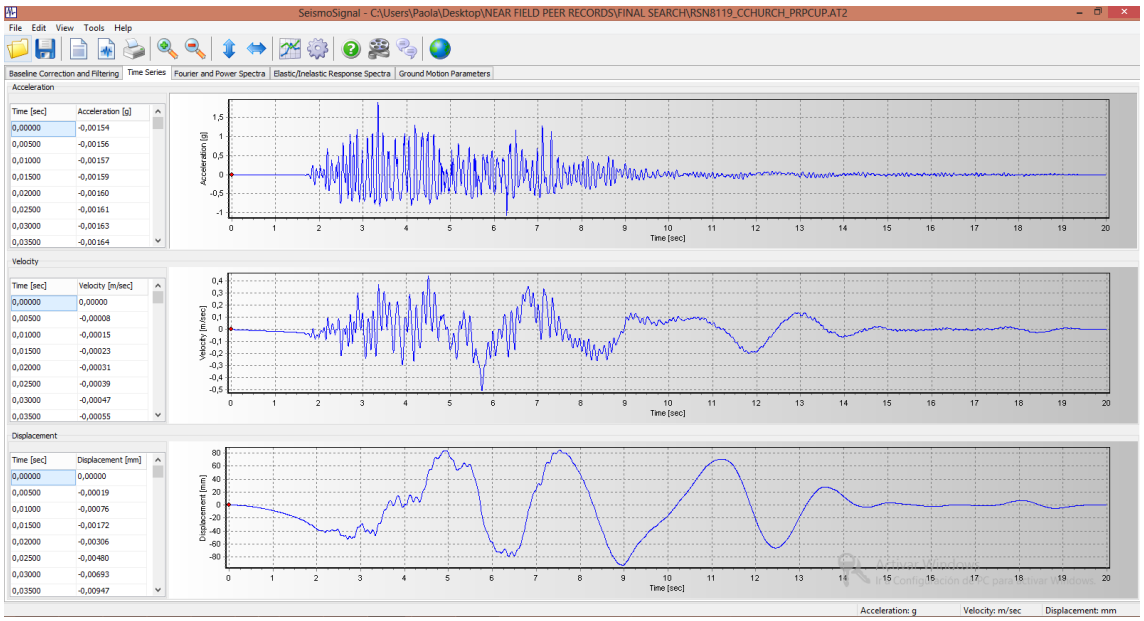

Figure 2.18 Seismosignal environment.

3. METHODOLOGY FRAMEWORK

As Méndez defined in 2007, a methodological framework should present in a clear and concise manner a delineation of each phase from the investigation. As a consequence, this chapter indicates the used methodological design with a description of how this investigation was conducted

3.1 Investigation Type.

According to Cesar Augusto Bernal classification, this is a sectional experimental investigation of a study case. It is experimental because a virtual model has been developed recreating (as close as possible to reality) each and every conditions of the study object -a Reinforced Concrete (RC) building- in order to analyze its behavior. Likewise it is sectional since this investigation was done with actual study case´s characteristics without taking into account any possible variation throughout time, for instance usage modification. As a consequence all the obtained data and respectively conclusions have been based in this time´s results.

3.2 Variables and dimensions.

In order to evaluate and classify the outcomes obtained from our representative model, 5 variables have been adopted. Their fundamental aim is to evaluate and confront the behavior of the building according to a classification. Nevertheless each variable has its individual role in pursuance of this aim. Moreover there is a dependence/independence relation among themselves, from which is important to be acknowledged.

The most significant variable is the reliability index which specifies how secure is the design parameter adopted (max displacement) in probabilistic terms. Then descending in order of importance the maximum displacement is found. This variable has been selected as the unique structural response of the building by pounding issues and practical matters (including more structural parameters would have meant a colossal increment of probabilistic analysis). Finally there are the "independent" earthquake parameters (Magnitude and Radio, PGA and Arias Intensity) which directly influence the ground motions sets obtained from databases, representing a variation the structural response. Although independent parameters have a reliance to geographic zone, soil conditions, and return period among other characteristic, they are independent from the other observed variables. In summary, table 3.1 lists the indicator, used techniques and the relation of each variable.

Variable	Dimensions	Technique	Independence from other parameters
Reliability index	Percent (%)	Sampling	Dependent
Max displacement	mm	Sampling	Dependent
Magnitude & Radio	dimensionless /km	PSHA	Independent
PGA	m/s2	PSHA	Independent
Arias Intensity	m/s	PSHA	Independent

Table 3.1 Variables and dimensions.

3.3 Sampling

From previous variables, 7 different sampling groups (for far-field analysis) have been formed and studied according to size and earthquake parameter. These sets are intended to determine the influence of a set dimension´s variation and a switch on parameters to select natural ground motion recordings. In addition an eighth group was created for near-field analysis. Although it is noteworthy to clarify that near-field results were not directly compared with the rest due to its singular properties.

Since same methodology has been applied, there are common characteristics among sets such as size. Per each earthquake parameter two size of samples seven (7) and thirty (30) were investigated. The first size (7) comes from Eurocode 8 minimum requirement in order to consider average response, (see at RL: Eurocode 8 procedure for references). The second set dimension (30) was determined from the Confidence Interval (CI) technique. Moreover a fifty (50) records called non scaled set was analyzed in order to verify stability results from 30-records sets. Theses sampling groups are summarized in Figure 3.1.

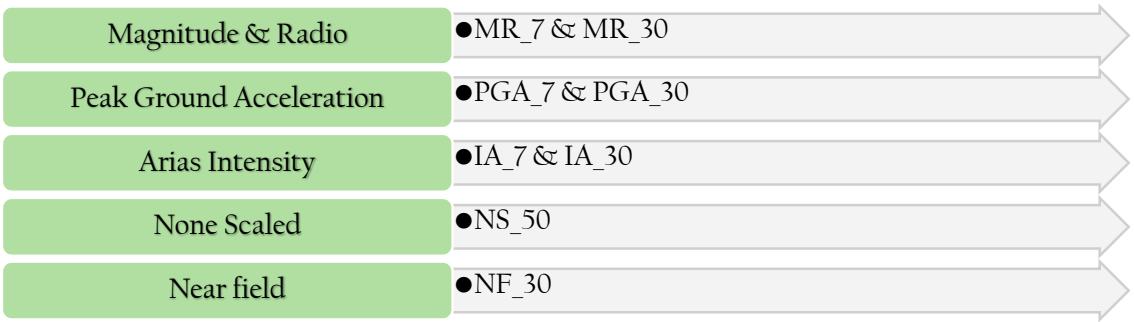

Figure 3.1. Sample sets by earthquake parameter.

Confidence Interval (CI) procedure employs a desired margin of error (MOE) and a level confidence to obtain a sample size (Yale University Department of Statistics, 1998). This procedure has some restrictions such as standard normal distribution anticipation and it is based on Simple Random Sample (SRS). In spite of these limitations it is assumed that this procedure is capable of providing a good approximation for our study case. Furthermore from Figure 3.2 it is observed in detail the confidence interval procedure.

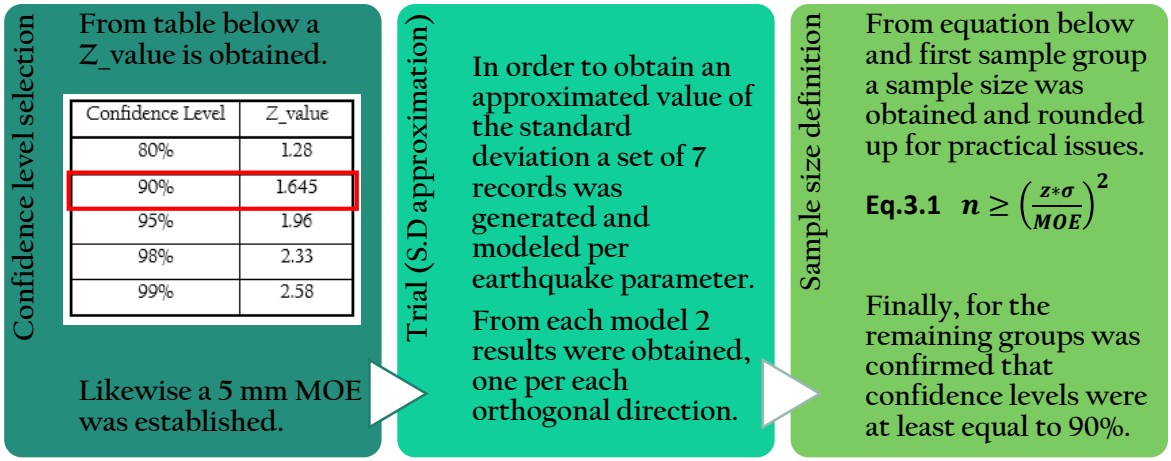

Figure 3.2 Confidence interval procedure.

In particular, CI procedure outcomes were used for set size dimensioning only and none conclusion were obtained in terms of maximum displacement behavior or earthquake parameter influence. From this small trial study 6 results came out and the confidence level calculated was always above 90% as summarized in table 3.1.

Replacing values for Eq.3.1

$$\left(\frac{1.645 * 15.7883}{5}\right)^2 = 26.98$$

$$26.98 \rightarrow 30$$

Sample Name	Trial (S.D)	Conf. Level (30)
MR_7_Xdirection	15.7883	91.4219
MR_7_Ydirection	9.0201	99.6100
PGA_7_Xdirection	15.6213	91.7163
PGA_7_Ydirection	11.1502	98.5044
IA_7_Xdirection	16.0097	91.0413
IA_7_Ydirection	11.6311	98.0982

Table 3.2 Confidence level results per earthquake parameter.

3.4 Step by Step methodology

In order to provide a better understanding of the complete process of this investigation a subdivision in 3 main blocks is performed. The first block involves strategies and procedures for the ground motion selection. The second block covers the steps for modeling of the study case. Finally third block includes: results handling, statistical analysis and the reliability index calculation. Figure 3.2 present the methodology outline per blocks.

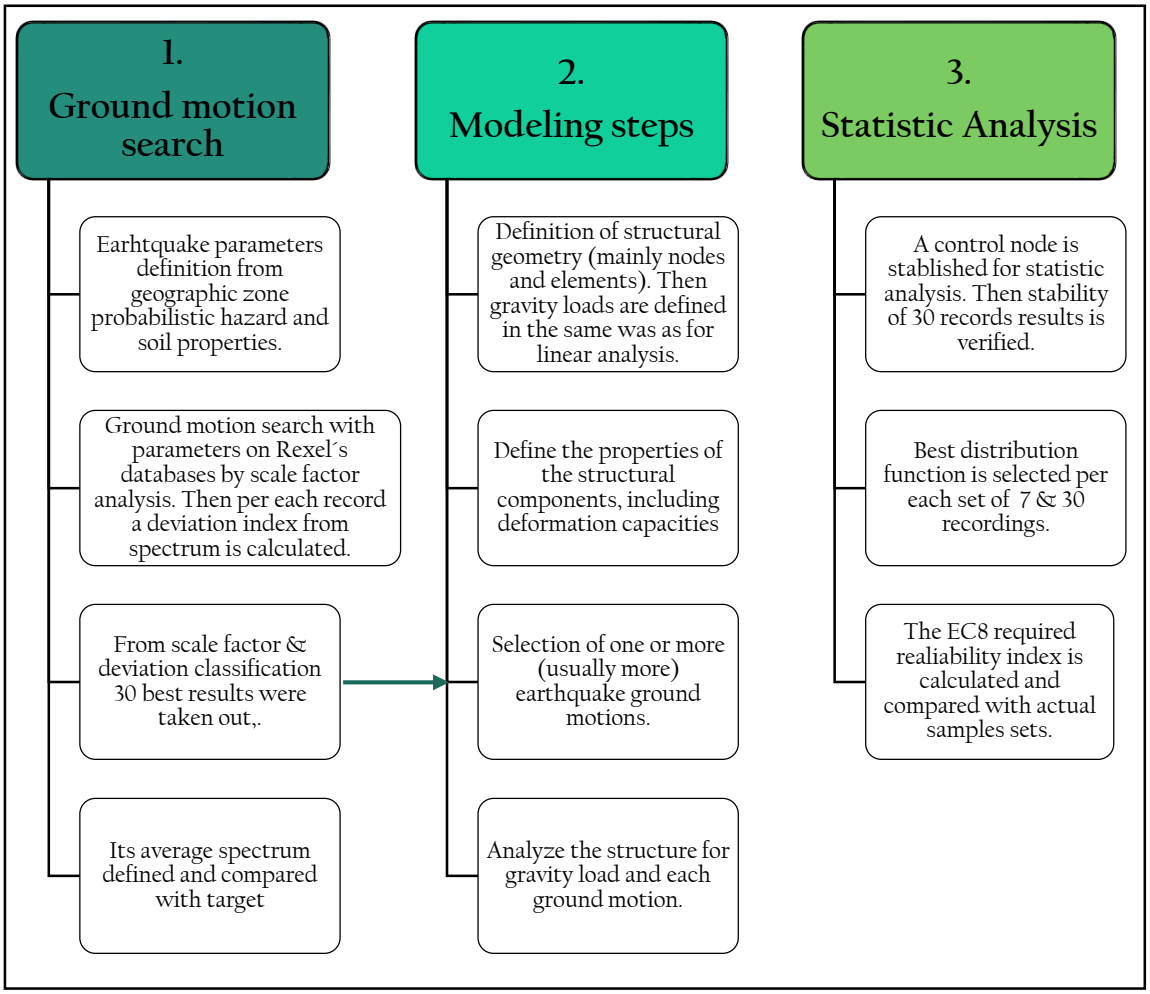

Figure 3.3 Methodology outline.

3.4.1 Ground motion search.

In order to define earthquake parameters characteristics of geographic zone and soil properties were analyzed. According to 2011 version of the parametric catalogue of Italian earthquakes, (Instituto Nazionale di Geologia e Vulcanologia) the expected Magnitude and Radio are 4.3-6.3 within a 35 radio or closer. Likewise same institution anticipates for Ferrara a PGA from 0.175-0.200 is with an exceedance probability of a 10% in 50 years. Respecting to Arias Intensity there is not any direct information. Hence 15 records were taken with previous parameters to determine Arias Intensity interval from 0.4-2 m/s.

Magnitude and Radio scale factor analysis.

This analysis aims to determine the "best interval" with the highest number of seismic events and closest Scale Factor (SF) to unity for ground motion selection. It was performed for European, Italian and Simbad databases using the software REXEL. From expected magnitude 4.3-6.3 (rounding up and down) magnitudes from 4 to 7 were studied in a 5 to 35 kilometer radio. The radio and magnitude intervals were analyzed using increments (illustrated in step 1 from figure 3.4). Finally 147 ranges were studied per database which are presented in Annex 1.

1.

Studied Intervals Radio & Magnitude For 7 radio categories (5-35)km	
Initial (M)	No. of intervals
4.0	6
4.5	5
5.0	4
5.5	3
6	2
6.5	1

Categories were defined from radio and magnitude increments.

2.

European database					
Range	M_min	M_max	Radio	SF	Events
0.5	4	4.5	5	3.8566	6
1	4	5	5	4.011	9
1.5	4	5.5	5	4.011	9
2	4	6	5	3.4697	11
2.5	4	6.5	5	3.4697	11
3	4	7	5	3.4697	11

(Fragment of 5km radio analysis.)

From each interval a scale factor and a number of events was determined.

3.

Scale Factor by magnitude range and radio.							
Range	5	10	15	20	25	30	35
0.5	1.20	0.48	0.54	0.71	0.77	0.84	0.84
1	1.20	0.84	1.16	1.38	1.42	1.88	1.87
1.5	1.20	1.00	1.36	1.82	1.93	2.40	2.46
2	1.44	1.14	2.10	2.19	3.01	3.41	3.44
2.5	1.44	1.14	1.91	2.19	3.01	3.41	3.44
3	1.44	1.14	1.92	2.19	3.01	3.41	3.44

From previous results best outcomes were introduced in a summary table.

4.

Seismic events by magnitude range and radio.							
Range	5	10	15	20	25	30	35
0.5	2	5	5	1	3	5	5
1	3	5	11	1	3	5	5
1.5	3	5	11	16	22	26	26
2	3	12	24	40	48	56	56
2.5	5	16	30	48	58	67	67
3	5	20	34	54	66	77	77

Same procedure was conducted for seismic events.

5.

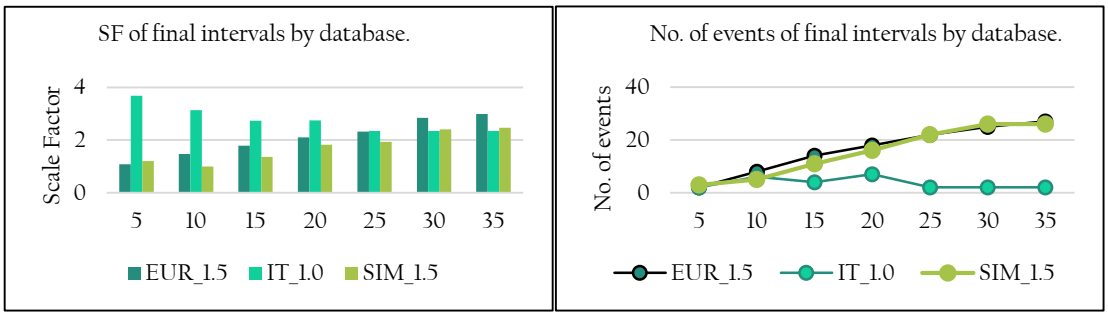

Finally results were plotted and it was confirmed a comparison among databases.

Figure 3.4 Magnitude and Radio scale factor analysis procedure.

PGA and Arias Intensity scale factor analysis.

Likewise previous analysis herein it is intended to determine the "best interval" per parameter with mentioned databases and software. This analysis was performed taking into account nominal life, limit state and functional use. Therefore considered intervals were as follows: (0.15-0.60) m/s^2 for Peak Ground Acceleration -PGA and (0.5-2.5) m/s for Arias Intensity (IA). Intervals increments were 0.05 m/s^2 and 0.5m/s, respectively. As a consequence 165 intervals were analyzed for PGA while 108 were studied for Arias Intensity. A summary of the analysis process is depicted in Figure 3.5. Complete results are in annex 1.

1

Studied intervals (PGA)	
Initial (PGA)	No. of intervals
0.15	9
0.20	8
0.25	7
0.30	6
0.35	5
0.40	4
0.45	3
0.50	2
0.55	1
Example_2 = 0.50-0.55 & 0.50-0.60	

Definition of categories from PGA increments.

Studied Intervals (IA)	
Initial (IA)	No. of Intervals
0.5	8
0.75	7
1	6
1.25	5
1.5	4
1.75	31
2	2
2.25	1
Example_ 3 = 1.75-2.00, 1.75-2.25, 1.75-2.50	

Definition of categories from Arias Intensity (IA) increments.

2

European Database				
Range	Min_PGA	Max_PGA	SF	Events
0.05	0.15	0.2	1.5268	4
0.10	0.15	0.25	1.368	21
0.15	0.15	0.3	1.2925	10
0.20	0.15	0.35	1.2157	12
0.25	0.15	0.4	1.1737	13
0.30	0.15	0.45	1.1151	14

(Fragment of PGA search.)
SF and events were obtain per intervals.

Simbad Database				
Range	Min_IA	Max_IA	SF	Events
0.25	1.00	1.25	0.8800	2
0.50	1.00	1.5	0.8590	3
0.75	1.00	1.75	0.7966	5
1.00	1.00	2	0.7253	7
1.25	1.00	2.25	0.7763	8
1.50	1.00	2.5	0.7763	8

(Fragment of IA search.)
SF and events were obtain per intervals.

3

Range	SF	Events
0.05	0.99743	2
0.1	1.0876	12
0.15	1.0047	18
0.2	0.97743	21
0.25	0.95258	23
0.3	0.91614	24
0.35	0.84939	26
0.4	1.0606	40

Best PGA results were summarized.

Range	SF	Events
0.25	1.1681	5
0.5	1.0073	10
0.75	0.98504	13
1	1.0697	22
1.25	1.0391	23
1.5	0.99055	25
1.75	0.99003	26
2	0.99003	26

Best IA results were summarized.

4

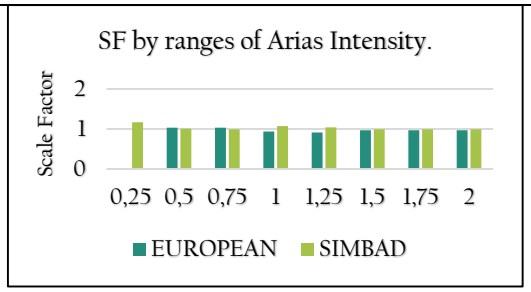

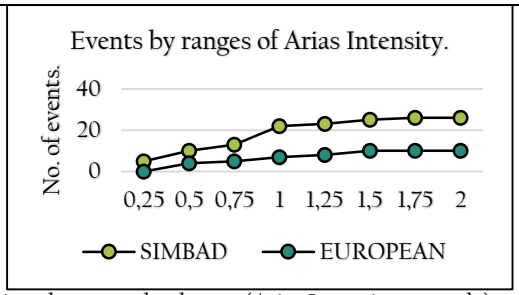

Finally results are plotted and it was performed a comparison between databases. (Arias Intensity example)

Figure 3.5 PGA and Arias Intensity scale factor procedure.

REXEL.

A program called REXEL (see RL: Rexel for more references) was used to complete this phase. REXEL is divided on 4 parts with sequencing dependencies, shown in Figure 3.6. Hence each of them on should be completed in order to perform the ground motion search. These stages are detailed below.

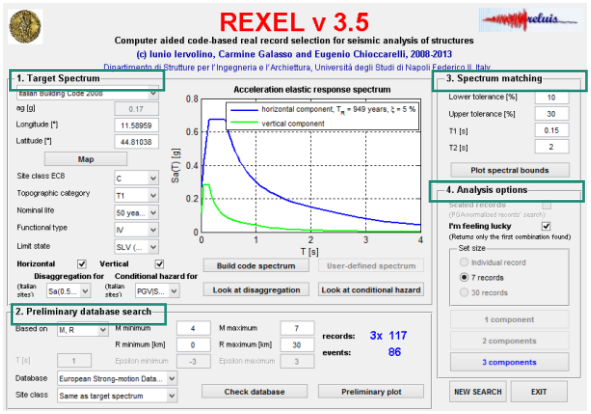

Figure 3.6 Environment of REXEL

1st Rexel stage: Target spectrum

In this part all the parameters are specified in order to create the objective spectrum. First the seismic code must be specified so that required parameters are subsequently supported. This spectrum will be the reference in order to match. Table 3.3 depicts the requirements detailed.

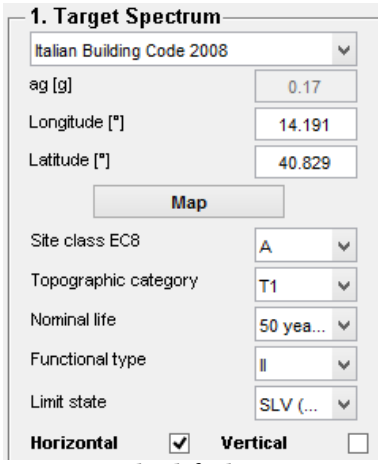

Rexel´s default view.

Code name	Italian08, EC8 type I/II, ASCE, user-defined
ag[g]	Acceleration *Not needed for Italy
Longitude	It is only required when acceleration is not specified.
Latitude	
Site class	From A to E (as EC 8 & NTC08)
Topographic Category	From T1-T4 (according to Italian code NTC08)
Nominal life	Eurocode 8 / Italian code
Limit state	Eurocode 8 / Italian code
Hor. / Vert.	This is specified which spectrum are required.

Table 3.3 Target spectrum stage.

Moreover there is a disaggregation and conditional hazard evaluation for Italian sites. This section has the aim to identify earthquakes having the largest contribution to the hazard for the spectral ordinates of interest (Iervolino, Galasso, & Cosenza, 2010). For disaggregation among the options are spectral acceleration segregation per periods of 0.5, 1 and 1.5 seconds for PGA, Magnitude and Radio or just the latter two. Likewise for conditional hazard are for Peak Ground Velocity, Np and ID values for a period 0.5 seconds only.

2nd Rexel stage: Preliminary database search

In this part the earthquake parameters are specified. First the parameter(s) in which the search is based and is selected. For spatial modeling (3 components) among the options are: Magnitude and Radio, Magnitude, Radio and Epsilon. In addition for horizontal components only the parameters available are: PGA (g), PGV, ID, IA, and Np. Finally following parameters are established: target interval, name of database and site class (by default is according to target spectrum).

It is noteworthy to explain check database and preliminary plot buttons, shown in Figure 3.7 First one provides the number of records and events founded with previous specifications. From these results you can decide to widen or restrict your intervals. Based on experience a good amount of records is between 30 and 50 records. On the other hand preliminary plot button depicts a graphic with all feasible records spectrum in contrast to target spectrum; this permits to observe the general behavior of the outcomes. In addition a general scale factor (because takes into account all records at the same time) is displayed with the graphic.

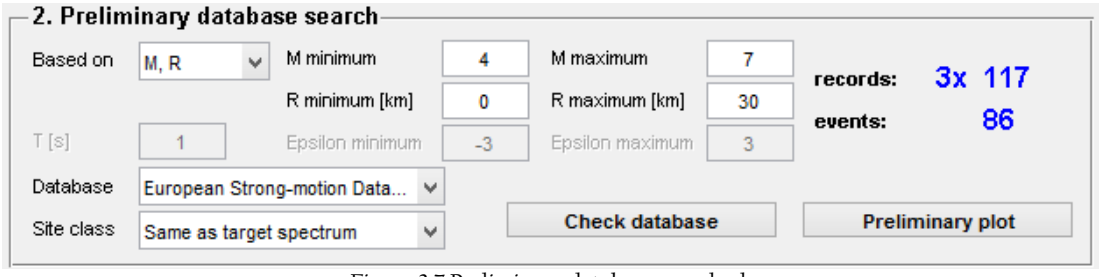

Figure 3.7 Preliminary database search phase.

3rd Rexel stage: Spectrum matching

This phase regards to the maximum tolerances of records in relation to the target spectrum. These margins are specified in percentage for lower and upper limits, while left and right boundaries are delimited by periods in seconds. Moreover there is the possibility of plotting previous spectral bounds in order to verify. Figure 3.8 presents an example of spectral boundaries plotting.

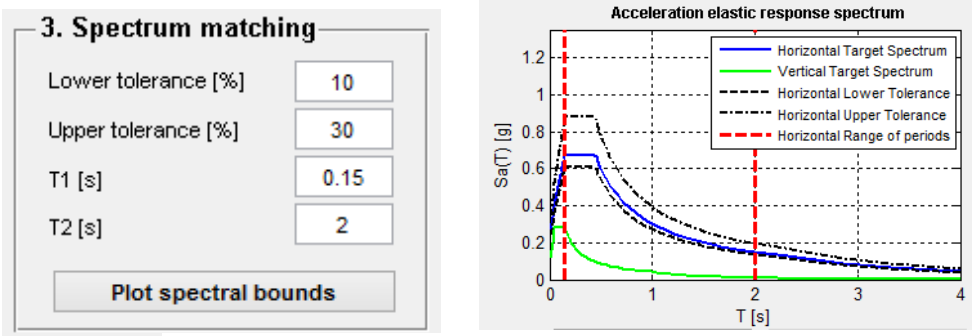

Figure 3.8 Spectrum matching and spectral boundaries

4th Rexel stage: Analysis options.

The parameters of set and combination are selected in this section. Among the options are: the specification of amount of combinations, set size (1, 7 or 30) and how many components from the record are needed. In addition just for Magnitude, Radio and Epsilon analysis, there is the possibility to select scaled records. The search starts when the amount of components button is pressed. Finally when the button of new search, works for restart, it returns default values and a new search can be done. Figure 3.9 displays the analysis options environment.

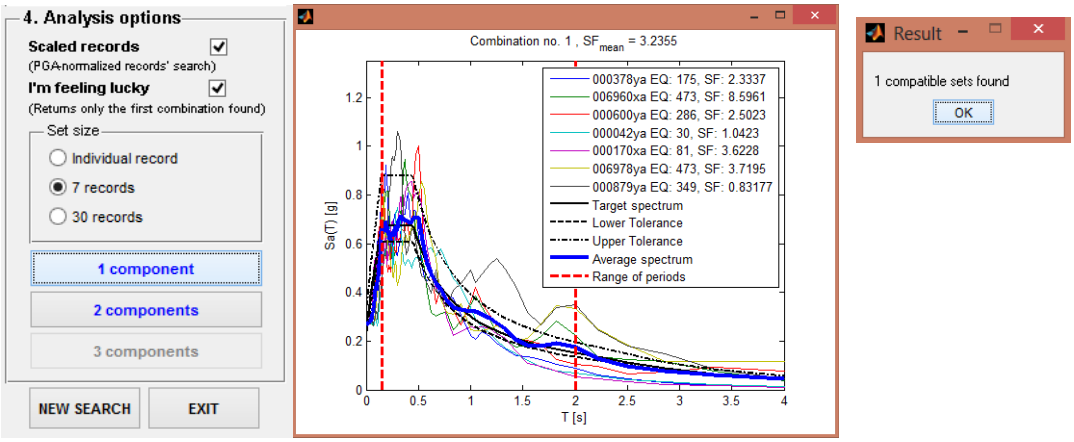

Figure 3.9 Analysis option stage

Final selection of records.

A deviation classification was performed to acquire the best records. Although REXEL returns deviation values for each record a complimentary analysis in excel was required. Excel analysis was done providing that deviation factor just express how far are the values from spectrum, but it does not describe if the records is has exceeding or defect from target spectrum. In consequence every record was plotted in excel in order to categorize them and select the 30 records that provide the average spectrum with the minor deviation from target spectrum. Finally each average record was plotted against target, shown in graphic 3.1.

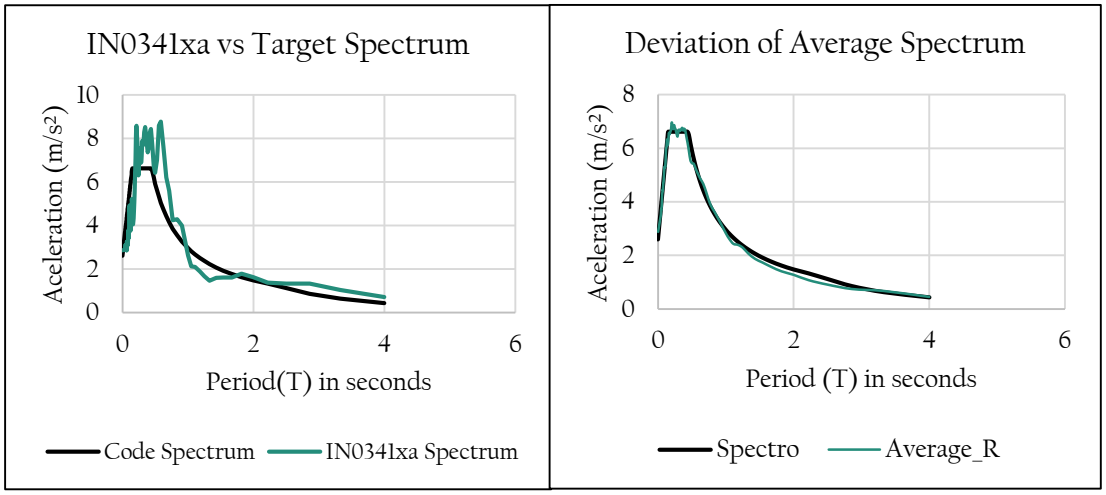

Graphic 3.1 Deviation Analysis in EXCEL

3.4.2 Modeling steps.

Following the methodology outline a virtual model was created using Midas Gen software. Some characteristics were consulted from (Bertaccini, 2014; Pizarulli, 2015) previous investigations. For further information these characteristics mainly structural geometry (including steel bracings and steel hysterical dampers) and gravity loads are defined in the following chapter ¨Building E¨ Case description. Regardless a brief description of the modeling process is presented.

Definition of structural geometry and gravity loads. Building E model (see figure 3.10) has been defined with as a 3D structure type. Since Building E regularity properties allows to ignore the earthquake's vertical component, its self-weight was adapted into X and Y directions only. According to previous research this model can be considered fixed hence every degree of freedom has been restrained at base. Moreover as part of (Pizarulli, 2015) proposal HEA 275 steel bracings and buckling restraining axial dampers (BRAD) with 56/30-b denomination were added. Regarding to gravity loads it was divided into permanent and variable loads.

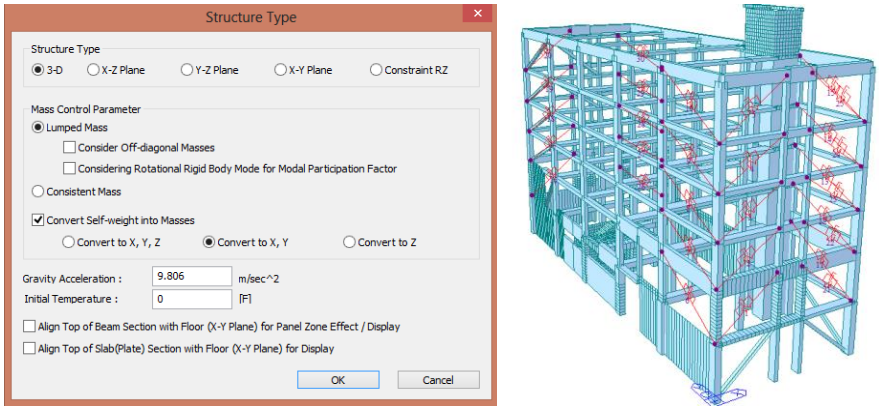

Figure 3.10 Structure type definition (left) and Building E model (right).

Definition of structural properties including deformation capacities. "Building E" 6 floors have been modeled with (25 kN/m^3) reinforced concrete. Furthermore for deformation capacity 4 inelastic hinges (column, beam, bracing and technical floor) were designated with lumped mass control parameter, Takeda properties and initial stiffness of 6EI/L. Finally BRAD 50/30-b system was defined with provided information specified by the manufacturer, shown figure 3.11

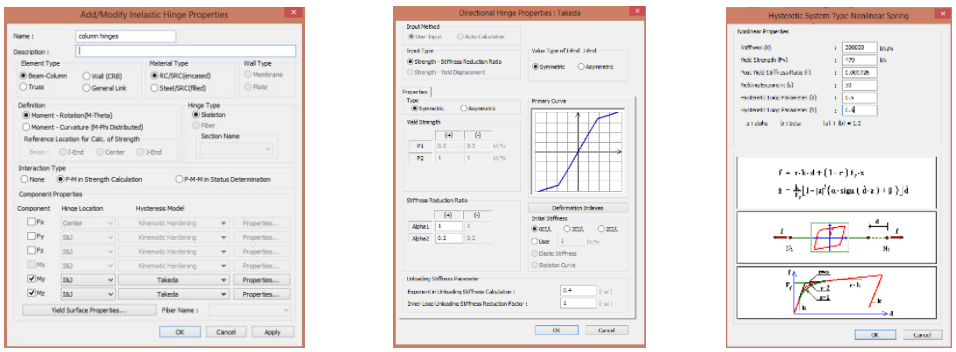

Figure 3.11 Inelastic hinge properties

Selection of one (or more) ground motions. This phase was realized on previous block. Therefore herein figure 3.12 is described how these ground motion records were defined in Building E virtual model. A load time history case was generated per each ground motion records. Among the specifications are nonlinear direct integration with transient history type and no consideration of P-Δ effect which means a small displacements assumption with the absence of geometric nonlinearity. Time increment were always small (0.005/0.001) seconds in order to get more accurate results. In relation to sequential loading it was applied after gravity loads, assuming that all structural elements are loaded during the earthquake.

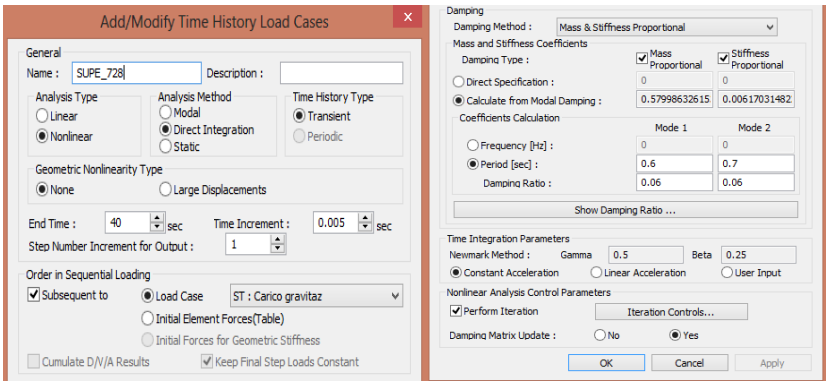

Figure 3.12 Time history Load Cases specifications.

Mass & stiffness proportionality was selected as damping method allowing matrix update. It was calculated from modal damping by period and damping ratio specification. These period and damping ratio were calculated from a previous eigenvalue modal analysis with target spectrum and a pushover analysis, respectively. Regarding to time integration parameter as direct integration was specified, a constant acceleration is considered with gamma 0.5 and beta 0.25 (see figure 3.12).

For integration control depicted in figure 3.13, the convergence failure was permitted for a displacement norm criteria. Likewise maximum step size of 0.00005, 10 times as maximum iteration and a tolerance of 1e-008 were stablished. Finally for boundary nonlinearity for Runge Kutta method the Fehlberg method (stepsize sub-division for non-convergence control) was selected.

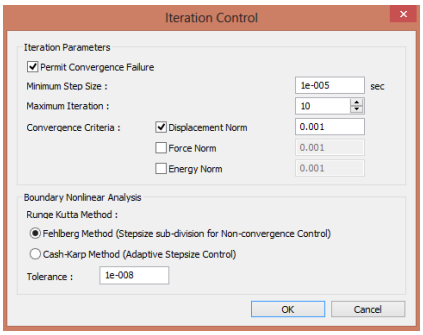

Figure 3.13 Iteration control view.

3.4.3 Statistical Analysis

"Building E" principal modes were verified throughout **a node controlling** for 7 ground motions on X and Y directions. This involves the displacement node observation in the "gap zone" (see building case description for further reference) along the whole building's height shown in figure 3.14. Every control established the first mode as principal as illustrated this was since added bracing and dampers provided a significant stiffness increment. Consequently in the rest of analysis only top roof nodes were evaluated to find maximum displacement reducing considerably analysis time.

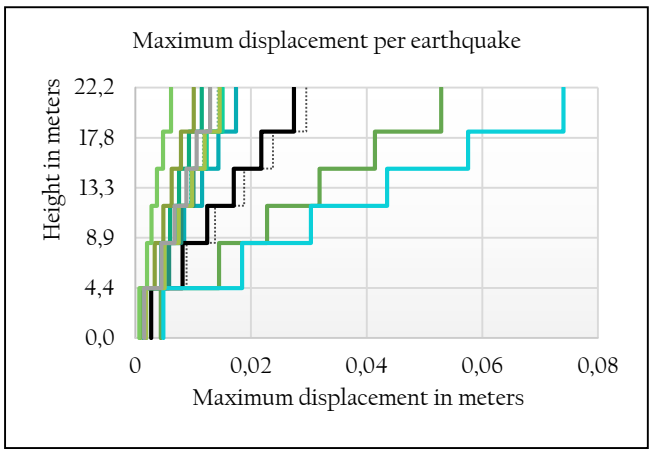

Graphic 3.2 Maximum displacement verification.

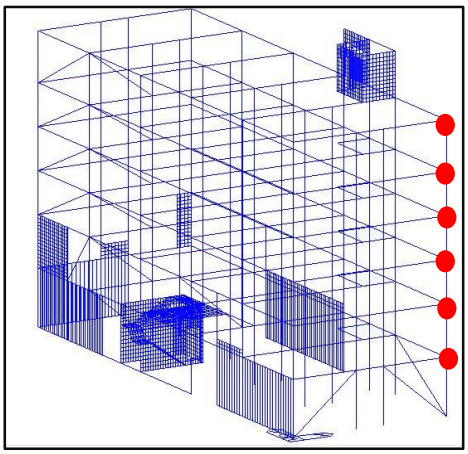

Figure 3.14 Studied point's example.

Results stability verification. This verification aims to determine whether average values change significantly after 30 records or not. For this procedure maximum displacement average is observed while set's size is increased from 7 records to 30 records, then from 7 to 50 records and both results are compared. Since both earthquake directions were considered, 30-records results augment to 60 and 50-records results augment to 100. Basic steps are detailed as follows:

i. First only seven maximum displacement are considered and 1st average is calculated.
ii. Second a single maximum displacement is added to previous set and 2nd average is obtained.
iii. Then previous step is repeated until 60 displacements have been taken into account.
iv. Steps i to iii are repeated till 100 displacements have been taken into account.

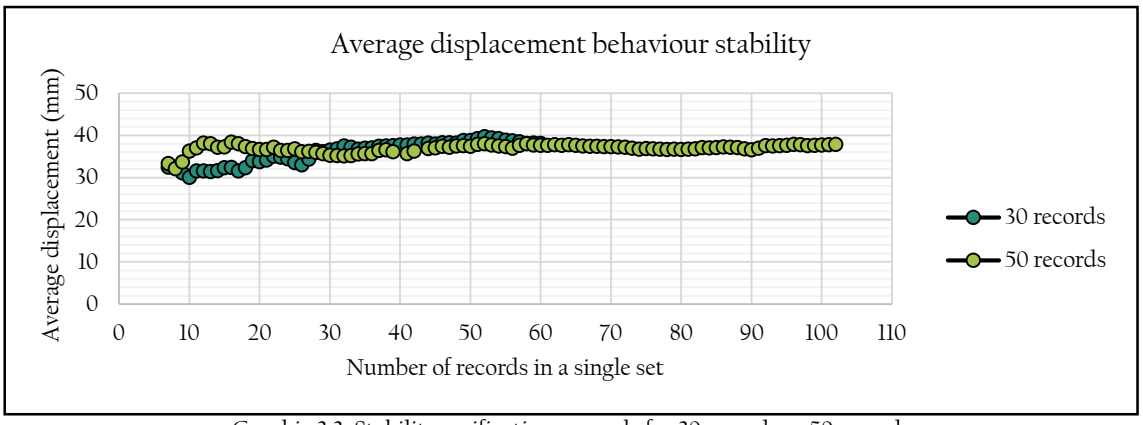

Graphic 3.3 Stability verification example for 30 records vs 50 records.

Distribution function fitting. From previous phase 6 density distributions were obtained because two orthogonal directions (X, Y) were observed for three different earthquake parameters (MR, PGA and IA). Therefore the distribution function fitting procedure was performed using Matlab software after stability was confirmed per each set. In this phase each density function was "fitted" to 17 different distribution functions using dfittool function from statistical MATLAB tools. Figure 3.15 presents an example of Normal distribution (Nigam, 1983) fitting procedure.

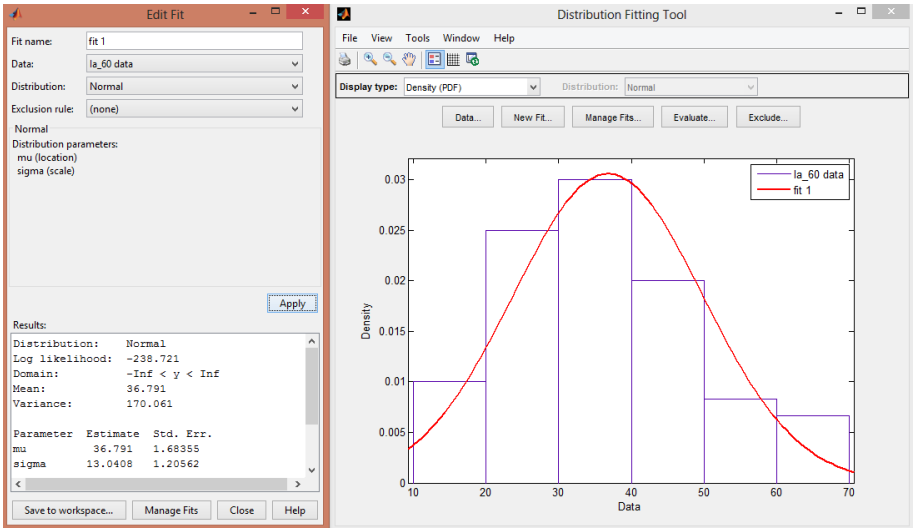

Figure 3.15 Distribution fitting example.

Chi-squared goodness of test. This phase was also performed using Matlab. Since basic conditions were achieved an evaluation throughout chi test was performed, shown in figure 3.16. This tests returns the probability of observing a test statistic as extreme as or more extreme than the observed value under the hypothesis that data in a vector comes from the "assumed" distribution. This procedure aims to determine the distribution that best fits each sample set by the organization of the returned probabilities (from major to minor) according to its statistical characteristics.

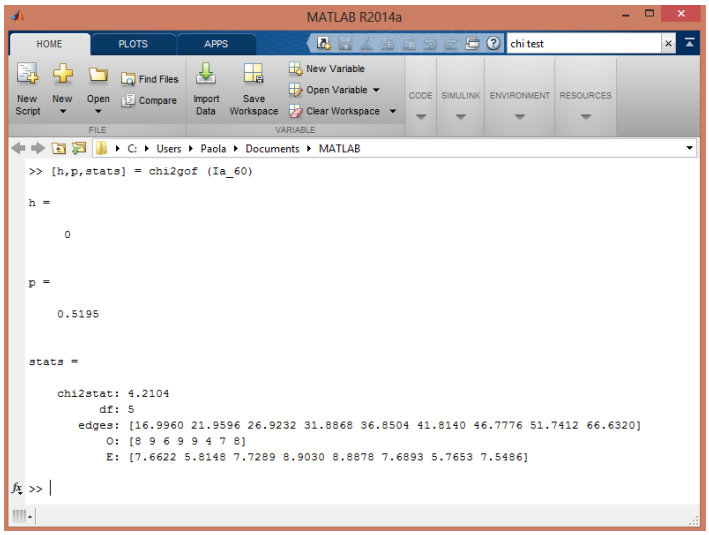

Figure 3.16 Chi squared test results of a normal distribution.

Verification of reliability index value. According to EN-1990, each project has a reliability index associated according to its cost of safety and failure consequences, shown in graphic 3.4. The target reliability selected for this case study las 3.7. This is because "Building E" is an existent structure with large consequences of failure and large safety costs due to its current function as municipal police offices. Nevertheless this procedure was performed using the failure probability 10^{-4}, which is the analogous from our target reliability, shown in table 3.4.

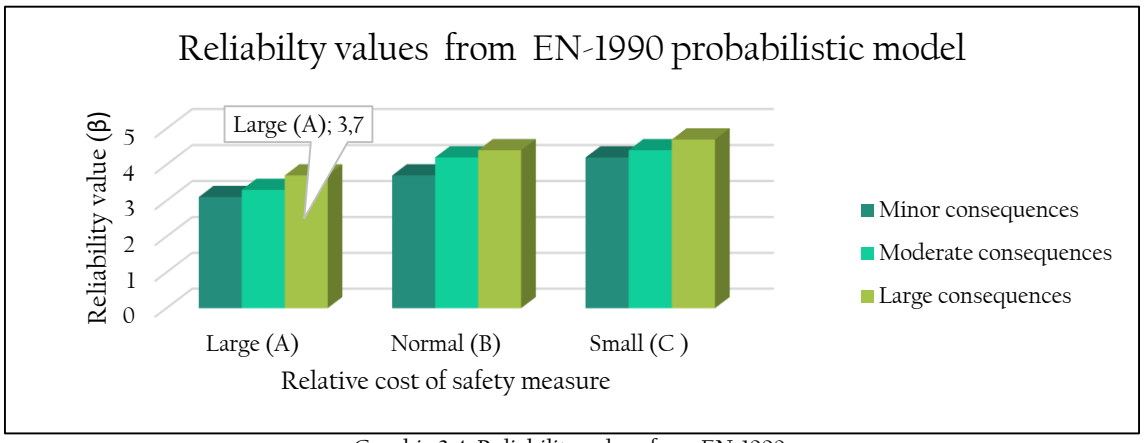

Graphic 3.4 Reliability values from EN-1990.

	Minor consequences of failure.	Moderate consequences of failure.	Large consequences of failure.
Large (A)	$\beta = 3.1$ ($p_f = 10^{-3}$)	$\beta = 3.3$ ($p_f = 5\,10^{-4}$)	$\beta = 3.7$ ($p_f = 10^{-4}$)
Normal (B)	$\beta = 3.7$ ($p_f = 10^{-4}$)	$\beta = 4.2$ ($p_f = 10^{-5}$)	$\beta = 4.4$ ($p_f = 5\,10^{-6}$)
Small (C)	$\beta = 4.2$ ($p_f = 10^{-5}$)	$\beta = 4.4$ ($p_f = 10^{-3}$)	$\beta = 4.7$ ($p_f = 10^{-6}$)

Table 3.4 Reliability and it analogous failure rates.

Most civil engineering failure probabilities are defined by the likelihood of being equal or smaller than a limit value (see left side of figure 3.17). However the failure probability of "building E" is referred to the possibility of finding a superior displacement than limit value. Hence this failure prediction could be defined as presented on the right side of figure 3.17, where Building E fails when it is obtained a greater displacement than limit from the analysis.

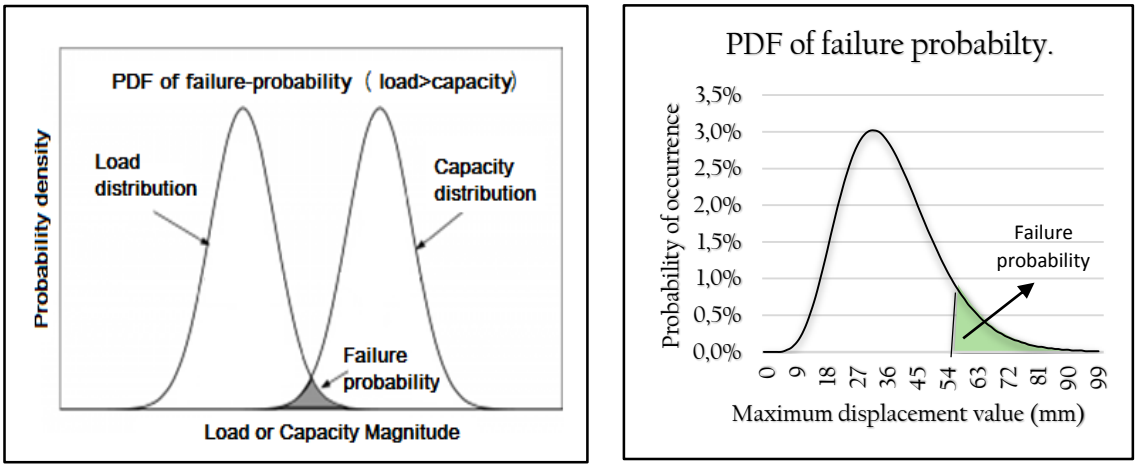

Figure 3.17 Failure probability analysis

4. "BUILDING E" CASE STUDY

This chapter presents a summarized description of the case study. The information detailed below was obtained from research and previous documentations. However most of it was acquired from a vulnerability assessment realized in 2014 and a seismic retrofit proposal in 2015.

4.1 General Structure Description

4.1.1 Location and usage

"Building E" designed and built in the 70s, it is located in Ferrara´s community at Via Bologna No. 534 is (see figure 4.1). According to WGS84 system its geographic location is: latitude: 44° 48´ 36.98" N, longitude: 11° 35' 23.25" E and altitude: 11 m. s. l.m -height level from the sea.

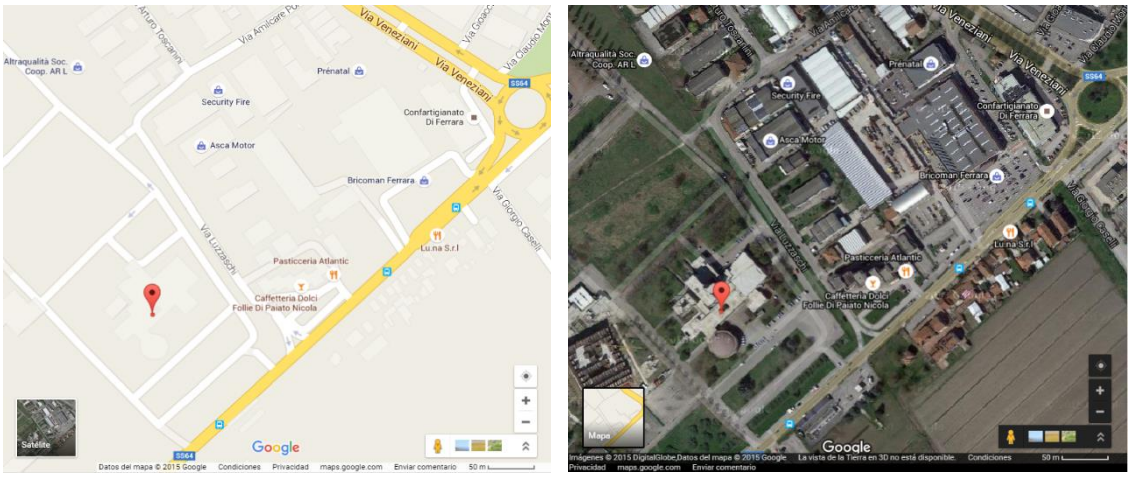

Figure 4.1 "Building E" geographical location courtesy of Google maps 2015.

"Building E" is property of the Emilia-Romagna Region. It belongs to "Ex Centro Operativo Ortofrutticolo" (Ex-C.O.O.) complex, which is constituted by 8 principal buildings communicated among themselves, but structurally speaking independent thanks to structural joints presence. At present time Building E works as offices and caretaker building presented in figure 4.2 along the complex description. Nonetheless in anticipation to intended use change which will modify its classification as "strategical building" a vulnerability study was developed (Bertaccini, 2014).

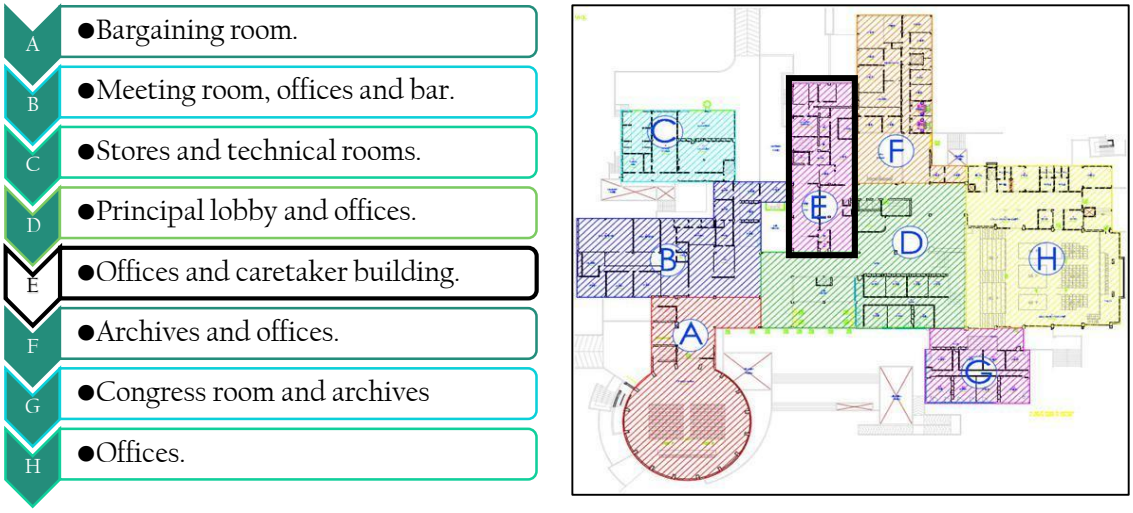

Figure 4.2 Description of "Ex-COO complex" by building function.

Figure 4.3 depict the usage variation of building E along its height. The basement has an air conditioning and an archive deposit. Ground floor has Municipal Police offices, ARPA's former offices and caretaker place. Likewise the first floor houses CSO offices. Finally on the second, third and fourth are located the rest of Municipal Police offices.

Figure 4.3 "Building E" function distribution per floor; from Bertaccini evaluation.

The flat roof is available only for maintaining activities. Likewise the roof has 2 technical compartments accessible only from itself. Inside building E there is a staircase that only connects the basement with the mezzanine floor and a technical room, being the latter which extends over the entire height of construction. First floor access is possible via an external staircase located on the South-West (former caretaker housing), or from inside F and D buildings.

4.1.2 Geometrical description

Building E is characterized by the following dimensions in plan and height: 36.75 m x 13.00 m, 21 meters height from ground level and 25.43 meters total height. It has 477.75 m^2 of superficial area per level. It also counts with 4 floors above ground a mezzanine floor, a basement and a flat roof.

As presented in figure 4.4, there are 6 frames in parallel 3 spans each, warps along the short side of the building (X direction) and connected from the floors and two perimeter beams (Y direction). The central columns are rectangular or square (they were tapered), while the perimeter columns are rather complex. Internal beams have a rectangular section. However there is an exception: the basement floor beams of the perimeter which have more complex shapes.

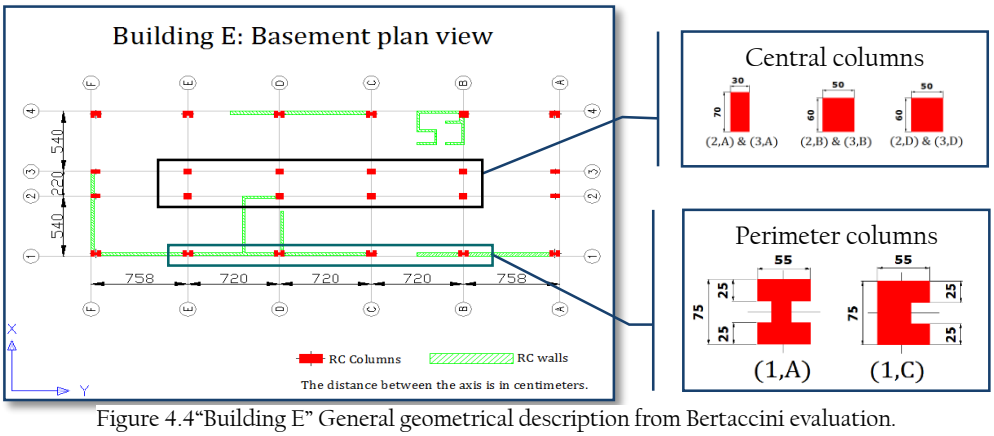

Figure 4.4"Building E" General geometrical description from Bertaccini evaluation.

Building E has a perfectly rectangular plant that is repeated for all 7 floors. Structural vertical support is constituted by separators and pillars of reinforced concrete (RC) which extend along the whole construction's height. In the basement, there are RC walls against land that terminate at the ceiling of the first floor.

All floor are "latero-cemento" type "TL 60", the beam's interspacing is 60 centimeters along all floors. Table No. 4.1 shows interstory heights and slab thickness of the whole building per level. As shown in the table the basement slab is the only one that differ from the rest.

Level Name	Interstory height (m)	Height (m)	Thickness (m)
Basement	4.17	Q+2.02	h= 0.24+0.04
Ground floor	4.00	Q+6.02	h= 0.20+0.06
First floor	3.30	Q+9.32	h= 0.20+0.06
Second floor	3.30	Q+12.62	h= 0.20+0.06
Third floor	3.30	Q+15.92	h= 0.20+0.06
Fourth floor	3.88	Q+19.80	h= 0.20+0.06

Table 4.1 "Building E" Interstory height and slab thickness.

4.1.3 Structural material's description

In general terms "Building E" is a framed reinforced concrete structure with latero-cemento floors and masonry walls. It has a technical compartment made with RC walls which it extends for the entire height of manufactured. From the standpoint of structural constitutes a stiffening core for the whole structure. Additionally the flat roof is paved with only waterproofing.

In order to know in detail all the components and materials of the building two experimental campaigns were established. The first one consisted on some thickness and materials type verifications implemented in situ by skilled workers from a hired firm. While the second one consisted in laboratory/ in situ tests aiming to confirm the material quality description; Figure 4.5 presents an example of a destructive test in a column.

Figure 4.6 Sample extraction in a column for a destructive test from Bertaccini evaluation.

The principals types of experimentations performed in the first campaign were: perforation of the floors, in order to directly measure the layer's thickness of the structural components and architectural package; drilling of plasterboard or brick walls, to verify the type, thickness and the possible presence of gaps and removal of the structural joints cover plates, for the assessment of thickness. From this operation the latero-cemento of the floors was confirmed along with its thickness shown in table 1. Moreover the type of brick was confirmed and no gaps were found.

On the other hand the second campaign, intended to describe the quality of the materials, was formed by: Semi-destructive testing (steel bar and cylindrical concrete extractions) and Non-destructive testing (Rebound hammer, ultrasonic test, SONREB, endoscopy and steel bar scanning), shown in figure 4.6.

Figure 4.7 Rebound hammer testing (left) and ultrasound testing (right); from Bertaccini evaluation.

According to the 2nd campaign, the concrete compression resistances were: 22.4 MPa (cylinder), 27.44 MPa (cubic), 17.4 MPa (cylinder) and 28018 MPa (cylinder) for medium, medium, characteristic and elastic modulus, respectively. Conversely for steel bars samples (shown in figure 4.7) the traction resistance obtained was 440 MPa and 627 MPa for elastic yielding and ultimate load, respectively.

Figure 4.8 Steel bars samples for testing; from Bertaccini evaluation.

4.1.4 Non-Structural Materials

In "Building E" all floors and ceilings are present almost everywhere, with the exception of the basement. All pillars are covered with plasterboard. Likewise its 4 facades are almost entirely covered by aluminum panels with solar shielding function, while the remaining parts and columns are in reinforced concrete at sight, see figure 4.8.

Figure 4.9 View of aluminum panels' facades; from Bertaccini evaluation.

4.1.5 Building E deterioration state

Building E has not been cracked or degradation resulting in a lack of load-bearing capacity of the structures to vertical loads. However some deterioration were found such as steel exposition, see figure 4.9.

Figure 4.10 Steel exposition on technical floor; from Bertaccini evaluation.

Figure 4.10 presents a summary all the found incidents per element. It is important to note that most of the degradation situations like infiltration of water, exposure to a lack of armor and / or expulsion of concrete cover resulting oxidation, and concrete segregation were encountered in the mezzanine. Despite of the conditions presented below in general terms Building E condition is considered satisfactory for static loads.

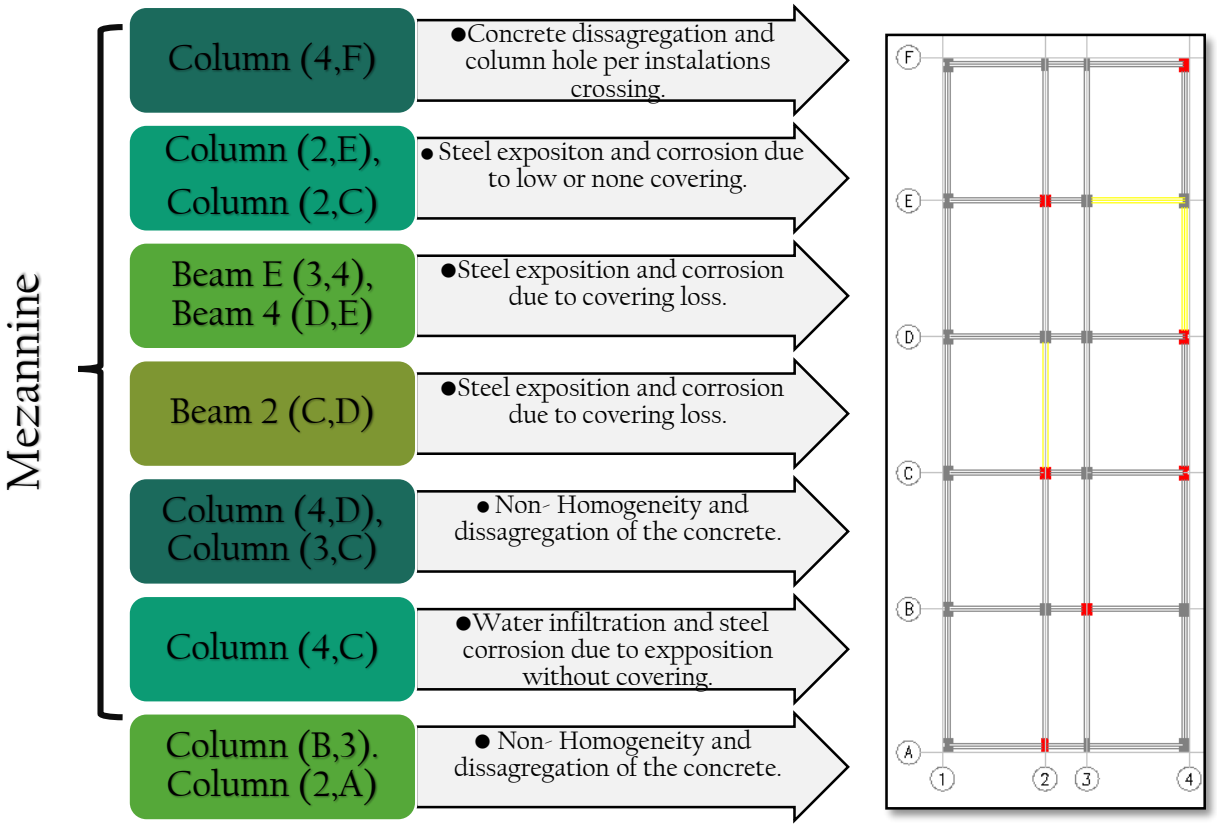

Figure 4.11 Degradation Situation Building E per elements.

4.2 Structure model analysis proceeding and results.

4.2.1 Static load analysis.

Before proceeding to determine gravity loads, a subdivision into homogeny zones (S_1, S_2... S_{17}) was made by distinguishing same type of floors. Then a load analysis was made taking into account material properties geometric dimensions of elements and present installation tubes. On the other hand for variable loads was assigned the NTC-08 recommended value according to its final usage. (Bertaccini, 2014). Table no. 4.2 presents gravitational and variable loads per zones and height.

Height (m)	Floor	G_1 (Structural W.)	G_2 (Non- structural W.)	G (Total weight)	Q_k (Variable load)
+2.02	S_1	3.40	4.01	7.41	5.00
+2.02	S_2	3.40	3.52	6.92	5.00
+2.02	S_3	3.40	4.01	7.41	2.00
+2.02	S_4	3.40	3.52	6.92	2.00
+2.02	S_5	3.40	3.82	7.22	2.00
+2.02	S_6	3.40	2.55	5.95	2.00
+2.02	S_7	3.40	3.58	6.98	2.00
+2.02	S_8	3.40	3.42	6.82	2.00
+2.02	S_9	3.40	4.38	7.78	2.00
+6.02,+9.32, +12.62,+15.92	S_{10}	3.35	2.13	5.48	2.00
+6.02	S_{11}	3.35	4.50	7.85	2.00
+6.02,+9.32,+12.62,+15.92	S_{12}	3.35	2.87	6.22	2.00
+6.02,+9.32,+12.62,+15.92	S_{13}	3.35	2.87	6.22	2.00
+6.02,+9.32,+12.62,+15.92	S_{14}	3.35	2.03	5.38	2.00
+9.32,+12.62,+15.92	S_{15}	3.35	4.40	7.75	2.00
+19.80	S_{16}	2.85	1.27	4.12	0.80
+23.30	S_{17}	2.85	1.10	3.95	0.80

Table 4.2 Building E Static loads summary per zones and height.

On the other hand some beam from perimeter were connected to the solar shielding for climate regulation. Therefore a valuation of solar shielding transferred load to the structural elements was made. Consequently its material and geometry were respectively identified as aluminum elements with a rhomboidal section (30x5) cm and a 1mm thickness in order to get the weight. Finally this weight was expressed in weight per length for practical appliance.

4.2.2 Seismic load analysis

Earthquake stroke is a natural phenomenon characterized by several parameters and conditions. For that reason it is considered a random event which is almost impossible to estimate with the same static loads accuracy. As a consequence of this situation seismic loads are estimated in probabilistic terms, taking into account geological conditions, structure usage and analysis type (Static, Dynamic, Linear or Non-Linear). Most of those parameters are defined in National and European Standard Codes in terms of previous studies and analysis.

Figure 4.11 is presented a brief summary of the seismic load estimation procedure made by (Bertaccini, 2014) for its seismic vulnerability study. This method starts with usage dependent parameters selection which are described and categorized according to the final intended use of the structure. Then from experimental results of the geological measured characterization soil type and topography category are specified. Hence depending on the limit state verification the probabilistic terms are defined and the periods and pseudo acceleration values for the design response spectra are obtained.

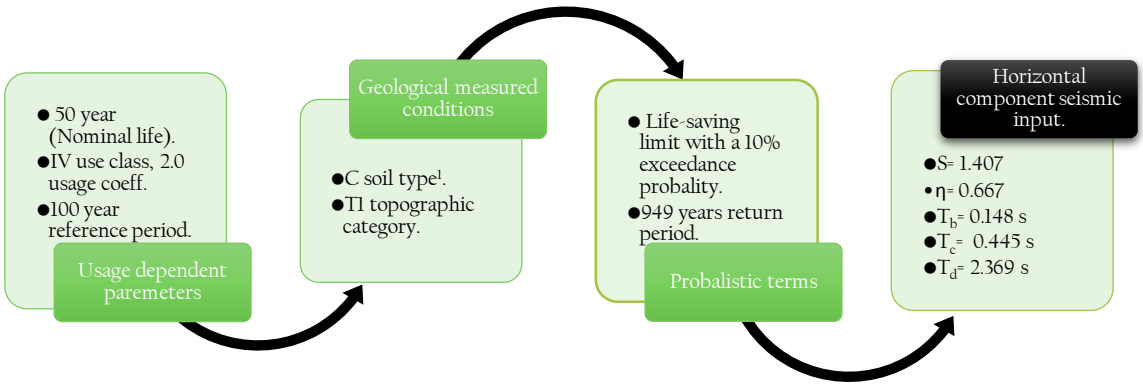

Figure 4.12 Summary of seismic load estimation procedure.

4.2.3 Model of calculus

Modeling is considered as a useful tool for engineering design and analysis. Although modeling´s meaning may differ depending on the application its basic concept remains the same: the process of solving physical problems by appropriate simplification of reality. In engineering, modeling is divided into two major parts: physical/empirical modeling and theoretical/analytical modeling, being the latter the subject of our concern. The figure number 4.12 presents the theoretical modeling general process that any actual software will follow in order to get the results. (Rock, Zhang, & Wilkinson, 2008)

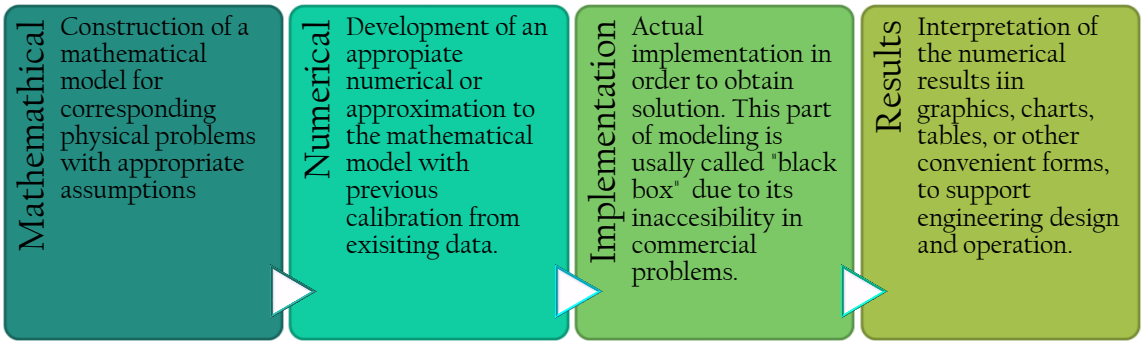

Figure 4.13 Theoretical model process ((Rock et al., 2008)

Along past years several numerical methods have been developed for suitable approximations to mathematical models. Among these methods one of the most popular is the Finite Element Method (FEM) because it can handle very complex geometry and a wide variety of engineering problems. Furthermore it manages complex restrains and loading. FEM cuts a structure into several elements (pieces) and reconnects the elements at “nodes”. This process results in a set of simultaneous algebraic equations. Finally the phenomena is expressed by governing equations and boundary conditions with infinite number of degrees of freedom (DOF). (de Weck & Kim, 2004).

Midas Gen enables practicing engineers to readily perform structural analysis and design for conventional and complex structures. Midas Gen utilizes a diverse range of specialty finite element analysis including finite element functions as well as modern theories of structural analysis to render accurate and practical results. These features contribute to higher and unprecedented standards of convenience, efficiency, versatility and productivity for structural design.(MIDAS Information Technology Co, 2015)

4.2.4 "Building E" static analysis

The structure was modeled using the geometric center of beams and columns as a reference to the axes while for floors the "package" (group of similar floors) center of geometry were used. Elements were modeled with finite concept as follows: beams and columns as "beam", masonry infill walls as "plate" with a 30/40 cm discretization, reinforced concrete (RC) wall as "walls" and discretized only in vertical direction, floors were considered "plate" with infinite stiffness due to a thickness higher than 4cm.

"Building E" was fully fixed at base, which means that every degree of freedom was blocked. In order to verify the structure subjected to vertical loads, all the structure acting actions were combined with the Ultimate Limit State (ULS) combination. ULS combination suggest a partial coefficient value regarding to load type and convenience (advantageous, disadvantageous).

Most of national standard code (NTC 08 for example) specify that in case of conducting a structural analysis with an automatic calculus code an accuracy verification should be made. In static load case, model validation is made with the vertical reaction totaling at structure base and own weight building with all variable load with nominal values confronting. Table No. 4.3 presents the static model validation made by (Bertaccini, 2014) for seismic vulnerability study. As shown the maximum found error is 3.77% which is minor than the 5% specified in the code, this means that the model was correctly validated.

Load type	Calculated (kN)	Midas (kN)	Error (%)
G1	21046.60	21250.78	0.97
G2	7393.62	7672.64	3.77
Q_k, no public off.[1]	4173.73	4173.40	0.01
Q_k, crowded[2]	481.76	481.89	0.03
Q_k, snow	367.33	359.47	2.14
Q_k, stairs	60.32	60.44	0.20
Q_k, maintaining	17.72	17.72	0.05

Table 4.3 Static Analysis Validation.

After model validation, a verification of the structural elements is realized. Figure 4.13 shows a 3D representation of "Building E" where elements with a ratio demand/resistance higher than unity are colored in yellow, orange or red in accordance to its vulnerability percentage. As presented in the left side due to flexion demand of vertical loads the entire building has ratios under unity. However, for shear demand approximately 15% of beams are colored in yellow due to a lack of transverse reinforcement.

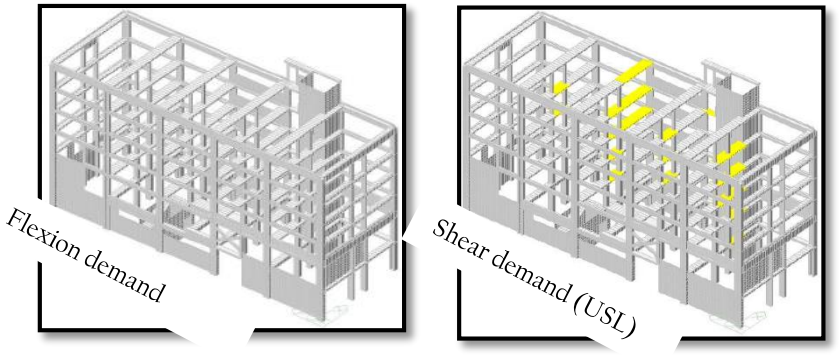

[1]No public offices (No open to the public building). [2]Possibility of crowing environment.

Figure 4.14 Demand/Resistance Building E response (Static Loads); from Bertaccini evaluation.

4.2.5 Seismic analysis procedure and results

The numerical model for building E seismic analysis was the same used for the previous static analysis including its vertical loads. However with the purpose of taking into account the masonry infills walls contribution into the global building response a single difference was introduced the equivalent truss insertion. Truss were modeled with a rectangular section finite element with the same name. Their geometric dimension were obtained with Al-Chaar model due to its simplicity and possibility of implementation for complete or partially closing.

To determine seismic action effects on building E a linear dynamic analysis was performed. According to NTC 08 this type of analysis must take into consideration every mode with a participant mass higher than 5% and a total amount of modes with a mass participation higher than 85%. Alternatively as a consequence for spatial variability of earthquake movements and center mass localization imprecision an accidental eccentricity must be applied. According to code this accidental eccentricity is 5% from measured perpendicular dimension to the seismic load application direction. Linear dynamic analysis basically consist of 3 parts:

1. Structure vibration mode determination.
2. Per every individual vibration mode the seismic action effects must be calculated, which are represented from the structure response spectra.
3. Step 2 effects combination.

For structure mode vibration Table no.4.4 lists the modal participation masses printout generated by Midas Gen software. This table indicates Mode 1 with the larger participation in X direction (37.19%) and Mode 2 in second place with a (19.75%). In the same manner for Y direction Mode 3 has the superior participation in the sum and Mode 2 was also found in second place. Furthermore it can be noted that a 94.98% is reached with 30 different modes in X direction while Y direction was little lower with a 92.50%. However both directions overpassed the 85% established in National Code.

MODAL PARTICIPATION MASSES PRINTOUT

Mode No	TRAN-X		TRAN-Y		TRAN-Z		ROTN-X		ROTN-Y		ROTN-Z	
	MASS(%)	SUM(%)	MASS(%)	SUM(%)	MASS(%)	SUM(%)	MASS(%)	SUM(%)	MASS(%)	SUM(%)	MASS(%)	SUM(%)
1	**37.1926**	37.1926	2.9994	2.9994	0.0000	0.0000	3.5807	3.5807	39.8406	39.8406	13.4734	13.4734
2	**19.7540**	56.9466	**19.7631**	22.7624	0.0000	0.0000	22.2503	25.8310	17.1546	56.9952	17.1145	30.5879
3	2.4922	59.4388	**36.5799**	59.3424	0.0000	0.0000	32.6557	58.4867	1.5788	58.5740	25.8864	56.4743
4	**5.8614**	65.3001	0.8000	60.1423	0.0000	0.0000	0.1499	58.6365	3.9192	62.4932	4.4372	60.9114
5	**13.1302**	78.4303	1.9964	62.1388	0.0000	0.0000	1.1723	59.8089	9.0997	71.5929	3.2664	64.1778
6	0.1324	78.5627	3.5756	65.7144	0.0000	0.0000	1.2060	61.0149	0.0013	71.5943	6.0776	70.2554
7	0.8391	79.4018	**8.3913**	74.1057	0.0000	0.0000	9.3366	70.3514	1.3048	72.8991	7.1635	77.4190
8	0.9258	80.3277	0.2578	74.3634	0.0000	0.0000	0.1090	70.4605	0.6159	73.5150	3.0859	80.5048
9	3.2083	83.5359	2.1102	76.4737	0.0000	0.0000	0.8732	71.3337	3.6476	77.1626	1.9278	82.4326
10	0.1826	83.7186	1.8960	78.3697	0.0000	0.0000	1.3839	72.7176	0.3301	77.4927	0.1236	82.5563
11	0.2905	84.0091	0.0124	78.3821	0.0000	0.0000	0.0014	72.7190	0.1404	77.6331	1.4648	84.0210
12	0.6273	84.6363	0.8323	79.2144	0.0000	0.0000	0.3904	73.1094	0.9616	78.5947	0.6549	84.6759
13	0.0201	84.6565	0.0048	79.2192	0.0000	0.0000	0.0072	73.1166	0.0466	78.6413	0.3208	84.9967
14	0.2407	84.8971	0.2531	79.4724	0.0000	0.0000	0.1850	73.3016	0.4089	79.0502	0.0022	84.9989
15	0.0186	84.9157	0.0276	79.5000	0.0000	0.0000	0.0208	73.3224	0.0357	79.0859	0.0030	85.0019
16	0.2651	85.1808	1.2120	80.7120	0.0000	0.0000	1.4019	74.7243	0.4281	79.5140	0.1583	85.1602
17	0.0056	85.1864	0.9497	81.6617	0.0000	0.0000	0.9054	75.6297	0.0041	79.5181	0.0066	85.1668
18	0.3649	85.5513	0.8907	82.5524	0.0000	0.0000	0.9056	76.5353	0.4604	79.9785	0.0116	85.1783
19	0.5830	86.1343	0.2207	82.7731	0.0000	0.0000	0.1788	76.7141	0.7589	80.7374	0.0047	85.1830
20	**6.7682**	92.9026	0.1865	82.9597	0.0000	0.0000	0.1968	76.9109	8.2027	88.9400	1.0901	86.2732
21	0.0372	92.9398	0.9494	83.9091	0.0000	0.0000	0.8974	77.8083	0.0542	88.9942	0.0050	86.2781
22	0.0517	92.9915	0.0042	83.9133	0.0000	0.0000	0.0053	77.8136	0.0341	89.0284	0.0025	86.2807
23	0.7919	93.7834	1.0866	85.0000	0.0000	0.0000	0.9789	78.7925	0.6786	89.7070	1.2041	87.4848
24	0.2992	94.0826	4.1817	89.1816	0.0000	0.0000	4.8765	83.6690	0.3971	90.1041	0.0165	87.5013
25	0.0003	94.0829	0.3713	89.5530	0.0000	0.0000	0.5797	84.2487	0.0455	90.1496	0.0337	87.5350
26	0.3348	94.4177	0.0003	89.5532	0.0000	0.0000	0.0052	84.2539	0.2494	90.3990	1.7520	89.2870
27	0.0886	94.5062	0.0183	89.5716	0.0000	0.0000	0.0281	84.2820	0.0418	90.4408	0.9920	90.2789
28	0.1899	94.6961	1.8858	91.4573	0.0000	0.0000	2.0699	86.3518	0.2668	90.7075	0.2144	90.4933
29	0.0231	94.7192	0.0502	91.5075	0.0000	0.0000	0.1275	86.4794	0.0269	90.7345	0.0301	90.5234
30	0.2652	**94.9844**	0.9933	**92.5007**	0.0000	0.0000	1.3127	87.7920	0.3009	91.0354	0.2466	90.7700

Table 4.4 Modal Participation Masses of "Building E"; from Bertaccini evaluation

In order to implement step 2, several scenarios were analyzed taking into account the directionality change of the seismic movement. Each set-up is represented by the following expression: $\pm 1.00 \cdot E_x \pm 0.30\, E_y \pm 0.30\, E_z$. Nevertheless, for "building E" the vertical component E_z was neglected due to building characteristics. Hence previous equation remains: $\pm 1.00 \cdot E_x \pm 0.30\, E_y$ and after considering signs alternating on both directions 8 base combinations are obtained. Finally due to accidental eccentricity 4 distinct situations for position mass center, so in consequence 32 events were investigated.

Respecting to step 3 effects combination is determined with compete quadratic combination (CQC) method. CQC was first published on 1981, is a method based on random vibration theories. It proposes to calculate the peak value of a typical force estimation from the maximum modal value double summation equation:

$$F = \sqrt{\sum_n \sum_m f_n \rho_{nm} f_m}$$

Equation 4.1 CQC method

Where f_n is the modal force associated with mode n. The double summation is conducted over all modes. Similar equations can be applied to node displacements, relative displacements and base shear and overturning moments.

The cross-modal coefficients, ρ_{nm}, for the CQC method with constant damping are:

$$\rho_{nm} = \frac{8\zeta^2(1+r)\,r^{3/2}}{(1-r^2)^2 + 4\zeta^2 r(1+r)^2}$$

Equation 4.2 Cross modal effects.

Where $r = \omega_n/\omega_m$ and must be equal to or less than 1.0. It is important to note that the cross-modal coefficient array is symmetric and all terms are positive.

Afterwards linear dynamic analysis is completed a model validation is indispensable. This validation confronts the sum of reactions generated on Midas from each direction with the base shear calculated trough a NTC-08 procedure which takes into account building weight and structure mode period. Table No. 4.5 presents base shear parameters and calculated result per each direction. Those parameters where analyzed for modes 1 and 3 which presented the larger mass participation for X and Y direction respectively on previous modal analysis. Period valued per each mode was determinate with an eigenvalue analysis, then design spectral acceleration was found and base shear calculated. Finally table number 6 demonstrate the calculated and software obtained values confrontation, where the higher error value corresponds to 0.29% which is under the specified range.

Direction / Parameter	X	Y
Mode Number	1	3
Mobilized Mass	37.1926	36.5799
Period (T) (sec)	0.8218	0.5152
S_d (T) spectra (g)	0.2480g	0.395g
Λ	1	1
W (kN)	30017.59	30017.59
F_h (kN)	**2768.75**	**4337.26**

Table 4.6 "Building E" base shear

Seismic load validation table			
Direction	Calculated (kN)	Midas (kN)	Error (%)
X seism	2768.75	2760.80	0.29
Y seism	4337.26	4334.78	0.06

Table 4.5 "Building E" seismic load validation

After model validation the structural a verification of elements was performed. Figure 4.14 and graphic 4.1 depict the 3D model of Building higher than unity are colored in yellow, orang percentage. This illustration display a large amount of structural elements most of them beams and columns with a low or medium vulnerability due to seismic loading. Being more specific, a total of 86% representing the 52% of the elements presents low vulnerability while 8% has medium, a total of a 60% of the elements at risk.

Seismic load validation table			
Direction	Calculated (kN)	Midas (kN)	Error (%)
X seism	2768.75	2760.80	0.29
Y seism	4337.26	4334.78	0.06

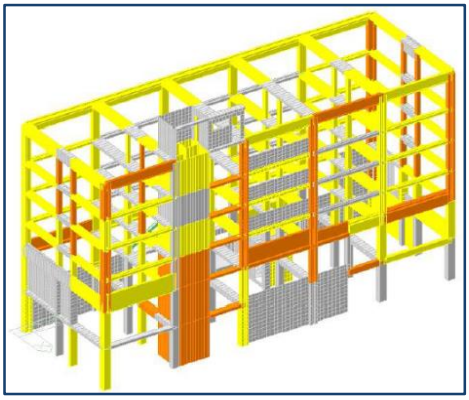

Figure 4.15 "Bldg. E" flexural vulnerability ratio

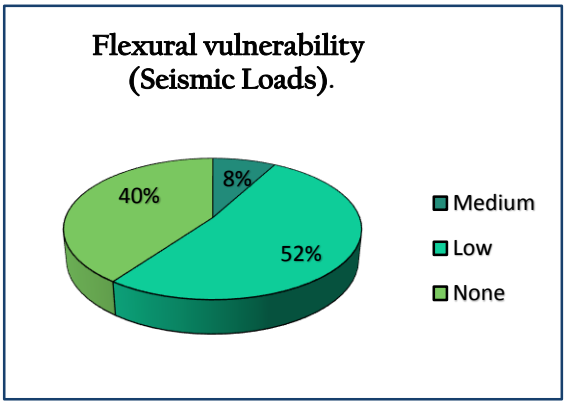

Graphic 4.1 "Bldg. E" flexural vulnerability.

In a similar manner figure 4.15 displays the 3D representation for shear stress. It can be noted that the ratio of vulnerable elements is lower than elements due to flexural bending. Even though there is not elements under high vulnerability, a 39% of the elements are subjected to low and 18% is subjected to medium vulnerability, making a total of 57% percent of elements at risk. Furthermore the primarily affected elements are columns and beam. However there is a higher percentage of affected walls due to shear stress than bending.

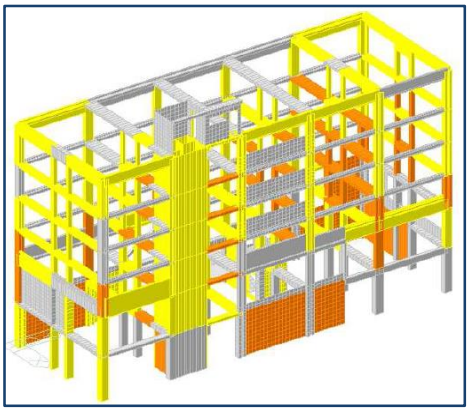

Figure 4.16 "Bldg. E" shear vulnerability ratio

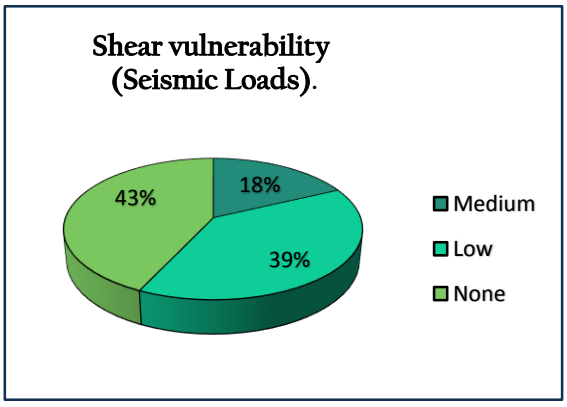

Graphic 4.2 "Bldg. E" Shear vulnerability by seismic loads.

Among the main reasons that caused a high percentage (over 50% in both cases) of structural elements with low and medium vulnerability were found: lack of transversal reinforcement which is critical for buildings under seismic loads, high distance between mass center and stiffness center therefore an additional torsional-type loading

Concerning to reinforced concrete walls verification, when are subjected to "flexo-compression" has a 64% percent of elements with none vulnerability and 36% with low is it important to note that any of the walls was subjected to medium or high vulnerability under this type of stress. However respecting to shear stress the situation is less favorable with a 52% percent with none vulnerability, a 39% with low and a 10% with medium

As seen in figure 4.16 the space between buildings is quite small. Owing to this limitation between Building E and their adjacent structures (Building F, D and B) the drift and deflection along the whole building height is evaluated in order to avoid damaging contact (pounding) between them. Moreover table 4.7 presents the results from (Bertaccini, 2014) seismic vulnerability evaluation where is verified that pounding between Building E- F and E-B does not happens so the dynamic behavior of either building remains invariable, this happens because F and B Building are not high enough to present a deflection. Nevertheless building D which is tall enough (more than double of previous buildings) after the height of 15.92 meters presents problems with the pounding effect.

Pounding between building E and F		
Height	Direction	Check?
+6.80	X	OK
+2.02	X	OK
Pounding between building E and D		
Height	Direction	Check?
+23.30	X	NO
+19.80	X	NO
+15.92	X	NO
+12.62	X	OK
+9.32	X	OK
+6.02	X	OK
+2.02	X	OK
+6.02	Y	OK
+2.02	Y	OK
Pounding between building E and B		
Height	Direction	Check?
+6.80	X	OK
+2.02	X	OK

Table 4.7 Pounding between Building E adjacent structures

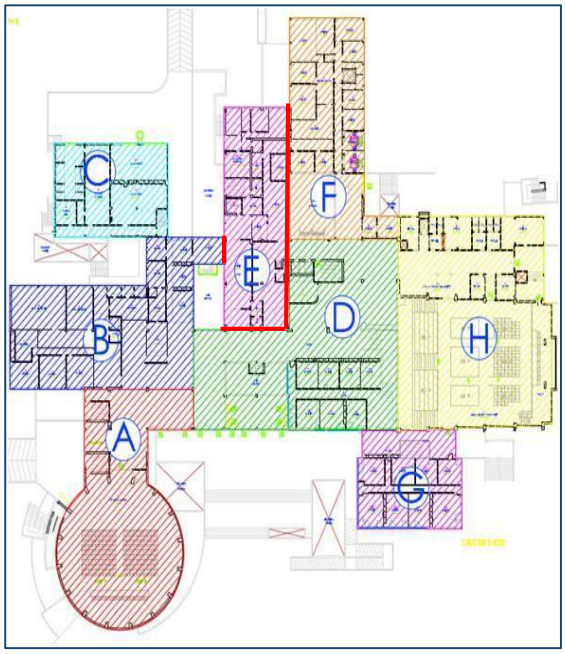

Figure 4.17 Building E complex plan view

From Bertaccini seismic vulnerability study it can be concluded that: the structure was projected for vertical loads only, has an important lack of reinforcing to resist shear and flexion stress, presents irregularity in height and some irregularities in constructive plan.

4.3 Pizzarulli´s Retrofit proposal.

As a solution for previous seismic vulnerability a retrofit assessment was proposed. (Pizzarulli, 2015). This proposal is divided in two main phases: the first aims to regularize Building E through a reduction of torsional effects while the second phase projects metallic dampers to dissipate the seismic energy that existing structural elements cannot tolerate. In this last phase Pizzarulli proposes three solutions varying damper´s size, distribution and quantities in both principal directions of the structure. These improvements have the purpose of presenting different levels of robustness which directly influence the short-term investment.

4.3.1 SP0 (Structure regularization)

The technic room generates a strong irregularity in plain view because is not in a symmetric position. As a consequence distance between mass center and stiffness center is increased which is traduced in future torsion problems. From this situation the principal aim of the first called SP0 arises.

SP0 intends to reduce the strong irregularity caused by the technical vain at all floor levels. To this end the insertion of metallic bracings in both orthogonal directions of the main building along it whole height and the removal of a reinforced concrete wall in ¨Mezzanine¨ floor is proposed. On the left side of figure 4.17 it is shown the reduction in the distance between centroids shown while the right side shows the 3D positioning of steel bracings along the entire height of the building. It is important to quote that metallic bracing insertion was not symmetric, as depict on the right side of figure 4.12 a HEA 260 profile was inserted in the X direction while for Y direction a larger denomination HEA 280 had to be used.

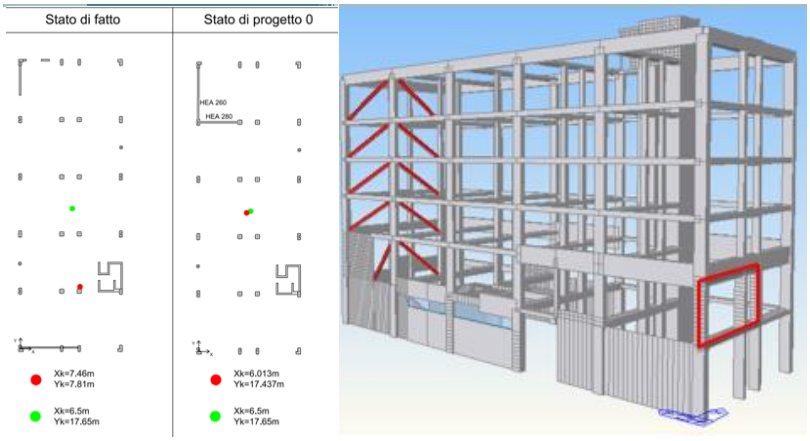

Figure 4.18 SP0 proposal from Pizzarulli's proposal.

4.3.2 SP1 (Buckling Restrained Axial Dampers insertion)

The main objective of this phase is to increase the building damping and reduce displacements and period throughout the increment of stiffness of the structure. In this phase it is proposed Buckling Restrained Axial Dampers (BRAD) insertion in the building, (see figure 4.18). This solution was adopted in series with a steel element to form the diagonal braces of the retrofitted structure.

From (Bertaccini, 2014) evaluation it was concluded that reinforced concrete frames and masonry walls of the building do not have the required detailing in order to develop a sufficient elastoplastic behavior capable of dissipate the expected energy. As a consequence this phase expects to improve the seismic behavior of the structure providing a better dissipation of the seismic input energy in the structure. In other words, it is anticipated that the seismic energy introduced to Building E will be absorbed by inserted BRAD dampers.

Figure 4.19 Buckling Restrained Axial Dampers.

SP1 design procedure.

In order to determine the amount and size of dampers for each direction a Displacement Based Seismic Design (Priestley et al, 2003) was performed. First of all a Pushover analysis was performed in order to determine the displacement capacity of the regularized structure (SP0 phase). Following the design method the demand displacement (40mm) was compared with the actual capacity of the building (26mm) due to a high proximity with next building. From this difference a damping value is obtained reducing the elastic spectrum, which in this case resulted in 21%. Then taking backwards the Displacement Based Seismic Design (DBSD) formula the required damping for the dampers was obtained and the dissipated energy in one hysteretic circle. Hence from the structure´s drifts, damper´s damping and one hysteretic circle area the demanding force for the damping device is calculated and a selection of the size device can be made.

SP1 Results

As a result of the stiffness inequity between both directions and likewise phase SP0 the Buckling Restrained Axial Dampers proposal insertion, is not symmetric at all in amount nor location. The amount dampers estimated for X direction (4 BRAD 56/30-b) corresponds to the double of Y dampers projected for Y direction (2 BRAD 56/30-b). Also their location in plain view do not correspond to a symmetric distribution, 4 dampers were added in the beginning of Y direction while just 2 were added at the end, depicted in figure 4.19.

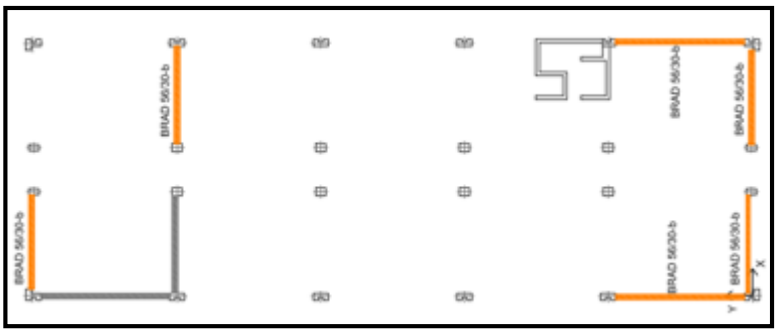

Figure 4.20 Plan view of BRAD's addition.

Even though BRAD dampers were inserted some elements did not verify due to shear stress. As a result, a local intervention is proposed for these elements, shown in figure 4.20. This intervention suggests Fiber Reinforced Plastic (FRP) procedure for 44 columns critical sections (near to nodes). Likewise recommends the embedded through section (ETS) with Carbon Fiber Reinforced Polymer (CFRP) procedure for the 27 beams in order to prevent potential shear cracking.

Figure 4.21 Local intervention procedure.

General observations.

From phase 0 (structure regularization) a period reduction from 0.70 to 0.64 seconds was obtained. However phase 1 indicated a more significant decrease of the period from 0.64 seconds to 0.444 seconds, which means that insertion of dampers brings a noteworthy reduction of displacements and a considerable increment of stiffness. Moreover this proposal satisfies all the demand requirements.

Turning to the financial aspect the estimated total cost of this proposal is EUR400, 000.00. Graphic 4.3 presents the costs distribution by procedure type. It can be observed that SP0_Structure Regularization along with SP1_Dampers Insertions cover the greater part of the budget with a contribution of the 69.7% percent. Then it is followed by Foundations with a participation of 18.2% and Local interventions with 11.3%, where the latter includes FRP and ETS procedures for columns and beams, respectively.

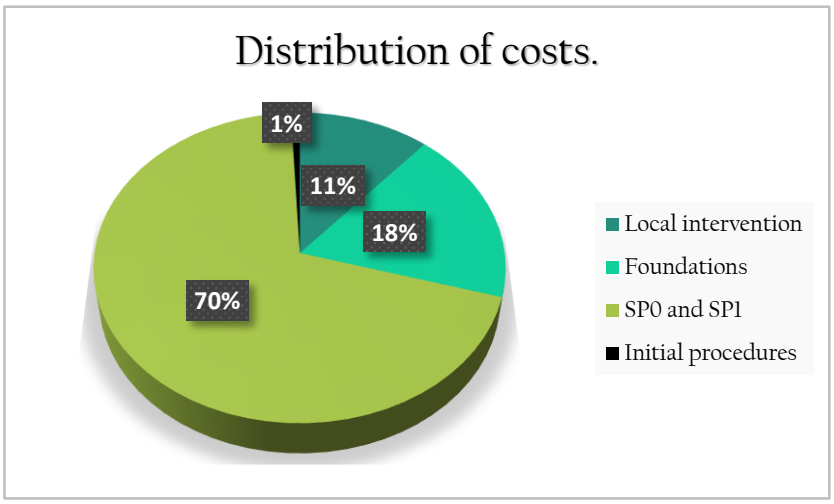

Graphic 4.3 Distribution of cost by procedure.

On the other hand the Direct Displacement Based Design was validated throughout the bracing design. Furthermore dampers insertion produced a significant reduction of the acting forcers on the floors and technical floor. In addition the convenience of this type of assessment is verified by the amount of total energy dissipated (326.4 Joules). Finally it is important to point out that the prediction of the structural behavior due to a variation on the dissipating system is impossible without an accurate design. (Pizzarulli, 2015)

5. PRESENTATION OF RESULTS.

In this chapter is presented the application results of previous established methodologies. Likewise preceding section, an organization by blocks is outlined to enable a better understanding of the outcomes. Moreover a statistical procedure is presented as a consequence of an unfeasibility of distribution fitting.

5.1 Outline of the chapter.

In order to organize the investigation procedure ground motion, modeling and statistic blocks were stablished at preceding chapter. Therefore results and statistical analysis were organized following same conditions with a sequence to follow, figure 5.1 presents the outline. Although same proceedings have been applied to all both types of recording (far field and near field), the latter one has been presented at the end of this chapter as a consequence of its own characteristics.

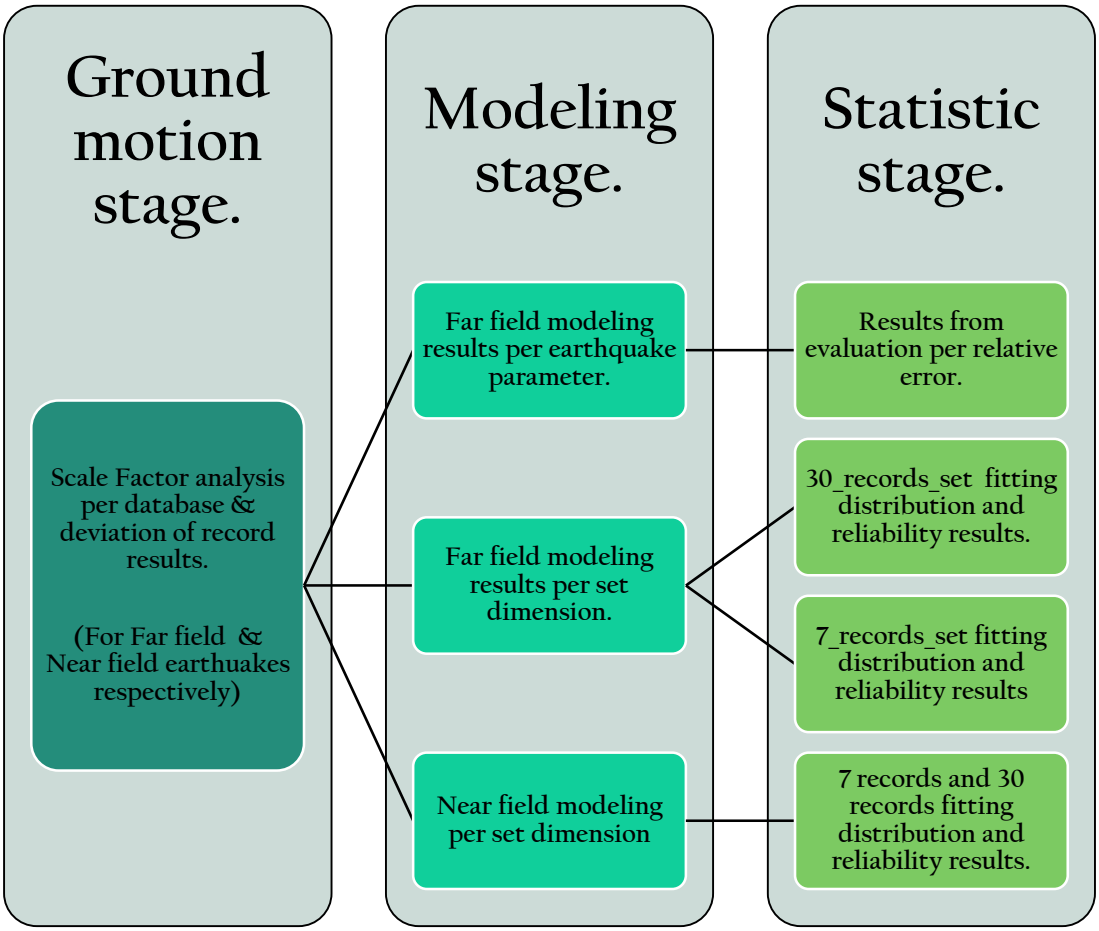

Figure 5.1 Outline of the chapter by stages.

5.2 Results from ground motion stage.

5.2.1 Scale factor analysis for far field earthquakes.

For REXEL search, a preliminary study analysis was performed aiming to detect best interval of earthquake parameters from the ratio between records and target spectrum. This ratio called Scale Factor (SF) denotes how large or small the recording is in a specific point from the objective. It is noteworthy to mention that Scale Factor analysis should be used only for initial ground motions discretization because it does not describes the whole ground motion behavior, an example and its formula is shown in graphic 5.1. Nevertheless ground motion time-search throughout databases was substantially reduced owing to obtained results of this analysis.

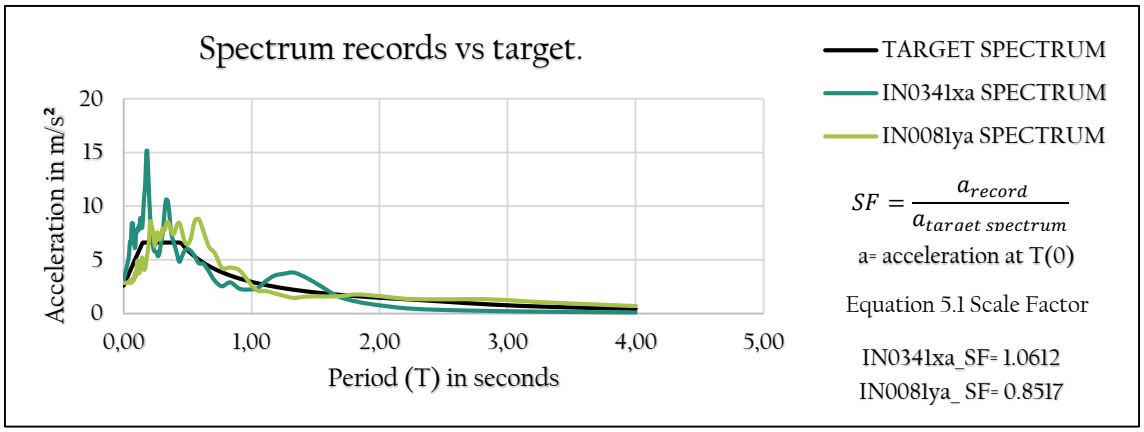

Graphic 5.1 Spectrum records vs target.

Radio & Magnitude (RM) analysis.

From this analysis a single interval was selected for European, Italian and Simbad databases, respectively (Smerzini, Paolucci, Galasso, & Iervolino, 2012; Smerzini & Paolucci, 2013). Graphic 5.2 presents European and Simbad databases best results with a 1.5 magnitude range (4.5-6) whereas Italian database shows a 1 magnitude interval of (5-6) as the most suitable.

Moreover European and Simbad describe a greater number of events than Italian when radio increases. Conversely Italian database has a greater SF for smaller radios and it is reduced when radio increases while for the European and Simbad databases is the opposite case.

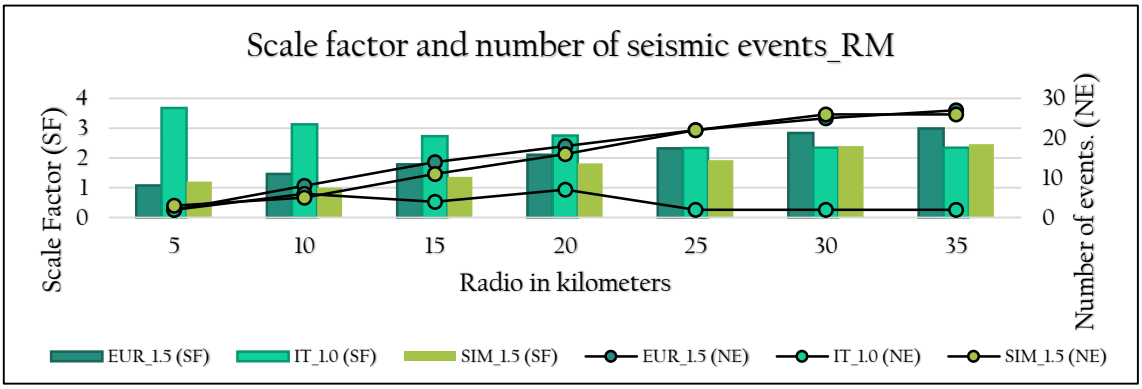

Graphic 5.2 Scale factor and events from radio & magnitude intervals.

Peak Ground Acceleration (PGA) scale factor analysis.

Unlike previous enquiry where two-variable correlation for Radio and Magnitude were necessary PGA only requires one variable, its own interval. From this analysis Simbad database presents a higher number of records in comparison with European and Italian, as shown in graphic 5.3. In general terms scale factors tend to be closer to unity in central intervals and increases at extremes. Moreover Italian database shows an outcome similar to RM (most of cases less than 10 events).

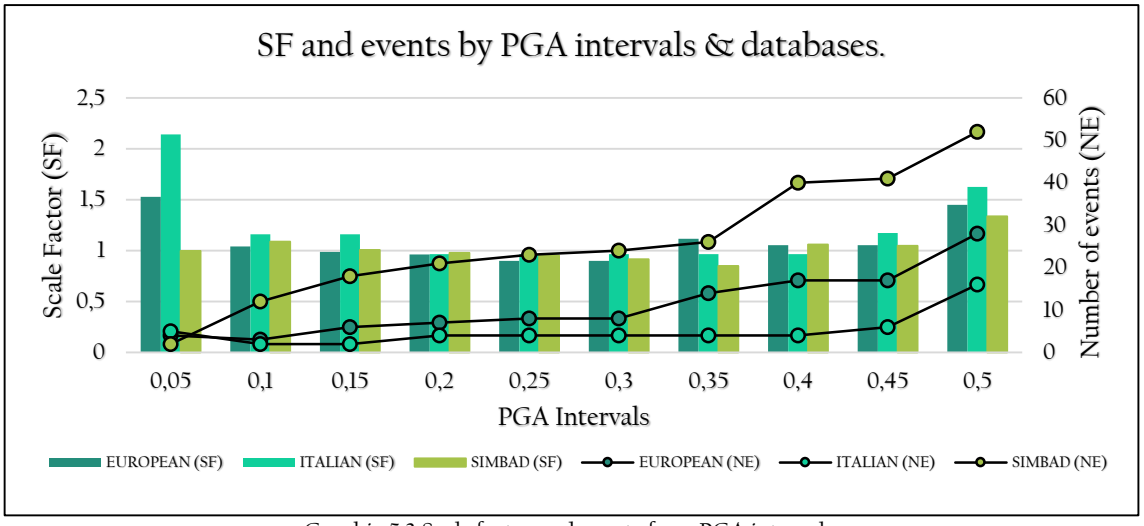

Graphic 5.3 Scale factor and events from PGA intervals.

Arias Intensity (IA) scale factor analysis.

From Arias intensity a notable difference was obtained in comparison with the previous results; non feasible events were acquired from Italian database. This outcome can be attributed to its size since Italian database doesn't account for this parameter. Furthermore Simbad provides a higher amount of feasible events without a significant increment on scale factor. Although a significant increment was no produced in any case.

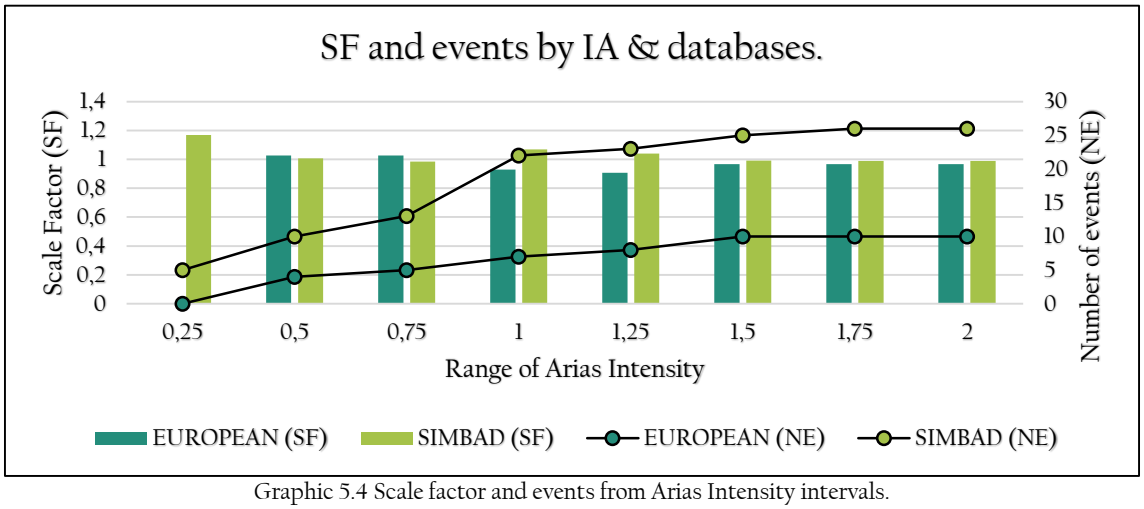

Graphic 5.4 Scale factor and events from Arias Intensity intervals.

General observations from scale factor analysis.

To sum up, table 5.1 presents scale factor analysis in terms of average by parameter and database. It can be seen that Simbad database has the most-effective outcome with higher number of events and lowest scale factor values, then continues European and finally Italian. Moreover Italian's average of events is less than 6 in all cases, indicating almost zero probability to find suitable events. As a consequence Italian database was neglected for later analysis. Additionally, for PGA and Arias Intensity following analyses the proportion of records obtained from databases is approximately 2:1 since Simbad results are twice times bigger than European results (emphasized values from table 5.1).

Earthquake parameter	Index average	European	Italian	Simbad
Magnitude and Radio	Scale Factor	2,08	2,76	1,74
	Number of events	16,57	3,57	15,57
Peak Ground Acceleration	Scale Factor	1,10	1,21	1,02
	Number of events	11,2	5,1	25,9
Arias Intensity	Scale Factor	0,85	0	1,03
	Number of events	6,75	0	18,75

Table 5.1 Scale factor summary analysis.

5.2.2 Deviation factor from target (far field earthquakes).

From scale factor analysis, at least 40 records were obtained for each earthquake parameter. As explained above scale factor does not describe a complete relation between spectrum´s recording and target spectrum. Hence deviation factors were calculated to categorize and select best recordings. This factor measure the difference of the spectral acceleration among spectrums for the same period value, using the same formula as standard deviation, see equation 5.1.

$$DF = \sqrt{\frac{\sum_0^n \left(\frac{(X_{ri} - X_{ci})}{X_{ci}}\right)^2}{n}}$$

X_{ri} refers to the acceleration at i period of the record; X_{ci} is the acceleration at i period of the code.

Equation 5.2 Deviation Factor

On the other hand Eurocode 8 and NTC 08 prescribes "in the range $0.2T_1$ and $2T_1$ no value should be minor than 90% of the corresponding value of the 5% damping elastic spectrum". As a result 2 deviation factor were established: total and partial, see graphic 5.5. The latter one aims to verify the 90% limitation prescribed on codes covering only from 0.15sec to 2sec.

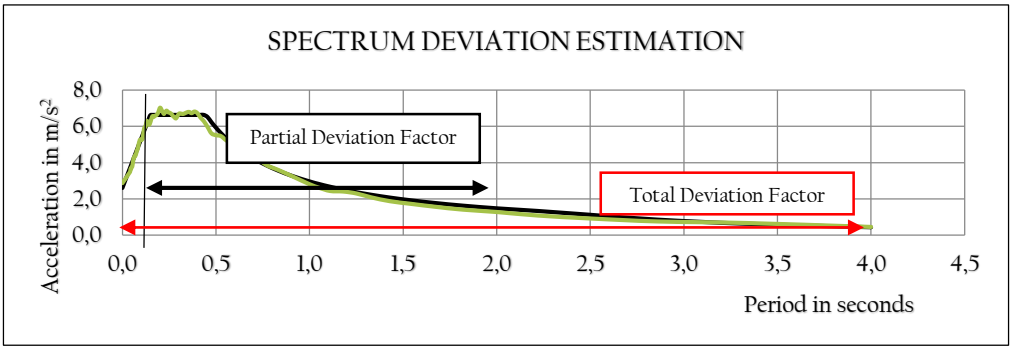

Graphic 5.5 Spectrum Deviation factor

However partial deviation cannot describe the nature of the deviation (exceedance or deficit). Therefore a visual classification was employed. Then from scale factor, partial deviation factor and visual classification sets of 30 records per earthquake parameter were assembled. On the other hand graphic 5.6 presents the divergence of average (from selected 30 recordings) responses from target spectrum. Likewise partial and total deviation factor from average spectrums are listed in table 5.2 where magnitude and radio presents the lowest partial deviation while Arias Intensity has the lowest total deviation.

Earthquake parameter	Partial DF	Total DF
Magnitude and Radio	3,06%	10,48%
Peak Ground Acceleration	4,66%	5,14%
Arias intensity	5,00%	4,98%

Table 5.2 Deviation factor by earthquake parameter.

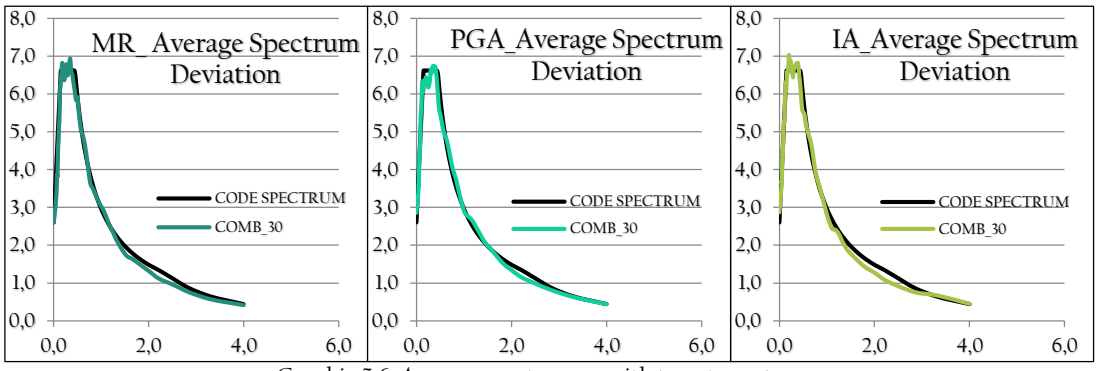

Graphic 5.6 Average spectrum vs with target spectrum.

5.2.3 Scale factor and Deviation factor for near field earthquakes.

Near field earthquakes search was performed using the Pacific Earthquake Engineering Research (PEER) database since previous databases can be only used for far field cases. As a consequence some aspects must be clarified due to found differences with preceding databases. First of all the database was designed for a geographical context outside Europe, so there is a significant proportion of records from other continents. Similarly, scale factor analysis was not necessary during near field search because there was a small amount of compatible records with the case study. As a result only deviation factor analysis was performed, shown in figure 5.2.

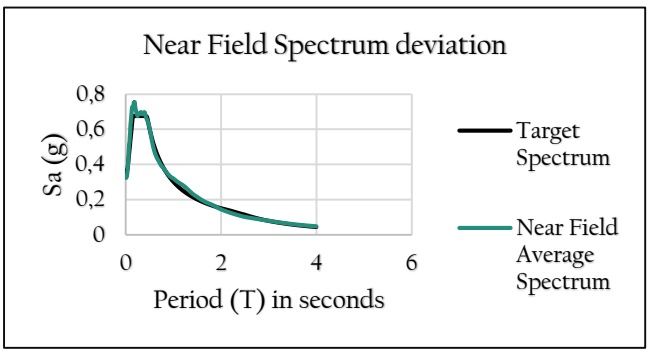

Near field	Deviation
Total	7,157%
Partial	7,223%

Figure 5.2 Near Field spectrum deviation.

5.3 Results from far field modeling stage.

In this section results from MIDAS Information Technology Co, 2015 analysis are presented. This phase aims to describe the average response behavior when the amount of analyzed records is increased. To this end, comparison among 50_recordings analysis, 30_recordings analysis and 7_recordings analysis are performed. Nevertheless it is noteworthy to mention that relative errors mentioned in this section do NOT refer to the reliability of the resulting values. The simply denote the observed difference in the average displacement due to size dimension. Reliability results and comparisons are presented in the statistical stage, which is the following section.

5.3.1 Results from 30-recordings analysis.

As previously explained in methodology chapter, maximum displacement was observed in both directions for this analysis, since the building has a pounding risk with an adjacent building. Moreover from previous chapter, it is known that first mode prevailed among others during the node controlling along building E height. As a consequence only top-roof points along "gap zone" were studied for the structural response statistical analysis, fore reference see figure 5.3.

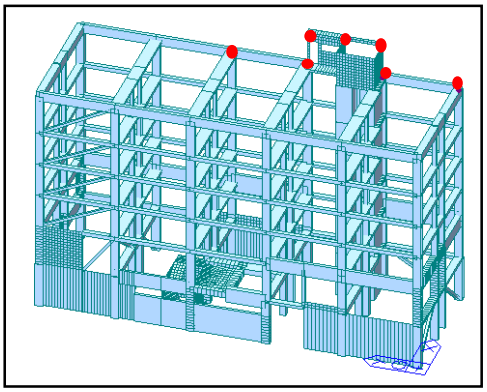

Figure 5.3 Studied points from modeling.

Thirty ground motion recordings were analyzed per each earthquake parameter. However sixty displacements were studied instead of thirty per parameter. This is because MIDAS returns maximum displacements for positive and negative direction and aiming to enhance the statistical population both possibilities were considered for subsequent analyses. Therefore a total of 120 displacements were observed and evaluated. Modeling results were analyzed as follows:

i. First only seven maximum displacements are considered and a 1st average is calculated.
ii. Second a single maximum displacement is added to previous set and a 2nd average is obtained.
iii. Then previous step is repeated until all displacements have been taken into account.

Magnitude and Radio average displacement behavior is displayed on graphic 5.7. It can be seen that the distance among X and Y direction average results is not stable along the increments of set dimension, on the contrary it seems to be increasing. On the other hand, X direction presents a more stable tendency line in comparison with Y direction.

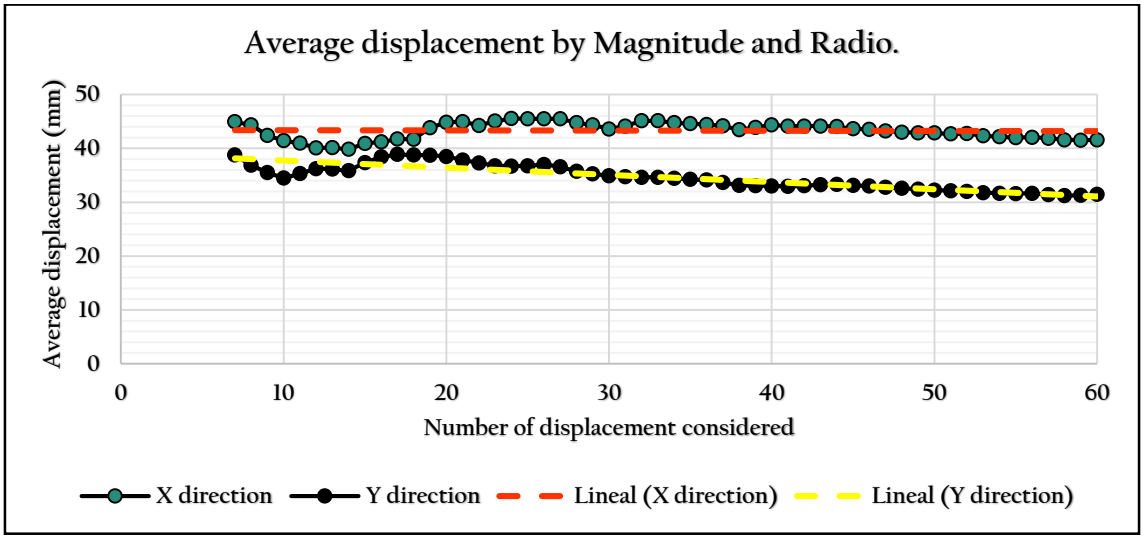

Graphic 5.7 Average displacement by Magnitude and Radio. (30_Recordings)

Peak Ground Acceleration (PGA) average results are illustrated in Graphic 5.8. Unlike magnitude and radio results, the distance between principal directions of the building are constant. Moreover, both directions present the same tendency with a slight positive slope. On the other hand the maximum difference between averages from X direction is 10 mm whereas for Y direction maximum difference is 8 mm.

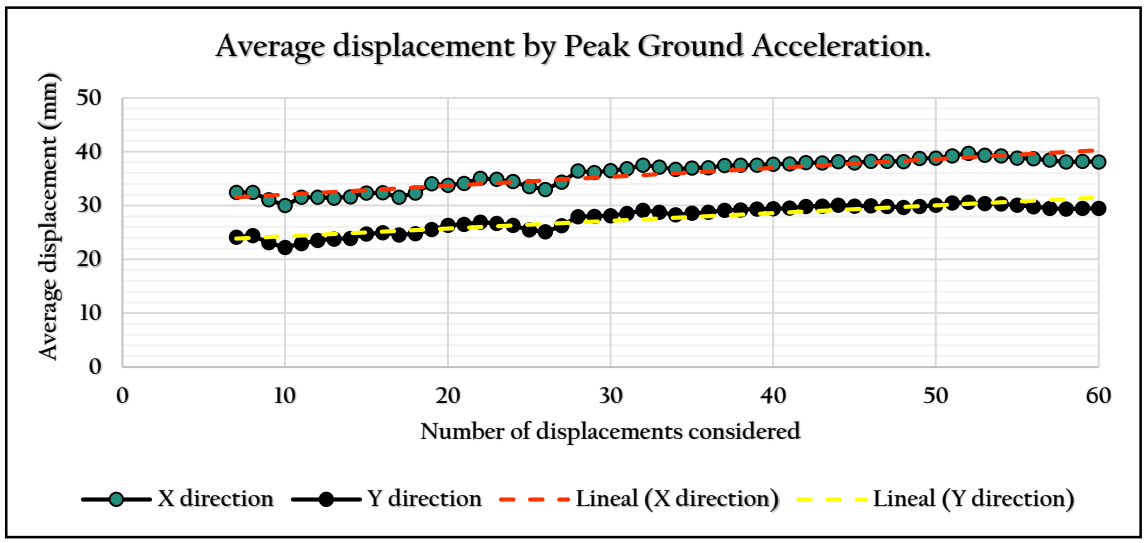

Graphic 5.8 Average displacement by PGA selection. (30_Recordings)

From **Arias Intensity results** it can be observed that for a smaller amount of displacement considered it presents a stronger oscillation than other parameters at initial values; from 10 to 18 varies from 32 mm to 38 mm in the X direction, shown in Graphic 5.9. However, it seems to become more stable for larger values. For instance, 21 and 60 values shows the same average displacement 37 mm. Moreover, if initial behavior (from 7 to 18 values) is neglected, difference between both directions seems to be unchanged by the increment of displacements. Finally, Y direction presents a reduced fluctuation in comparison to X direction, see graphic 5.9.

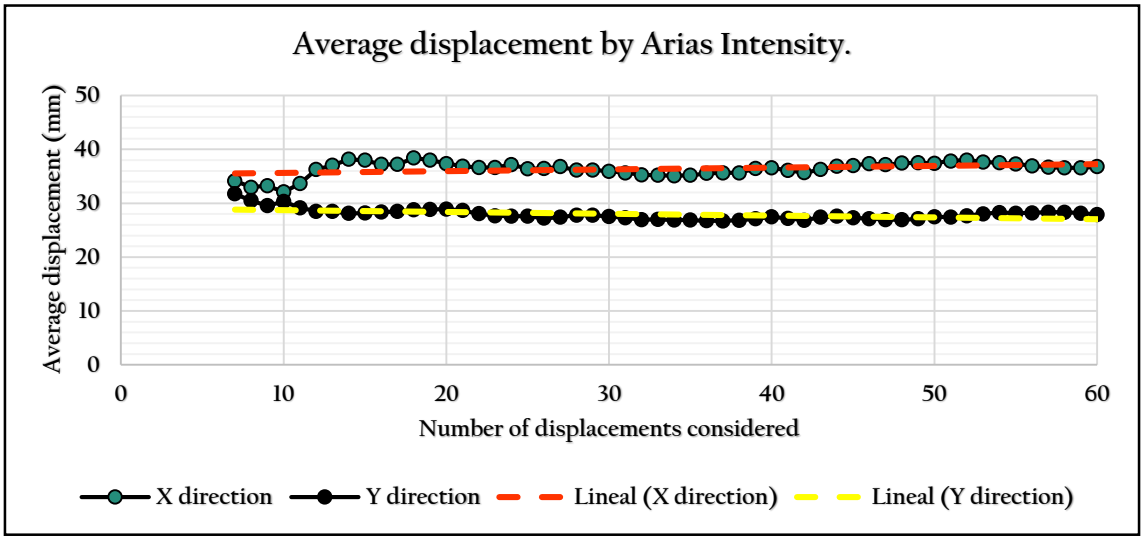

Graphic 5.9 Average displacement by Arias Intensity. (30_Recordings)

5.3.2 General observations 30 recording analysis by earthquake parameter.

In order to appreciate differences between selections methods table 5.3 presents the standard deviation of previous averages by earthquake parameter. From this table it can be seen that PGA has the greatest standard deviation for both directions, meaning that is most variable of the group under Building E conditions. Conversely for the smallest deviation there are two parameters involved; Arias Intensity presents the smallest standard deviation for Y direction. Whereas the minimum standard deviation for X direction was obtained from Magnitude and Radio analysis. Turning to differences among directions there is clear evidence that stiffness of the investigated structure affects the average trend since standard deviation from Y direction were at least a 20% lower in the best of cases.

St. Deviation	MR	PGA	Arias Intensity
X direction (mm)	12,713	14,894	13,041
Y direction (mm)	9,937	11,732	8,909
Dif. (%)	27,94%	21,23%	31,68%

Table 5.3 Standard deviation by earthquake parameter.

Magnitude and Radio presents the average displacements on the safest side since the highest average values were obtained from this analysis, see graphic 5.10. On the contrary, Arias Intensity seems to present the lower averages while the number of considered displacements is increased. Moreover it can be appreciated that differences among average displacements due to parameter variation is notably reduced when the number of considered displacements increases. Moreover for all parameters it is observed a tendency to achieve the same value.

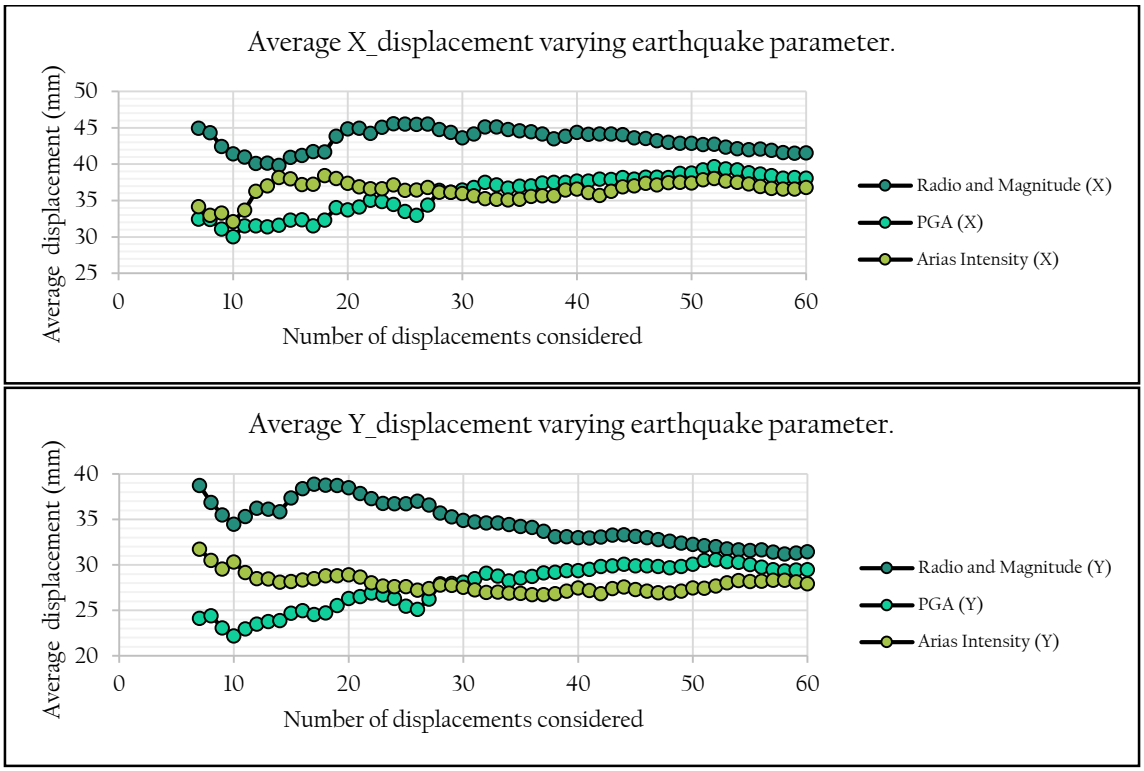

Graphic 5.10 Average displacement by earthquake parameter and direction. (30_Recordings)

5.3.3 Stability verification (50 recordings analysis).

As a consequence of previous presented tendencies or instability on average results a further investigation was performed. This verification aims to corroborate that 60 displacements values is a stable and reliable number for statistical purposes. Therefore the average behavior of a greater population was studied.

This set was called "no scaled" because no parameter in specific was taken into account and it was formed by 50 records. Likewise previous analysis (default and its opposite directions) were considered, thus 100 displacements were observed. Results from this verification are depicted on graphic 5.9 where a steadiness can be perceived above 60 displacements since values do not fluctuate with a significant difference among them. In addition final averages (when a 100 displacements are observed) have been used as reference values for further comparisons and analysis.

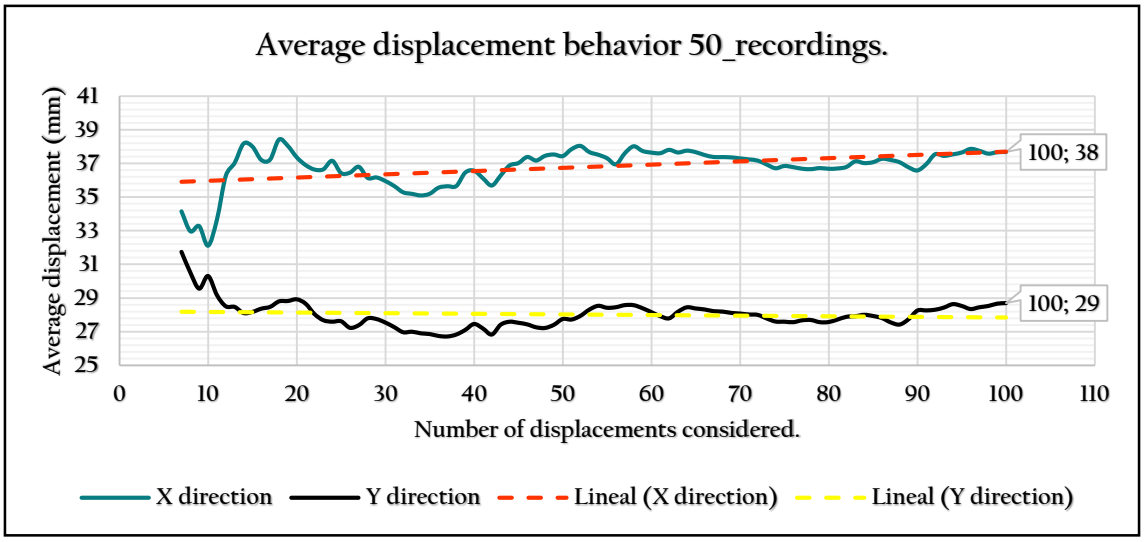

Graphic 5.9 Average displacement stability verification. (50_Recordings).

5.3.4 Comparison of 50-recordings and 30-recordings by earthquake parameter.

In order to perform this comparison final averages (when 60 displacements are considered) of 30_recordings analysis were contrasted with final average from 50_recordings analysis. This comparison aims to detect differences due to earthquake parameter variation and amount of considered earthquakes.

Graphic 5.11 presents the relative error by earthquake parameter and direction. It can be seen that PGA is the closest parameter to 50_recordings results while Magnitude and Radio is the farthest one. Moreover both parameter show positive relative error, meaning that they are superior to the average obtained from 50_recordings analysis. This implies that PGA and MR results might get a more reliable value from further analysis. On the contrary Arias Intensity results are inferior to 50_recording implying that a lower reliability will be obtained from these results.

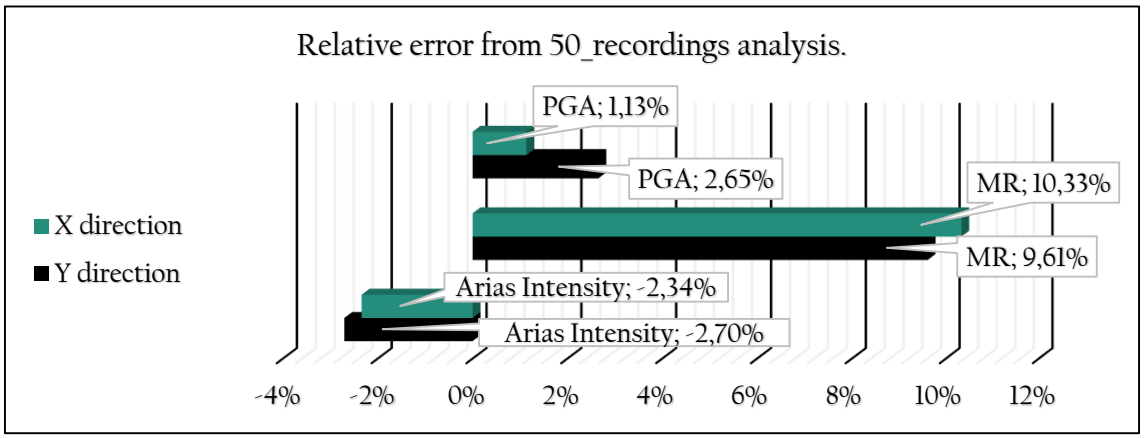

Graphic 5.11 Relative error from 50_recordings by earthquake parameter. (30_recordings)

5.3.5 Results from 7-recording analysis.

Since 7-records is a very small sample size there is a great variability of possible results. As a consequence from REXEL more than 100.000 combinations were obtained for 7_recordings analysis. Despite of the great amount of available data a significant reduction of observed combinations was performed due to available time and computational capacity.

On the other hand Rexel only returns combinations from a single database at a time, which means that combination of SIMBAD and European best results was not available using the software. As a consequence Rexel procedure was studied in order to recreate less combinations using both databases at a time. From REXEL recreation, 12 best recordings were selected and 792 combinations generated per direction and earthquake parameter. A summary of this performed procedure is presented in figure 5.4.

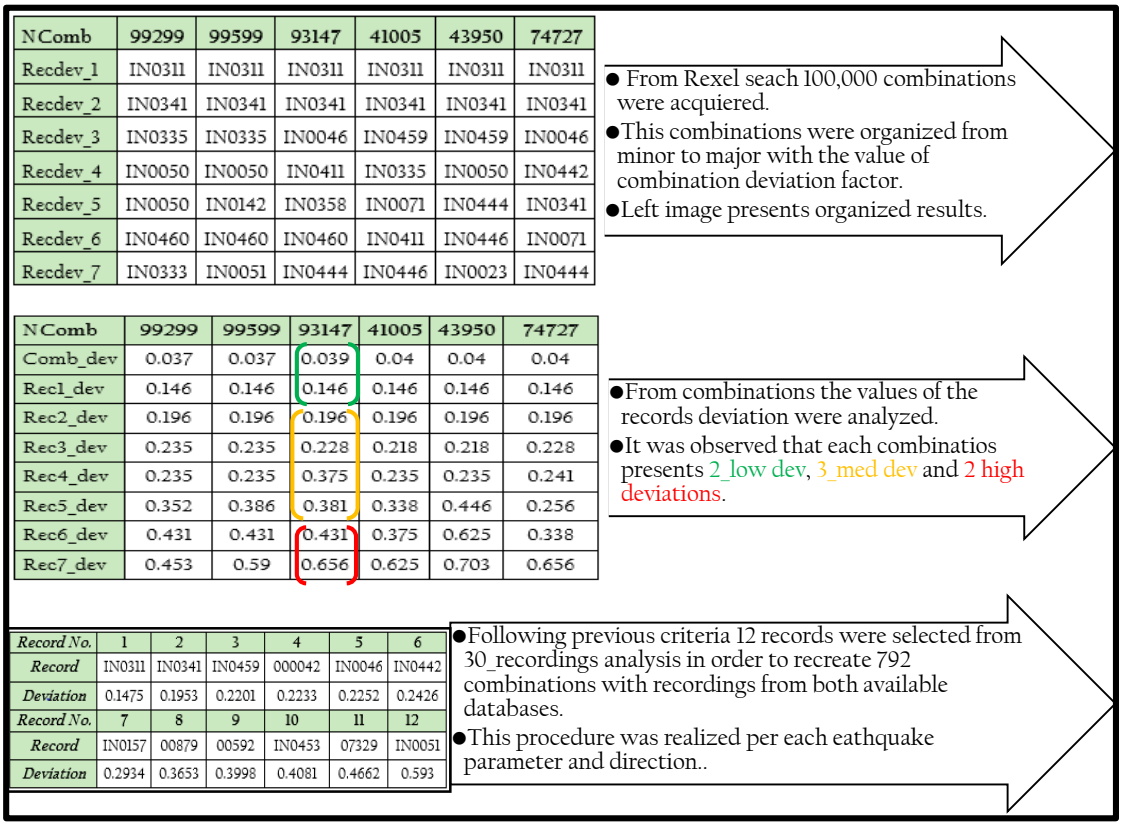

Figure 5.4 Summary of the combination procedure for 7_recordings.

From previous procedure 792 combinations were obtained per each earthquake parameter and direction. Hence this sections aims to determine the behavior of 7_recordings results, such as variability among results and median values. Moreover a comparison among earthquakes parameter results is presented in order to detect differences due to parameter variation. Likewise 30_recordings analysis a comparison with 50_recordings results is performed to determine if the behavior is affected by sample size.

Magnitude and Radio average displacement behavior for X direction is displayed on graphic 5.12. It can be perceived that X direction average results presents a significant fluctuation of the values. Being more specific the average displacements oscillate from 31 mm to 51 mm, representing an increment of 64,51%. Although there is a strong instability among results, it can be appreciated that the averages oscillates around (40 mm) which can be considered the median value of the combinations.

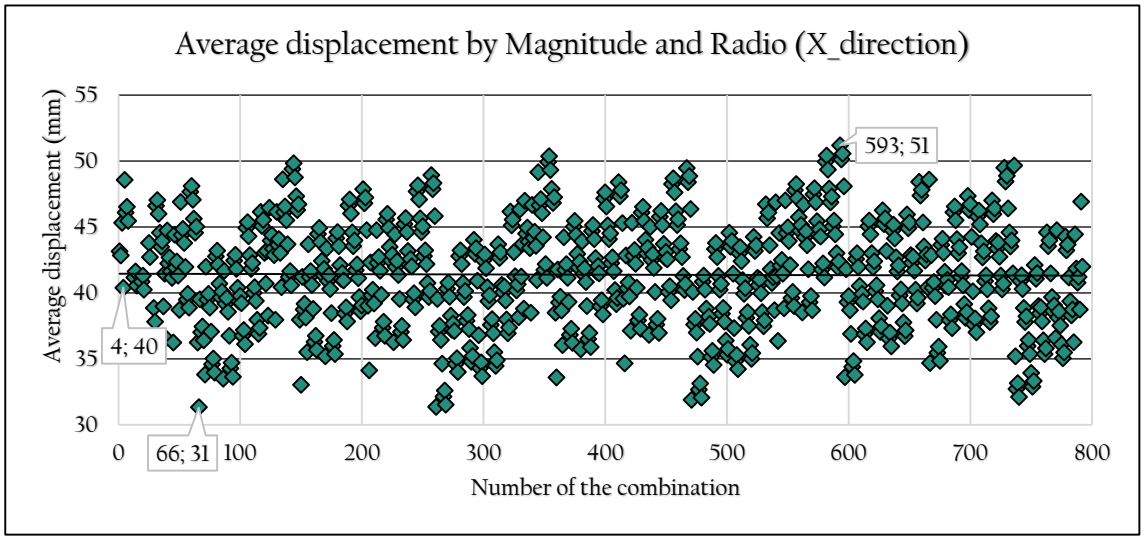

Graphic 5.12 Average displacement by Magnitude and Radio (7_recordings)

Graphic 5.13 presents the average results of Y direction by Magnitude and Radio. Y direction presents a value oscillation similar to X direction, although it seems to be inferior. Moreover Y average displacements fluctuates from 27mm to 38mm (a 40.74% increment) almost 20% lower than X displacements. This reduction of the variability can be a consequence of the stiffness increment from the case study.

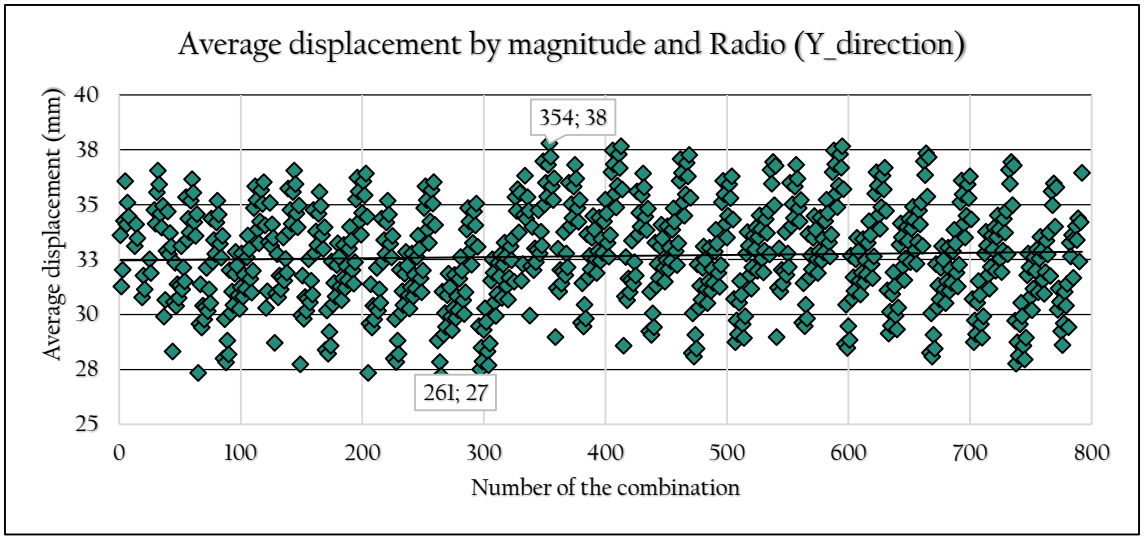

Graphic 5.13 Average displacement behavior of 7_recordings by magnitude and radio.

Peak Ground Acceleration and Arias Intensity outcomes have shown a reasonably resemblance with Magnitude and Radio in terms of value fluctuation. Hence a general graphic (summarizing the results) is presented instead of individual ones. Graphic 5.14 presents the maximum, median and minimum values obtained from the 792 combinations per earthquake parameter and direction. In general terms no substantial differences were detected due to parameter variation. The greatest difference was found at minimum values of Y direction with a 24,70% between Magnitude and Radio and Arias Intensity. The number of considered combinations (792) could be among the possible causes of these observed similarities. However only 12 records were used to recreate the combinations, thus further studies are required.

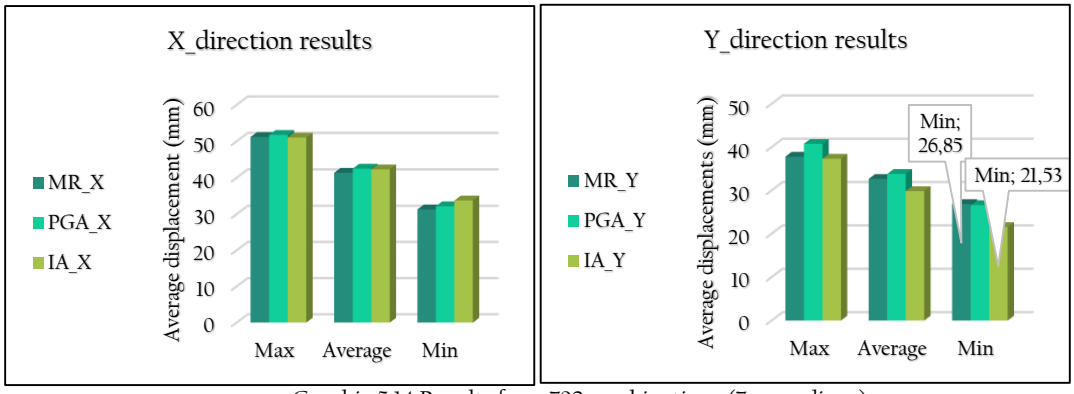

Graphic 5.14 Results from 792 combinations (7_recordings).

5.3.6 Comparison among 50-recordings and 7-recordings by earthquake parameter.

Unlike 30_recordings analysis where 1 combination was studied per parameter, for 7_recordings 792 combinations were evaluated since there is a significant fluctuation of the results. As a consequence the relative error (taking 50_recordings as a reference) was analyzed with another perspective in order to be acquainted with worst and best scenarios. Graphic 5.15 presents the relative error obtained when the maximum, median and minimum values from the 792 combinations are compared with 50_recordings values. The greatest overestimation was obtained from PGA analysis while Arias intensity was the closest with a 3,91%.

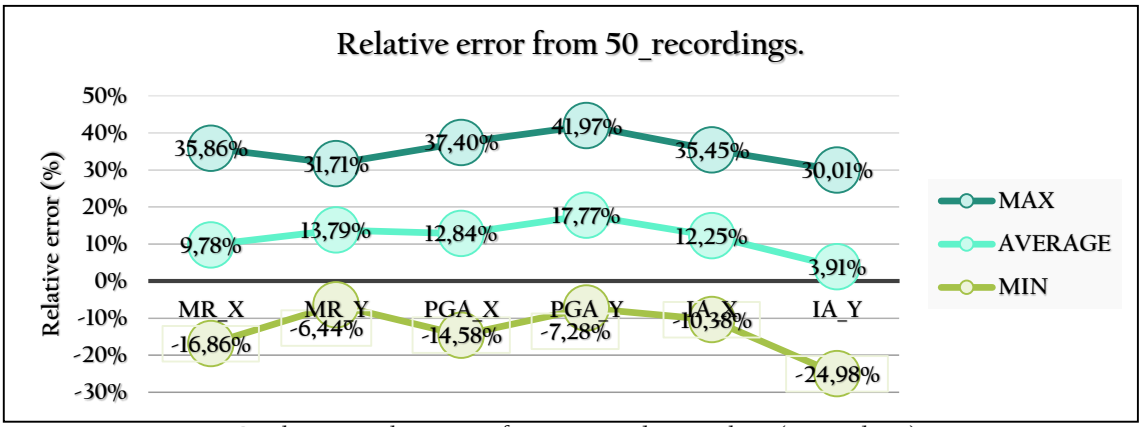

Graphic 5.15 Relative error from 50_recordings analysis (7_recordings)

5.4 Results from far field statistical stage.

5.4.1 Reliability and probability of failure analysis.

From Eurocode EN: 1990, structures should satisfy reliability values in relation to its safety level and economical costs of repairing. According to mentioned standard for an existent structure with large economic consequences of repairing and social importance the reliable value should be equal to or greater than (P_s)= 3,72 in a year (see methodology chapter for further references).. Nevertheless this value is not comparable with the available data. Therefore from the equation 5.1, its corresponding failure rate was calculated in order to be compared with the probabilities obtained from the fitted distributions (see review literature chapter for further references).

$$P_f = \phi(P_s)$$ Equation 5.3 Failure rate

Where ϕ returns the cumulative probability of a normal distribution with mean value 0 and standard deviation equal to unity, see figure 5.4. Consequently a failure probability in a year of 10^{-4} was obtained using the function pnorm from Mathcad. However the maximum displacement average of Building E has been verified due to a pounding risk. This implies that all the analysis have been performed under survivability limit state conditions. Besides Building E has a strategic usage, so the return used period was 949 years for all the analysis. Owing to this significant difference among years the probability was converted to an equivalent for mentioned period.

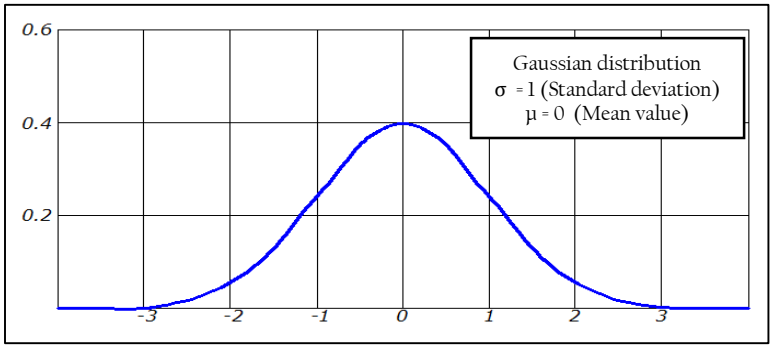

Figure 5.5 Gaussian distribution function; μ= 0 σ=1.

In order to perform the conversion equation 5.2 was used. (Gulvanessian, Calgaro, & Holicky, 2010). From the application equation 5.2 a 9,05% was obtained as maximum failure probability in a return period of 949 years, meaning that any displacements from previous analyses should have a failure probability equal or minor to 9,05% in order to be reliable. Therefore a displacement with an approximately 9% of exceedance was taken from the fitted distribution of 50_recordings for both directions. So like in previous analysis the values will be the reference to compare with the average displacements from earthquake parameters.

$$P_n = 1 - (1 - P_1)^n$$
$$P_{949} = 1 - (1 - 10^{-4})^{949}$$ Equation 5.4 Failure rate conversion
$$P_{949} = 0{,}0905\ (9{,}05\%)$$

5.4.2 Statistical analysis for 50-recodings set.

From 50-recording set a function fitting distribution was performed in order to obtain the reliability of an average response and compare it with the required with current codes. A Matlab analysis was performed with 17 different distribution functions for continuous variable. This study was mainly divided in 2 sections: first best fitting according to a distribution function and then its evaluation with a chi squared test (Nikulin, 1973) . As a result Gamma distribution came out with the higher probability of occurrence: a 90% for X direction and 91% for Y direction.

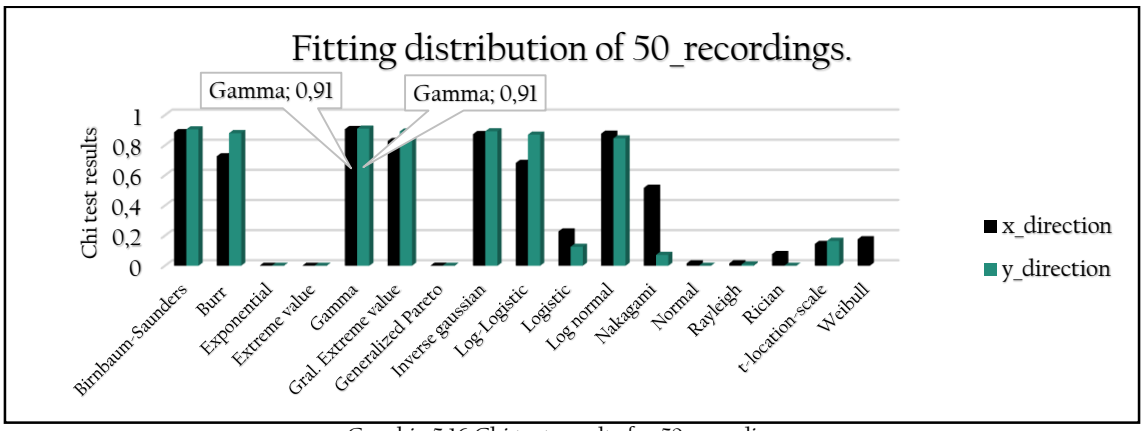

Graphic 5.16 Chi test results for 50 recordings.

Reliability analysis for 50_recordings.

Graphics 5.17 presents the probabilistic density function (PDF) and probabilistic cumulative function (CDF) using the gamma distribution for 50_recordings results on X direction. From this graphic it can be appreciated that X direction describes a wide curve which denotes a certain deviation among values. The difference between a 50% and 9% exceedance values was determined and it can be observed that displacement increases from 36 mm to 57,25 mm (60,33% raise) to satisfy current codes. Moreover the failure rate obtained with an average response is 7,03e-04, which means a 7 times greater value than the failure rate prescribed in current codes.

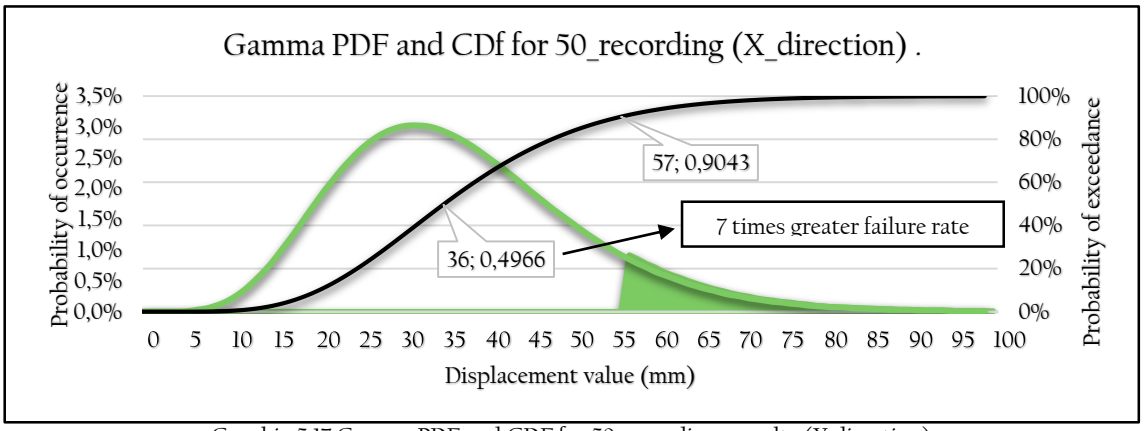

Graphic 5.17 Gamma PDF and CDF for 50_recordings results (X direction).

On the other hand Y direction results are presented in graphic 5.18. Herein Y direction describes a narrower curve than X direction, which means it presents an inferior variability among results and a lower deviation. Likewise X direction if an average value is considered a 7 times greater failure rate is being considered. Moreover it is also perceived a significant increment of the displacement value (from 27,5 mm to 44 mm) in order to satisfy code reliability conditions. This increment represents a 60% from the considered initial value, which is very similar to the 60,335% obtained from X direction.

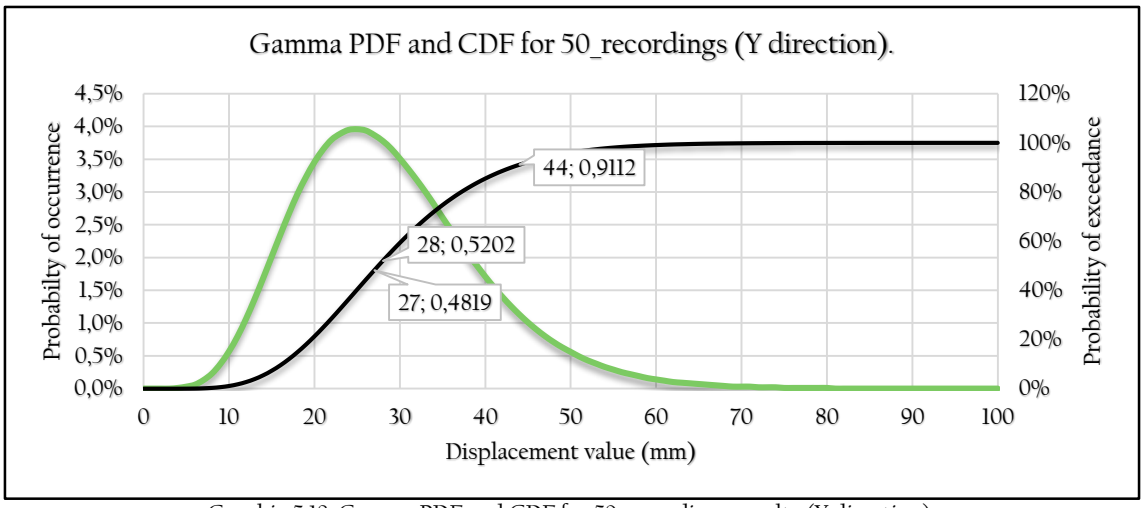

Graphic 5.18 Gamma PDF and CDF for 50_recordings results (Y direction).

5.4.3 Statistical analysis for 30 recordings.

Likewise for 50 recordings a fitting distribution was performed for 30_recordings results varying the earthquake parameter. These results are displayed on graphic 5.19 with 50_recordings results to make some comparisons. The first aspect to notice is the variability of best fitting distribution. This is verified when among 6 results (excluding 50_recording analysis) there are 4 different functions distributions. Likewise there is a wide range of the probability of occurrence of the chi test result since there are observed values from 52,18% to 97,25%. From this situation it is believed that 30 recordings still could be a small size to find function distributions due to earthquake uncertainties and randomness.

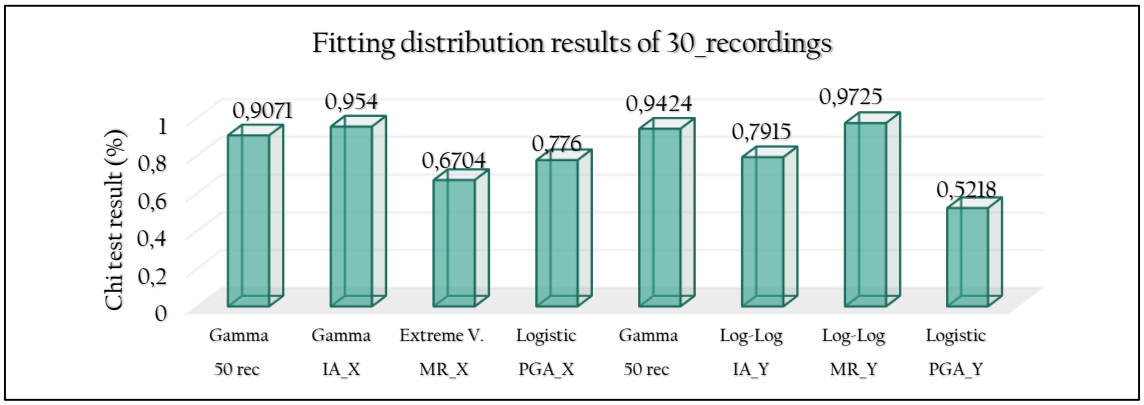

Graphic 5.19 Fitting distribution results of 30_recordings.

Reliability analysis for 30_recordings.

The procedure previously describe was repeated for 30 recordings analysis. Then 50_recordings results were contrasted with obtained reliable displacements from the earthquakes parameters in order to determine its feasibility and efficiency. Graphic 5.20 presents the reliable displacements against 50_recordings results. Magnitude and Radio denotes in the X direction the highest value for codes prescription. On the other hand for Y direction the greatest value was acquired from PGA analysis with a 45,80mm. It is important to highlight that despite the variability of founded distributions no significant differences were appreciated due to earthquake parameter variation.

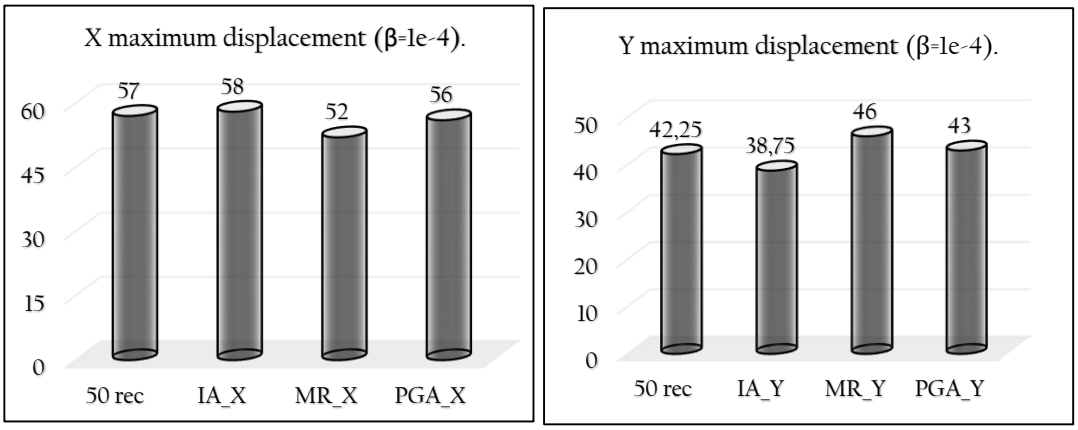

Graphic 5.20 Maximum displacements by earthquake parameter. (30 recordings)

Graphic 5.21 presents a comparison throughout increments of the maximum displacement values. Graphic 5.21 presents displacements with a 50% of being exceeded and a light green part (increment) denotes the augment of the maximum displacement to achieve the code reliability. It can be seen that Magnitude and Radio (X direction) presents the lowest percentage increment while the greatest increment was obtained from Arias Intensity in the same direction. Furthermore it is important to note that Y direction increments are very similar (45%-47%) with the exception of Arias intensity (38%). Whereas for X direction percentage increments have a larger range of variation from (25%-51%).

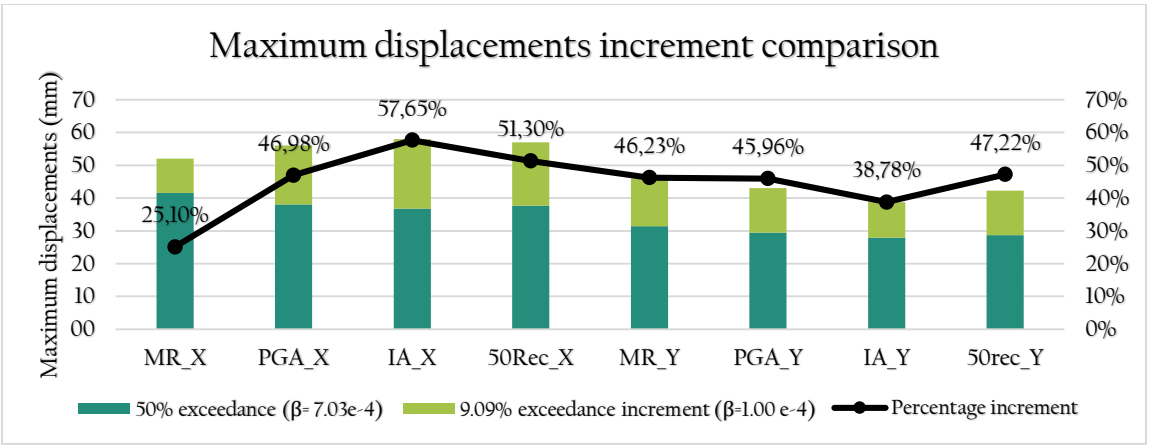

Graphic 5.21 Maximum displacements increment comparison. (30 recordings & 50 recordings)

5.4.4 Statistical analysis for 7-recording set.

Even though 30-records behavior was studied, professional engineers in real life do not have the time to perform this amount of analysis, so a conventional analysis of 7-records set was realized to determine its behavior. Aiming to recreate the 7-recording scenario as closer to reality as possible, 12 best- recordings were extracted from each parameter and all possible combinations (792) were studied. From this combinations a distribution fitting was intended, shown in graphic 5.22. As a result for fitting distribution trial a final function distribution was not reached since the highest probability of occurrence was 27.65% which means that a 72.35% of the times it does not belong to this distribution.

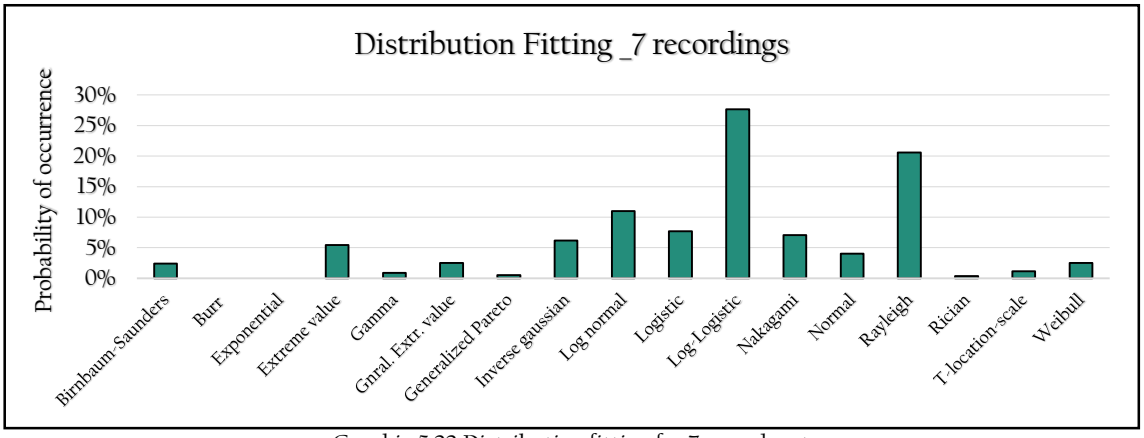

Graphic 5.22 Distribution fitting for 7 records set.

5.5 Results from near field recordings

In order to analyze near field recordings same procedures from far field were applied, such as positive and negative analysis of recordings. However the amount of results was significantly reduced due some variances found. One of these differences is that earthquake parameter variation analysis was not be performed since the search parameters from the PEER database were different. Nevertheless, although parameters would have been exactly the same from far field databases, there is a significant possibility that compatible results per parameter would have been under 30 recordings since without any parameter in specific only 35 feasible records were found. As a result, instead of three studies (one per earthquake parameter) a single 30-recording analysis was performed. Moreover both 50-recordings analysis and comparison among 30 & 50 recordings were not completed due to a lack of compatible records.

Turning to 7-records analysis, the exact same procedure from far field analysis was conducted for the 792 combinations recreation. Likewise 30-recordings analysis, comparison among 50-recordings and 7-recording was not possible due to a lack of feasible events.

5.5.1 Results from modeling stage.

Results from 30-recordings.

From graphic 5.23, it can be observed that for a smaller amount of displacement considered (less than 15) it presents a slight positive slope which disappears as the number of displacements considered is increased. This is verified when 7 displacements are considered a 25 mm average displacement is found while for 14 recordings a 33 mm, representing an increment of a 32% increment. However, it seems to become more stable for larger values. For instance, 22 and 60 values shows the same average displacement 30 mm. Moreover, if initial behavior (from 7 to 18 values) is neglected, difference between both directions seems to be unchanged by the increment of displacements.

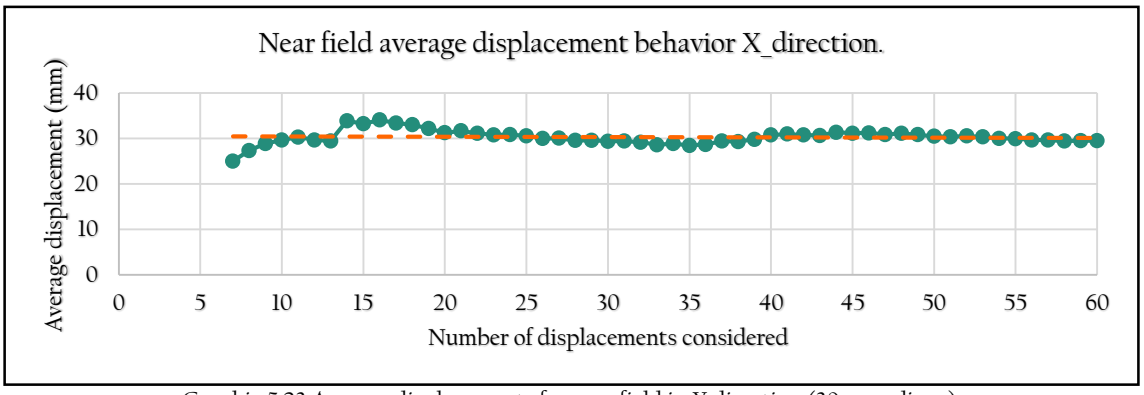

Graphic 5.23 Average displacements for near field in X direction (30 recordings).

Concerning to Y direction (represented in graphic 5.24), it is perceived a slight negative slope when a small number of displacements. However analogously to X direction as the number of displacements considered is increased it seems to increase stability. This is verified when the average for 20 observed displacements is 19mm while for 60 displacements is 20 mm. Finally it is important to note that the biggest deviation among results is only 4mm, which implies more stability than X direction for present case study.

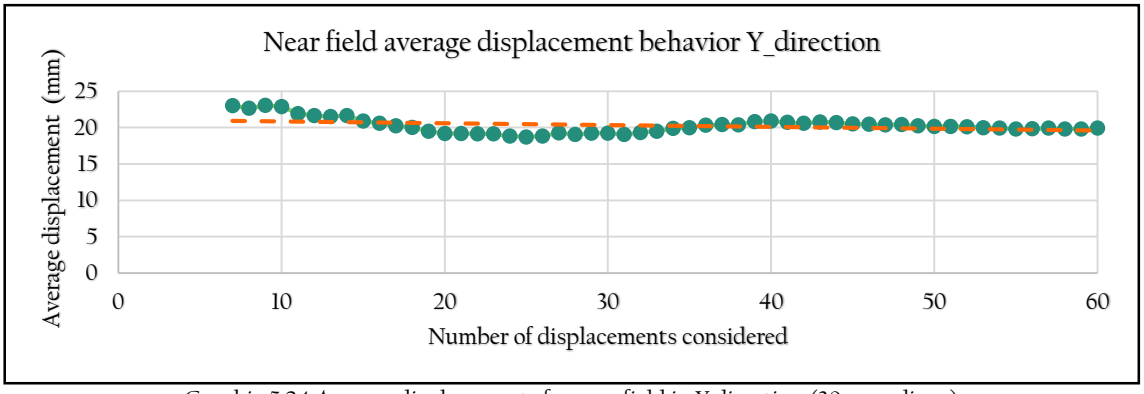

Graphic 5.24 Average displacements for near field in Y direction (30 recordings).

Results from 7-recordings.

The average displacement behavior for X direction is displayed on graphic 5.25. It can be perceived that X direction average results presents a significant fluctuation of the values with and slight negative slope. Being more specific the average displacements oscillate from 26 mm to 47 mm, representing an increment of 83,07%. Although there is a strong instability among results, it can be appreciated that the averages oscillates around (36,5 mm) which can be considered the median value of the combinations.

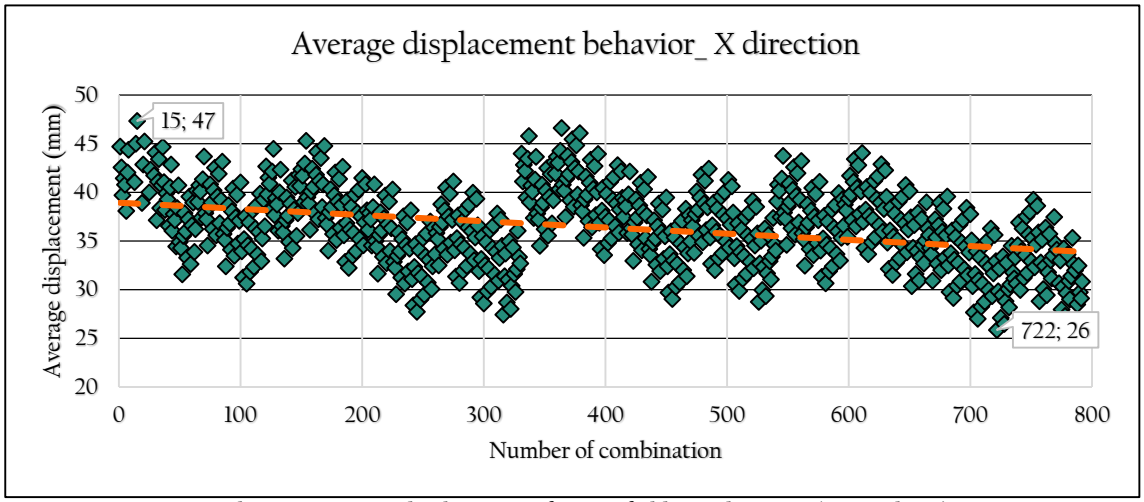

Graphic 5.25 Average displacements for near field in X direction (7 recordings).

Graphic 5.26 presents the Y direction average results from near field earthquakes. Y direction presents an inferior oscillation than X direction. Moreover Y average displacements fluctuates from 20mm to 30mm (a 54,22% increment) almost 33% lower than X displacements. This reduction of the variability can be a consequence of the stiffness increment from the case study. Fur

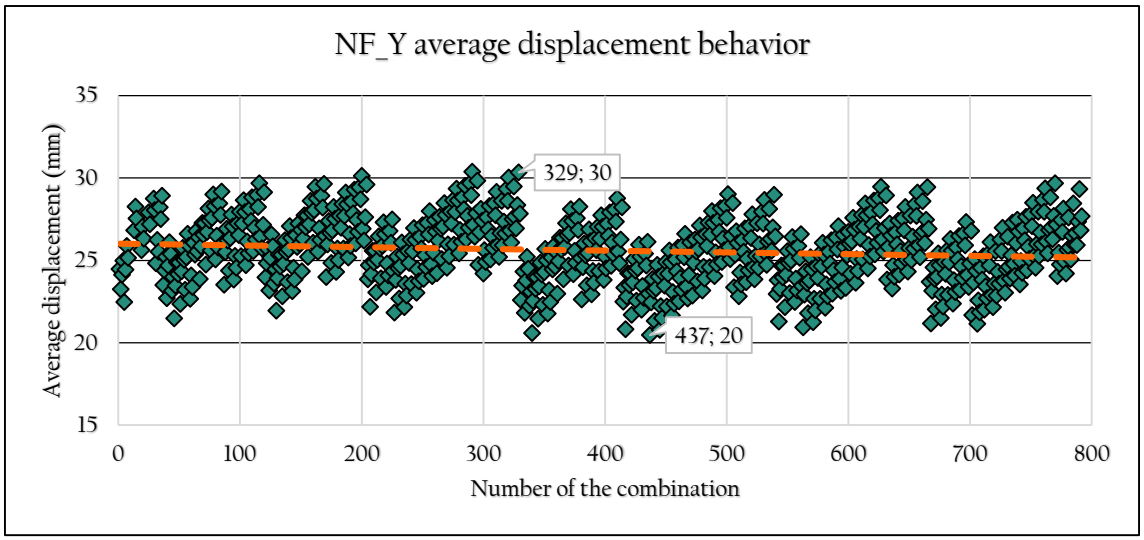

Graphic 5.26 Average displacements for near field in Y direction (7 recordings).

5.5.2 Results from statistical stage.

Fitting distribution.

Same proceedings from far field earthquakes were performed for near field analysis. This implies that distribution data was fitted to 17 different functions and its probability of occurrence was determined by chi test throughout MATLAB software. Graphic 5.27 presents the chi test results from fitting distribution. It can be observed that Log-Logistic is the distribution that bests fits near field analysis with 89,92% for X direction and 89,81% for Y direction.

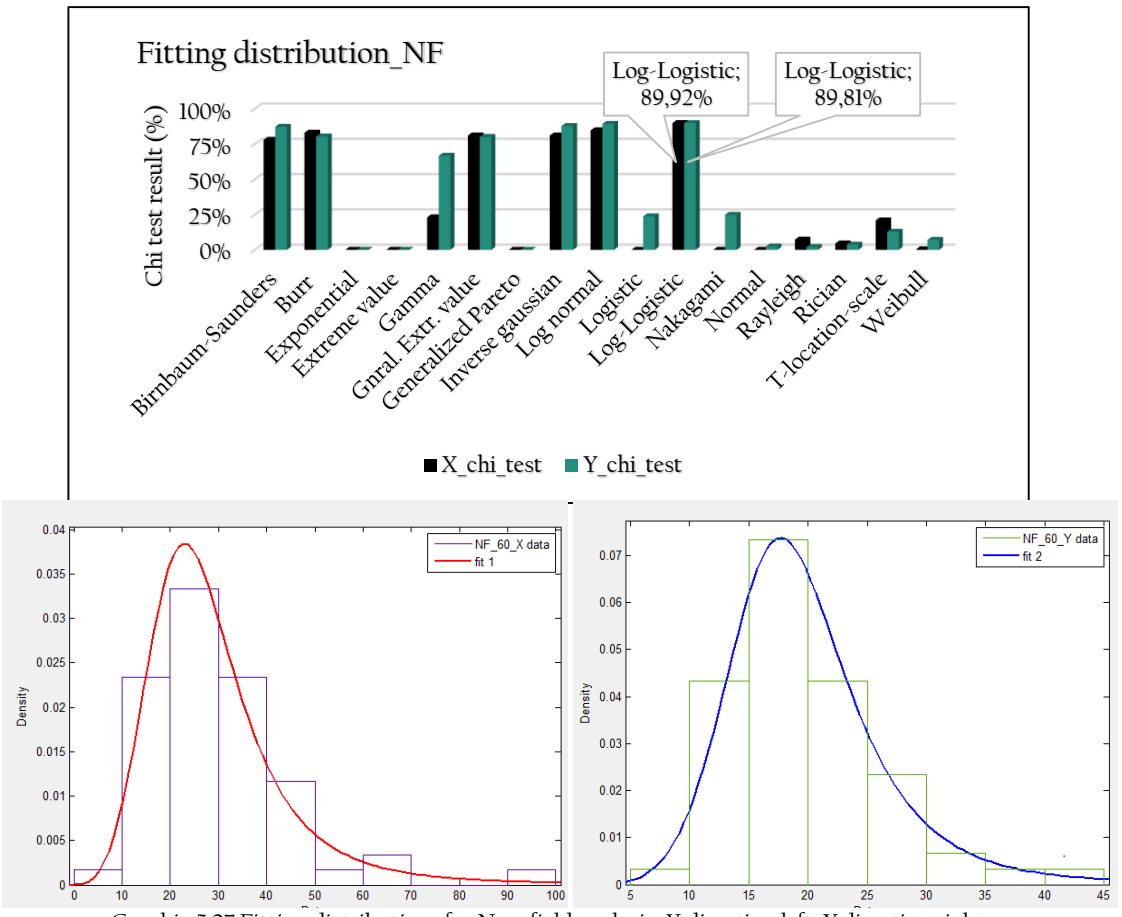

Graphic 5.27 Fitting distributions for Near field analysis; X direction left, Y direction right.

Graphics 5.28 presents the probabilistic density function (PDF) and probabilistic cumulative function (CDF) using the log-logistic distribution for near field results on X direction. From this graphic it can be appreciated that X direction describes a wide curve which denotes a certain deviation among values. The difference between a 50% and 9% exceedance values was determined and it can be observed that displacement increases from 26,50 mm to 48,75 mm (83,96% raise) to satisfy current codes. Likewise previous studies, if average value is considered the failure rate is 7,03e-04, meaning a 7 times greater value than the current code failure rate.

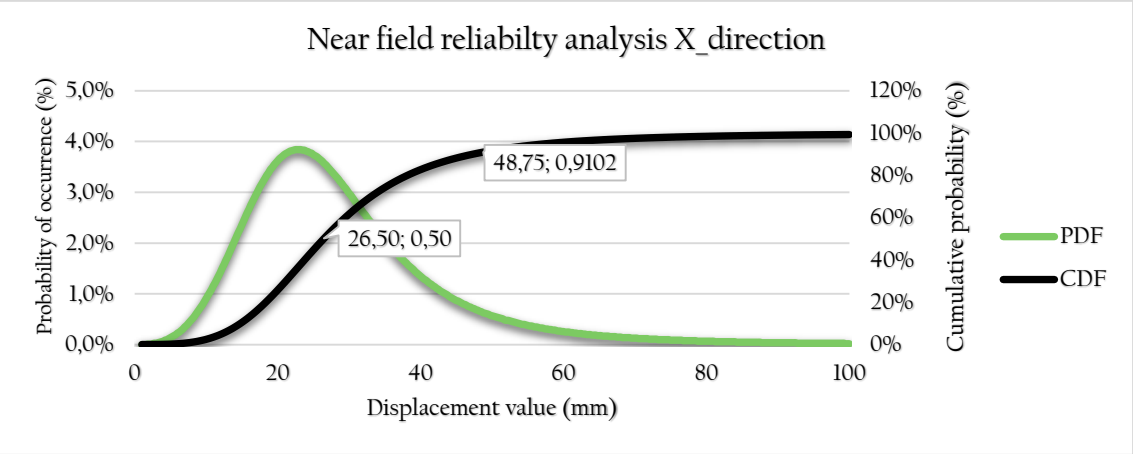

Graphic 5.28 Near field reliabilty analysis in X direction.

Graphics 5.29 presents the probabilistic density function (PDF) and probabilistic cumulative function (CDF) using the log-logistic distribution for near field results on Y direction. It is perceived a significant increment of the displacement value (from 19 mm to 29,50 mm) in order to satisfy code reliability conditions. This increment represents a 55,26% from the considered initial value, which is significantly minor than the 83,96% obtained from X direction. Herein Y direction describes a narrower curve than X direction, which means it presents an inferior variability among results and a lower deviation.

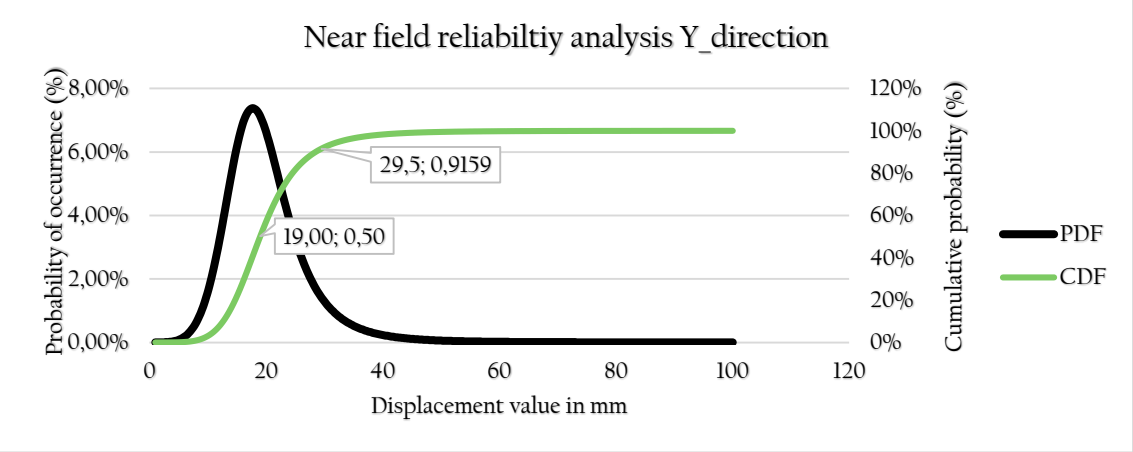

Graphic 5.29 Near field reliabilty analysis in Y direction.

5.6 Displacement Reliability Upgrade Procedure (DRUP)

5.6.1 Motivation of the procedure.

There is an absence of distribution function for 7_recordings. Therefore a statistical analysis of 792 combinations was performed to understand its characteristic in order to propose a procedure that allows to get reliable displacement trying to take as much minor times the maximum displacement. Graphic 5.30 present an example of average behavior of 7-recording set. It can be seen that it is has a considerable amount of fluctuation. Moreover average rounds near to 41mm with a standard deviation of 7mm.

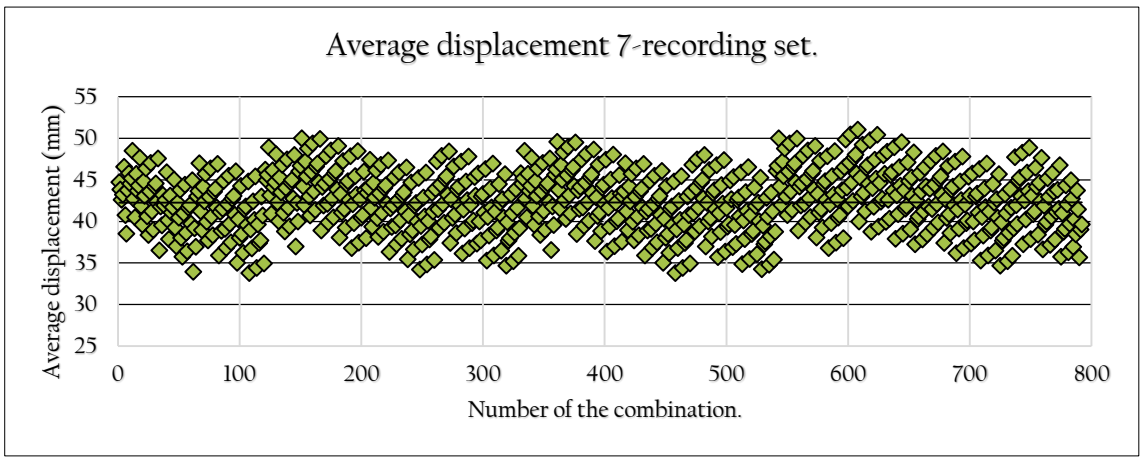

Graphic 5.30 Average displacement of 7-recording set.

5.6.2 Development of the procedure.

This procedure was developed using common statistical characteristics such as standard deviation, median value and average. Moreover its main objective is to obtain from the 792 combinations at least a 90% of reliable values minimizing as possible the selection of maximum value as final displacement. Since current codes prescribes for Building E case a reliable value with only a 9% of being exceeded, the desirable range is between average value and major observed displacement.

Table 5.4 presents the actual situation and how the procedure intervenes. In general terms, the average value is always outside the desirable range, indicating that always a different final value will be obtained. From Table 5.4 can be appreciated that there are 2 ways to get into the desirable range: increasing the average displacement or decreasing maximum value. Moreover this decision mainly depends on the distance among average and major displacement. Hence the procedure establishes in which situation is the evaluated 7-recordings set and takes an action.

Situation	Procedure intervention
1. 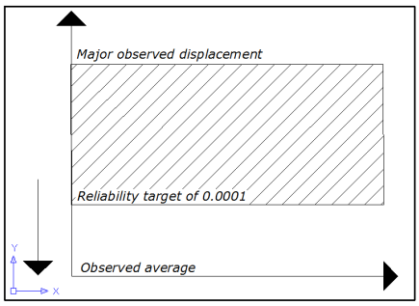	In the situation number 1, the major value is too distant from average, so in order to get a reliable value is more accurate to reduce the major value than increase the observed average.
2. 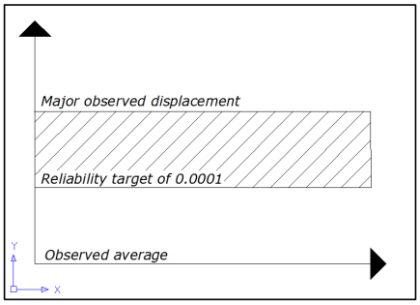	In situation number 2, major value is not distant nor close from average so, a there is no security to get in a reliable range by reducing the major value or increasing the average.
3. 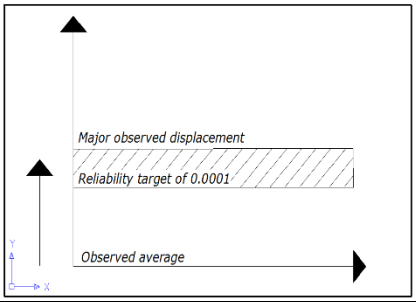	In Situation 3, the difference between major value and average is small. In order to get a reliable value would be more secure if the average is increased than reducing the major observed value.

Table 5.4 Procedure Intervention from actual situation.

5.6.3 Description of the procedure.

This procedure consists in a classification of the 7-recording set in terms of its own statistical conditions and taking into this classification average value will be increased or maximum value will be reduced to satisfy reliability values. In order perform this cataloguing a Dispersion Factor (DF) is calculated from 7-recordings set results, see equation 5.3 from table 5.5. This factor mainly depends on 2 aspects: the median value of the set and the 7-recording set Major Value Influence (MVI), which is the squared difference among the average of the whole set and the average without the major value, described on equation 5.4 from table 5.5.

Equation	Components Equation Description
$DF = \frac{MVI}{Median^{\,2}}$ Equation 5.5 Dispersion Factor	MVI is the major value influence in the set Median is the central value of when the results are sorted in ascendant.
$MVI = (set\ average^{\,2} - average\ without\ major^{\,2})^2$ Equation 5.6 Major Value Influence	Set average takes into account all the results (7 values). Average without major neglects the greatest one, which means only 6 values are considered.

Table 5.5 Deviation Factor (D.F) and Major Value Influence (M.V.I)

After the Dispersion Factor is computed, 3 different outcomes are possible according to previous interventions mentioned in table 5.4. As a result, table 5.6 presents the possible outcomes and its final displacement value. It can be appreciated that even though median value and major value influence are used during DRUP procedure, after dispersion factor is calculated the standard deviation is the only parameter used to modify the final displacement (FD). Unless there is not possibility of modification and major value should be considered as final displacement.

Dispersion Factor possible outcome	Final displacement value (FD)
DF is major than a 90, meaning that major value is too dispersed from central values and it needs to be reduced.	The major value is reduced by standard deviation. $FD = Mv - \sigma$
DF is between 90 and 50, meaning that dispersion of the set is regular and no action is needed.	Major value $FD = Mv$
DF is below 50, meaning that major value it too close from central values.	Average result is increased 2 standard deviation. $FD = Av + 2\sigma$

Table 5.6 Final displacements values from DRUP procedure.

5.6.4 Example application of the procedure.

A summary of DRUP procedure is shown in figure 5.6 to clarify the methodology. It mentions the major parts from the method along with a brief description below. This summary is followed by the presentation of three examples representing each possible outcome, respectively, see table 5.7. From these examples it can be seen that major final displacements outcomes will always come from the second situation since it takes the major value of the set without any modification.

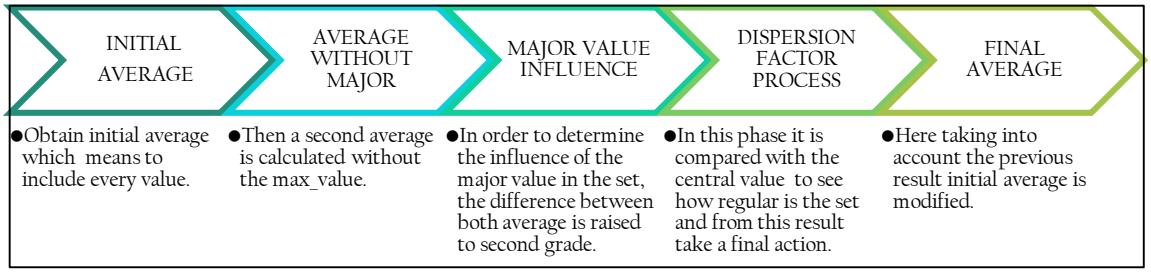

Figure 5.6 Summary of DRUP procedure.

First situation (major value is distant from average)			
Name of the phase	**Dimension**	**Formula**	**Values**
Sorted maximum displacements (MD) values	mm	Values organized from minor to major.	18,106_18,905_37,571_41 ,415 45,843_58,573_ 74,324
Standard deviation of the set	mm	$SD=\sqrt{\frac{\sum(x_i-m)^2}{n-1}}$	20,242
Average of the set	mm	$average_{set}=\frac{\sum_{i=0}^{7} MD_i}{7}$	42,105
Average (without major value)	mm	$average_{wmv}=\frac{\sum_{i=0}^{6} MD_i}{6}$	36,733
Major Value Influence (M.V.I)	mm⁴	$MVI=(42{,}105^{\,2}-36{,}733^{\,2})^2$	179.232,102
Dispersion Factor (DF)	mm²	$DF=\frac{179.232{,}102}{41{,}415^{\,2}}$	104,496
Final Displacement	mm	$FD=74{,}324-20{,}242$	**54,082**
Second situation (is not distant nor close)			
Sorted maximum displacements (MD) values	mm	Values organized from minor to major.	18.106_18.905_ 27.679_28.009 37.571 _41.415_58.573
Standard deviation of the set	mm	$SD=\sqrt{\frac{\sum(x_i-m)^2}{n-1}}$	13,4638
Average of the set	mm	$average_{set}=\frac{\sum_{i=0}^{7} MD_i}{7}$	32,894
Average (without major value)	mm	$average_{wmv}=\frac{\sum_{i=0}^{6} MD_i}{6}$	28,614
Major Value Influence (M.V.I)	mm⁴	$MVI=(32{,}894^2-28{,}010^{\,2})^2$	69.297,77
Dispersion Factor (DF)	mm²	$DF=\frac{179.232{,}102}{41{,}415^{\,2}}$	88,333
Final Displacement	mm	$FD=58.573$	**58,573**
Third situation (average and major values are close)			
Sorted maximum displacements (MD) values	mm	Values organized from minor to major.	18.106_18.90_ 27.679_37.571 38.83_41.415_45.843
Standard deviation of the set	mm	$SD=\sqrt{\frac{\sum(x_i-m)^2}{n-1}}$	11,094
Average of the set	mm	$average_{set}=\frac{\sum_{i=0}^{7} MD_i}{7}$	32,621
Average (without major value)	mm	$average_{wmv}=\frac{\sum_{i=0}^{6} MD_i}{6}$	30,417
Major Value Influence (M.V.I)	mm⁴	$MVI=(32{,}621^{\,2}-30{,}417^{\,2})^2$	19.297,77
Dispersion Factor (DF)	mm²	$DF=\frac{19.297{,}77}{37{,}571^{\,2}}$	13,671
Final Displacement	mm	$FD=32{,}621+2*11{,}094$	**53,162**

Table 5.7 Examples from DRUP procedure.

5.6.5 Application of DRUP procedure (results for far field analysis).

The graphic below displays the modified average displacements from Arias Intensity case for X direction (IA_X). It can be appreciated that most of the cases were rounding 45 mm and after procedure they oscillates around 60 mm while the target was 57mm. Moreover it can be seen that after DRUP procedure values oscillates from 50mm to 65 mm, if maximum values cases are neglected. Similar results were obtained for the rest of earthquake parameters and directions. As a consequence a summary is presented in graphic 5.31, for further references refer to annex 1.

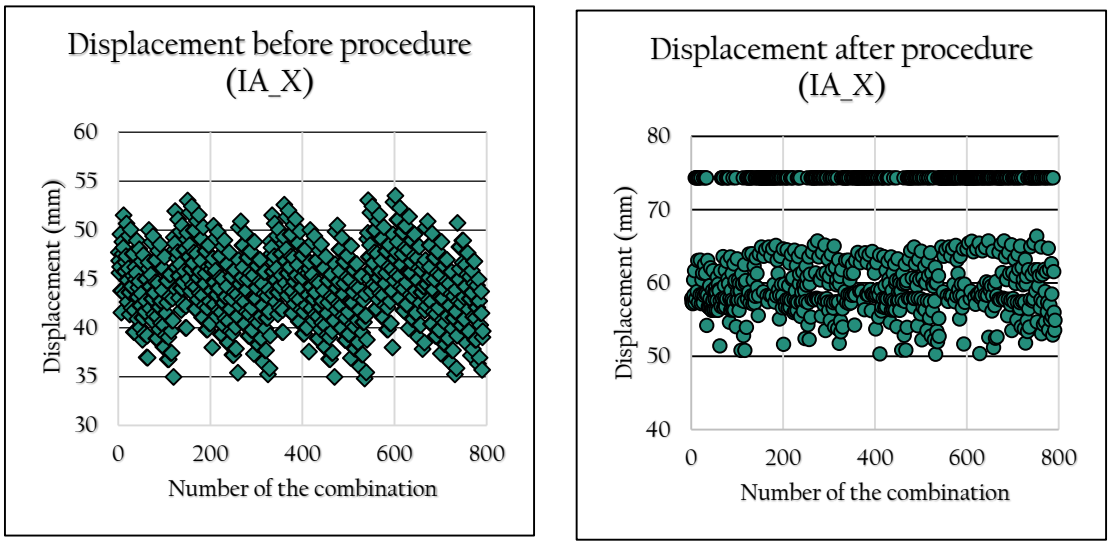

Graphic 5.31 Displacements before and after DRUP procedure

Graphic 5.32 presents two different aspects: the percentage of displacements above threshold and the percentage of results that are equal to the maximum displacement of the set. Most of the cases exceed the threshold with a percentage near or superior than 90%. Whereas the percentage of results equal to maximum displacement presents feasible outcomes most of the time; with the exception of Magnitude and Radio in Y direction where a 60% percent was observed.

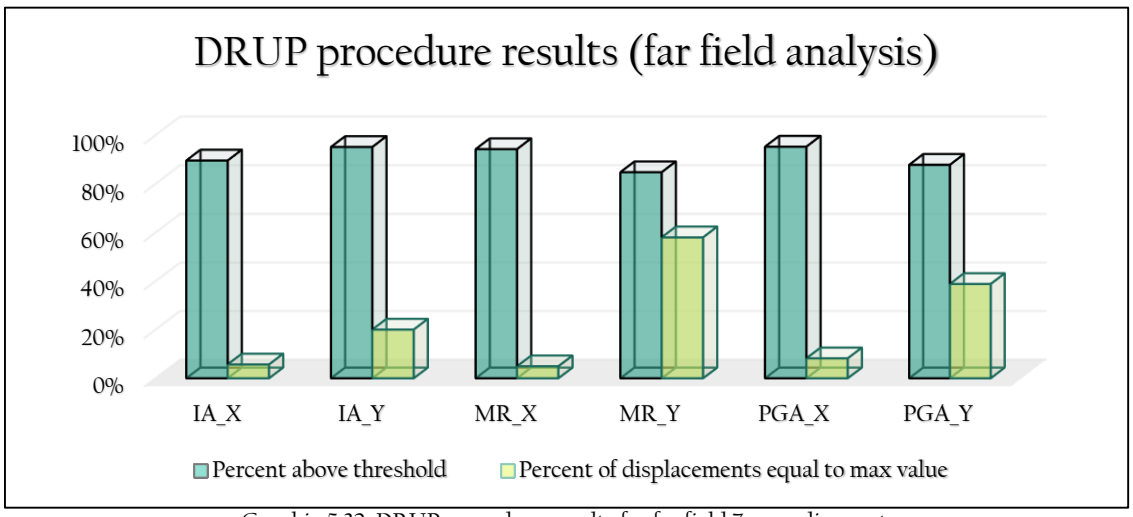

Graphic 5.32 DRUP procedure results for far field 7-recordings sets.

5.5.6 Application of DRUP procedure (results for near field earthquakes).

The graphic below presents near field earthquakes displacements results before and after DRUP procedure for X direction. It can be seen that values were oscillating around 37.5mm and after DRUP procedure they oscillate around 55mm while target was 47,25mm. This is a consequence of the relationship between the standard deviation and the procedure.

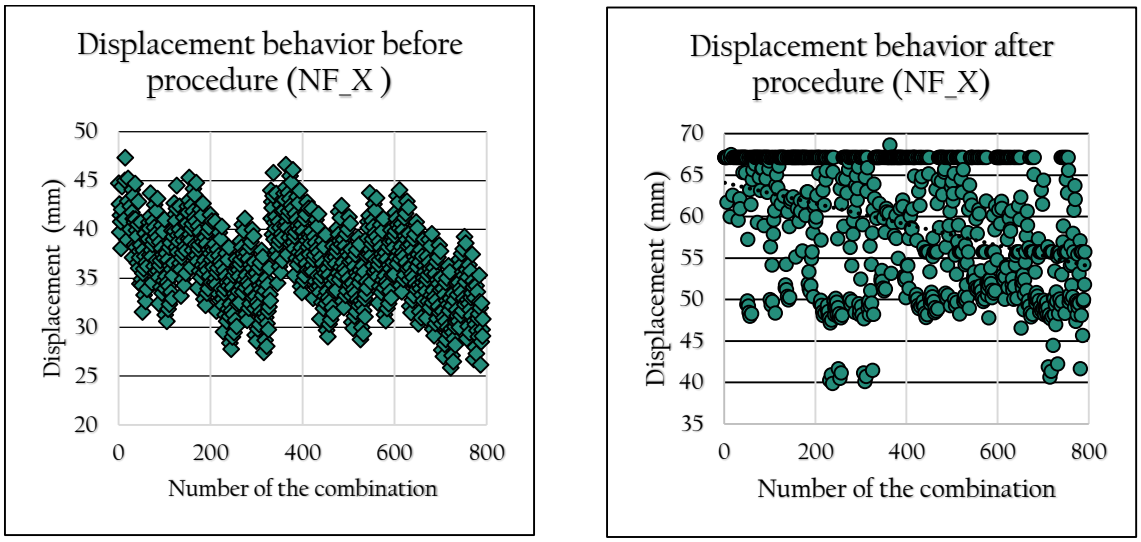

Graphic 5.33 Average displacement behavior of Near field analysis.

The percentage above threshold and the percentage of final displacements equal to max value were calculated using previous same procedure. The obtained results are described in graphic 5.27. It can be appreciated that Y direction presents a large percentage of maximum value used. It is considered that among the causes is that Y direction presents standard deviation under 10mm most of the time. Therefore further analyses should be performed.

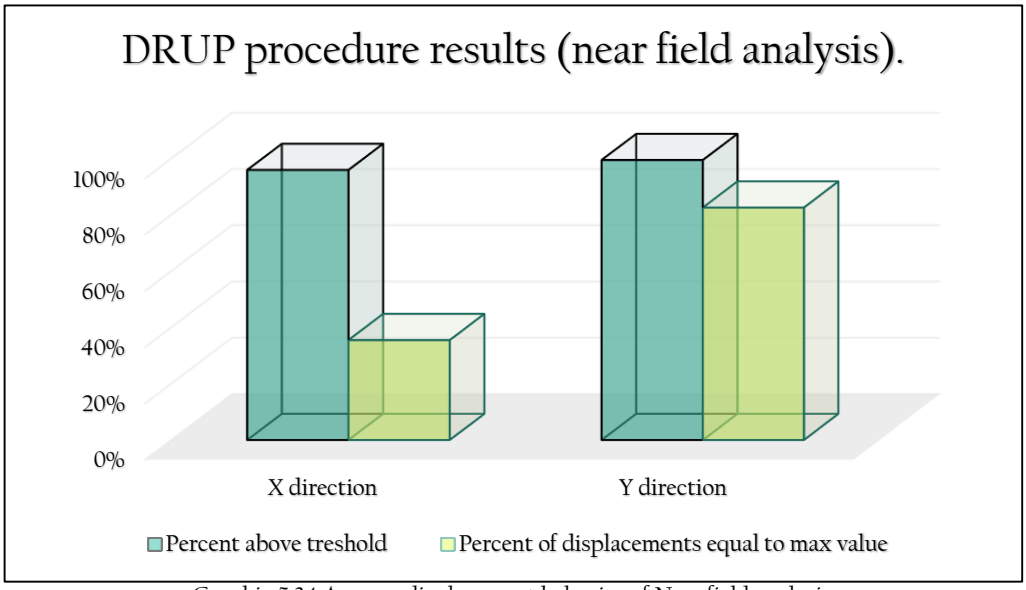

Graphic 5.34 Average displacement behavior of Near field analysis.

5.5 Comparison among far field and near field.

Herein a comparison is presented in terms of the minimum increment required to achieve current reliability prescriptions for far field and near field result. Nevertheless is important to mention that conditions among earthquakes types presents some differences. Hence this comparison is merely descriptive of the found results and an ulterior conclusion cannot be considered. Graphic 5.35 presents how the considered maximum displacements for an average value with an (7e-04 reliability) is increased to reach the minimum (1e-04). It can be appreciated that near field responses are inferior to any of the far field result. Likewise near field presents the largest increments in order to get the minimum reliability value. Nevertheless near field values remains with the smallest displacements from the complete study.

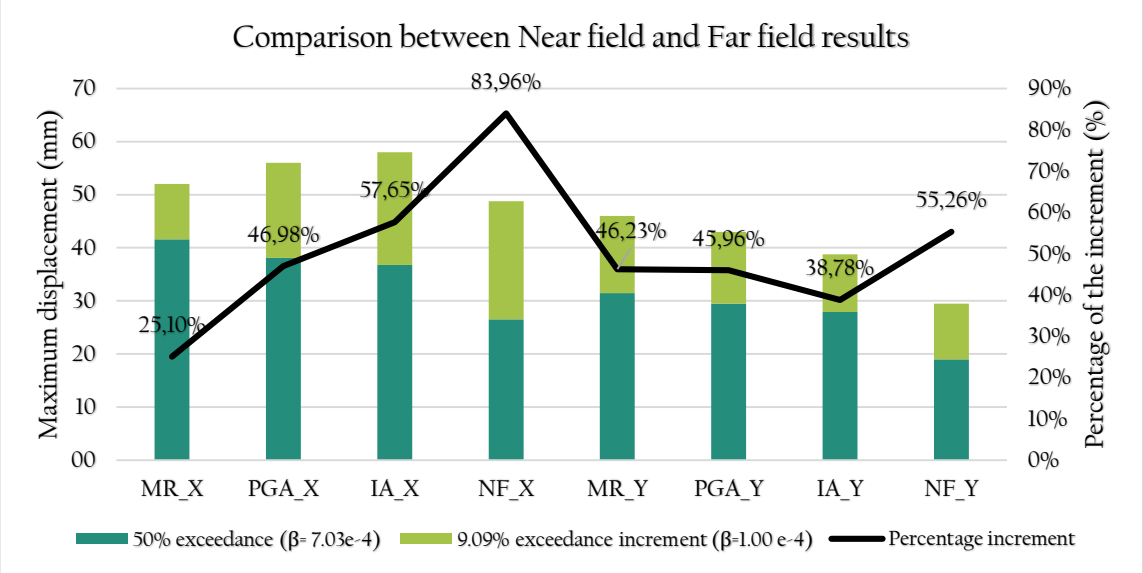

Graphic 5.35 Comparison among near field and far field displacements results.

6. CONCLUSIONS & RECOMMENDATIONS.

This sections presents the observations from general and specific objectives. Likewise herein it is defined the innovative aspects of the research along with recommendations for further developments.

6.1 General observations.

Nonlinear dynamic analysis has evolved from a calibration method to the most accurate tool for seismic assessment. In the same manner natural earthquakes recordings are becoming more popular as a dynamic analysis input. Consequently there is a clear need of adequate ground motion selection procedures and nonlinear dynamic reliable results.

Therefore average displacement behavior has been observed from modeling results of a RC retrofitted building from 1970s. Among general observations it is found that average results tend to be stable when the number of observed recordings is higher than 30, which means 60 observed displacements since both directions (positive and negative) have been considered. Moreover from the variation of the earthquake parameter, Magnitude and Radio (MR) presents the highest average of maximum displacement for both directions. Therefore MR is considered the "safest parameter" since in case of unreliable values it will have the lowest failure probability. Conversely, Arias Intensity (IA) was the parameter with the lowest maximum displacement average, which implies worse reliability values. Nevertheless it is important to mention that observed differences

On the other hand from the average maximum displacement contrasting between far and near field, the latter one has shown the inferior values. However this result should not be extrapolated to another structural response since near field analysis takes into consideration the vertical component, which surely alter (with a greater impact than displacement) the rest of structural responses.

Finally from statistical analysis it is concluded that no average response (value with a 50% probability of being exceeded) satisfies the reliability index prescribed for Building E study case in the EN-1990 standard. As a consequence from fitted distribution functions a value with a 9% probability of being exceeded is suggested for 30-recordings analysis. Whereas for 7-recordings analysis a procedure called DRUP is proposed since no distribution function was founded. Such procedure aims to achieve current reliability prescriptions at least 90% of the time.

6.2 Specific conclusions.

In this section far field and near field findings are separately presented and compared. In the far field section, conclusions related to the variation of the selection earthquake parameter are detailed. Likewise findings about the influence of set increment in the average response are described. In near-field section only the effect of recordings increment in the average response is discussed since the amount of feasible events is significantly lower.

6.2.1 Far Field findings.

→ Identification of 3 earthquakes parameters.

From literature review analysis it is concluded that Radio and Magnitude (RM) is one of the simplest approach to define a seismic event. Moreover Peak Ground Acceleration (PGA) is considered one of the most popular earthquake parameter since in the beginning of seismic analysis most of structures were low-rise (rigid). This implies that their worst situation are short-lived earthquakes where PGA has its greater efficiency. Nevertheless PGA is not useful for all structures since nowadays buildings have a wide range of height. As a consequence integral parameters have been proposed such as Arias Intensity (IA) which measures ground motion strength in terms of velocity (m/s).

Consequently MR, PGA and Arias Intensity (IA) were selected as parameters for the ground motion selection process. However it does not implies that the rest of available parameters should not be used for ground motion selection. This categorization was realized because there was a limited computational and time capacity. What it is more it is encouraged to realize further investigations with more parameters.

→ Definition of feasible databases for ground motion.

European, Italian and Simbad databases were available for far-field ground motion selection. Nevertheless after a preliminary analysis Italian database was neglected due to the little amount (less than seven in all cases) of feasible records viable records for the seismic hazard and soil conditions of Building E case. In addition from previous exploration and conditions Simbad is considered the most efficient database of the group for our study case. In other words, Simbad has the largest quantity of feasible events with scale factor closest to unity.

→ **Ground motion set assembling.**

European and Simbad databases provided at least 40 recordings per each earthquake parameter. Hence a categorization was required in order to arrange a 30-recordings and 7-recording sets. The applied procedure basically consisted in a classification by scale factor, deviation factor and a visual cataloguing of (exceedance or deficit) from target spectrum. Moreover two deviation factor were determined (partial and total) to prioritize the range $0.2T_1$-$2T_1$ where no value should be minor than 90%.

From ground motion 30-recording assembling, Magnitude and Radio presented the lowest partial deviation (3.06%) and the highest total deviation (10.48%) from the reference average spectrum. Likewise MR was the parameter with the largest difference between partial and total deviation with a 6.42% while PGA and Arias Intensity shown 0.58% and 0.02%.

→ **Contrast average maximum displacement according to earthquake parameter.**

From the evaluation of sets with a 90% of confidence (30 recordings sets) following conclusions were obtained: PGA is considered the most unstable parameter since it presented the highest deviation more than 30% on both directions. In general terms, Arias intensity is the most stable parameter since it has shown the lowest deviation (less than 20% for both directions). Conversely if only one direction is considered Magnitude and Radio (MR) presents the lowest deviation among results with a 14.358%. Moreover highest values of displacements were obtained from Magnitude and Radio selection. As a result MR is considered the safest parameter because in terms of reliability it will also have the highest value.

→ **Evaluation of the average response behavior.**

From increasing record analysis average maximum displacement the behavior showed notable divergences due to variation of the selection earthquake parameter. Magnitude and Radio displayed an increment tendency of the difference between orthogonal directions while PGA showed a very steady behavior all the time. Moreover Arias Intensity exhibited the lowest distance amid directions at the beginning of the evaluation. However after a few recording´s increment (10 observed recordings) the distance increased substantially and remained stable.

From 7-recordings analysis a constant fluctuation of values was detected in all cases. Among the observations are differences till 64% were appreciated. From this situation is inferred that there is a significant uncertainty respecting to the expected value from a 7-recording set. Besides it is important to note that Magnitude and Radio presented the largest exceeding (45.99%) and the shortest deficit (7.09%) from references values, which supports the general observation as the safest parameter.

→ **Reliability analysis**

The reliable reference value was obtained from 50-recordings set since it is the largest statistical population available. Then reliability index was calculated for average maximum displacement of 30-recordings sets and contrary to expected no average value satisfies EN-1990 prescriptions. On the other hand, reliability index of 7-recordings set could not be determined because no distribution function was properly adjusted with a feasible probability of occurrence.

Since for 7-recording sets no function was found to fit, a Displacement Reliability Upgrade Procedure (DRUP) was proposed in order to reach a reliable value as requested by the Eurocode EC0 for the considered case study. It consist in an average increment depending on statistical characteristics of the set. This procedure has managed to achieve a satisfactory displacement at least 90% of the times. Besides only for Magnitude and Radio (Y direction) was observed a high percent of cases where maximum value the searched value taken.

Despite of the differences founded on average displacement behavior analysis of 30-recordings, where Magnitude and Radio was denominated as the safest parameter. From reliability analysis the differences among reliable displacements were considerably lower from 30-recordings, which implies that earthquake parameters do not affect significantly

6.2.2 Near Field findings.

As explained in research restrictions near field analysis presented some limitations due to available data. Therefore there is no identification of earthquakes parameters since only one (multi-parameter) search was performed. Regarding to feasible databases definition near field recordings were obtained from Pacific Earthquake Engineering Research (PEER) database From this situation it is noteworthy to state that European near field information needs to be widen since it is generally know that soil conditions and types fault are different so there is an evident lack of knowledge in this field. Finally concerning to records assembling since only 30-recording were found there is no necessity of records classification.

→ **Evaluation of the average response behavior.**

Average response behavior of near field presented some divergences among 30-recordings and 7-recordings results. Likewise far field results 7-recordings presented a severe fluctuation among their results function distribution could not be found. From this situation, it is inferred that 7 is not a sufficient amount of samples in statistical terms.

→ **Reliability´s set determination**

After same procedures were applied for 30-recording near field sets, log-logistic was the distribution that best fitted for both direction with an approximate 90% of occurrence probability. Then the same situation was observed for 7-reccordings sets, no function was accurately fitted with a realistic probability of occurrence. Hence DRUP procedure was performed for 792 combinations and reliability was satisfactory more than 90% of the times.

→ **Comparison between Far Field and Near Field results**

The first difference between far field and near field results was the availability of ground motions. In my opinion was the most important difference since comparisons among earthquakes parameters could not be performed. Although near field and far field were matched to the same spectrum, ground motions from near field were shorter (time duration). As a result most of near field cases presented an inferior average structural response than far field. However this results should not be extrapolated to other structural responses.

Respecting to the statistical analysis, Gamma was the distribution that best fitted far field results while Log-Logistic was obtained for near field. This difference is attributed to near ground motion characteristics mostly short duration less than 20secs. Finally after DRUP application for 7-recordings sets, near field shows a larger percent of reliable displacements than far field. This could be a consequence of the standard variation, where near field presented a lower deviation, (graphics with an inferior dispersion of the points).

6.3 Innovative aspects of the research.

This thesis has taken into account recent scientific material from journals, conferences proceedings and other forms. Therefore this research presents 2 innovative features: natural earthquakes selection methods and reliability analysis. The first aspect makes emphasis on the research of an accurate earthquake parameter. Furthermore it provides a better understanding of the influence of these parameters in final outcomes of the analysis. Turning to reliability analysis it has been demonstrated the importance of its verification in order to fulfill the safety requirements from EN-1990.

6.4 Research restrictions.

Nowadays most of knowledge fields are very extensive and interrelated among themselves. As a result the introduction of restrictions in a research is a very common technique. This approach aims to narrow down the study field so that investigations can be completed in a feasible time with existing resources.

In this investigation some restrictions have been introduced due to computational capacity and available time. Among these limitations are: only one study case (Building E) and only one structural response (average maximum displacement) have been observed since both consume a large amount of time. In the same way only three (3) earthquake parameters have been employed for variation of ground motion selection procedure in order to reduce time-results processing.

However not every limitation was introduced at the beginning of the research planning. A fourth limitation was found during the investigation process. The analysis of near field earthquakes for nonlinear dynamic analysis is a very recent study subject. As a consequence the amount of available data is substantially inferior in comparison to far field ground motions. Hence in order to find a feasible amount of events (at least 30-recordings) more than one earthquake parameter was used at the same time. This means that near field analysis was performed only one time with a general characterization, which implies that no earthquake parameter in specific could be related to the selection procedure.

6.5 Future developments and recommendations.

The development of natural earthquakes selection methods permits an improved description of existing structures seismic behavior and a further enhancing of new structures seismic design. However an accurate set of ground motions is impractical if the reliability of the project is unknown. Hence this research contributes to acquire a better understanding of current available selection methods for real ground motions. Likewise a reliability analysis is presented as complement of the behavior study.

Nevertheless further studies are needed in order to get general procedures since restrictions were applied. Several ideas for continuing the research presented in this thesis may be considered. An immediate example may be represented by the modeling of structures from other materials and characteristics with an increment of selection earthquakes parameters. Likewise another one could be the observation of more than one structural response to perceive near field influence against far field.

7. REFERENCES.

Abrahamson, N. A., & Somerville, P. G. (996). Effects of the hanging wall and footwall on ground motions recorded during the Northridge earthquake. *Bulletin of the Seismological Society of Americal*, *86*, S93–S99.

Ammon, C. J. (2011). Earthquakes effects. Retrieved March 23, 2016 from http://eqseis.geosc.psu.edu/~cammon/HTML/Classes/IntroQuakes/Notes/earthquake_effects.html

Ancheta, T. D., Darragh, R. B., & Stewart, J. P. (2013). PEER ground motion database. Retrieved April 8, 2016, from http://ngawest2.berkeley.edu/

Arya, A. S., & Agarwal, A. (2002). Seismic Evaluation and Strengthening of Existing Reinforced Concrete Buildings. New Delhi: National Disaster Management Division. Retrieved March 25, 2016, from http://nidm.gov.in/PDF/safety/earthquake/link12.pdf

Bertaccini, A. (2014). *Vulnerabilitá Sismica di construzioni in c.a. ad uso civile site nell´area EX-C.O.O. di Ferrara. Corpi E-F*. Universitá degli studi di Ferrara.

Bolt, B. A. (2015). Earthquake. Retrieved April 4, 2015, from http://www.britannica.com/science/earthquake-geology

Bozorgnia, Y., Niazi, M., & Campbell, K. W. (1995). Characteristics of free field vertical ground motion during the Northridge earthquake. *Earthquake Spectra*, *11*, 515–525.

Bradley, B. A., Cubrinovski, M., Macrae, G. A., & Zealand, N. (n.d.). Ground Motion Prediction Equation for Spectrum Intensity Based on Spectral Acceleration Equations, (Im), 1–30.

Chambers, J., & Trevor, K. (2004). Nonlinear Dynamic Analysis - the Only Option for Irregular Structures. In *13th World Conference on Earthquake Engineering*. Vancouver, B.C., Canada.

Cornell, C. A. (1968). Engineering seismic risk analysis. *Bulletin of the Seismological Society of America*, *58*(5), 1583–1606. http://doi.org/http://dx.doi.org/10.1016/0167-6105(83)90143-5

De Weck, O., & Kim, I. Y. (2004). *Finite Element Method. Engineering Design and Rapid Prototyping*. Retrieved from http://web.mit.edu/16.810/www/16.810_L4_CAE.pdf

Douglas, J. (2003). Earthquake ground motion estimation using strong-motion records: a review of equations for the estimation of peak ground acceleration and response spectral ordinates. *Earth-Science Reviews*, *61*(1-2), 43–104. http://doi.org/10.1016/S0012-8252(02)00112-5

eurocodes.us. (2013). Nonlinear methods of analysis. Retrieved Febraury 20, 2016 from http://www.eurocode.us/earthquake-resistance-eurocode-8/nonlinear-methods-of-analysis.html

Fahjan, Y. M. (2008). Selection and scaling of real earthquake accelerograms to fit the Turkish design spectra. *Teknik Dergi/Technical Journal of Turkish Chamber of Civil Engineers*, *19*(SPEC. ISS.), 1231–1250.

Fahjan, Y., & Ozdemir, Z. (2008). Scaling of earthquake accelerograms for non-linear dynamic analysis to match the earthquake design spectra. In *14th World Conference on Earthquake Engineering*. Retrieved from ftp://ftp.ecn.purdue.edu/spujol/Andres/files/02-0165.PDF

Fardis, M. N. (2009). *Seismic Design, Assessment and Retrofitting of Concrete Buildings* (Vol. 8). Dordrecht: Springer Netherlands. http://doi.org/10.1007/978-1-4020-9842-0

Filiatrault, A., & Cherry, S. (1988). Comparative performance of friction damped systems and base isolation systems for earthquake retrofit and aseismic design. *Earthquake Engineering & Structural Dynamics*, *16*(3), 389–416. http://doi.org/10.1002/eqe.4290160308

Giovenale, P., Cornell, C. A., & Esteva, L. (2004). Comparing the adequacy of alternative ground motion intensity measures for the estimation of structural responses. *Earthquake Engineering & Structural Dynamics*, *33*(8), 951–979. http://doi.org/10.1002/eqe.386

Grimaz, S., & Malisan, P. (2014). Near field domain effects and their consideration in the international and Italian seismic codes. *Bollettino Di Geofisica Teorica Ed Applicata*, *55*(4), 717–738. http://doi.org/10.4430/bgta0130

Gulvanessian, H., Calgaro, J. ., & Holicky, M. (2010). *Guida all' Eurocodice Criteri Generali di Progettazione struturale: EN 1990*. (P. Rugarli, Ed.). Roma: EPC Libri.

Hancock, J. (2006). *The Influence of Duration and the Selection and Scaling of Accelerograms in Engineering Design and Assessment*. *Integration The Vlsi Journal*. University of London; Imperial College. Retrieved from www3.imperial.ac.uk/pls/portallive/docs/1/7293267.PDF

Housner, G. W., & Trifunac, M. . (1967). Analysis of accelerograms -Parkfield earthquake. *Bulletin of the Seismological Society of America*, *57*, 1193–1220.

Iervolino, I., Galasso, C., & Cosenza, E. (2010). REXEL: computer aided record selection for code-based seismic structural analysis. *Bulletin of Earthquake Engineering*, *8*(2), 339–362. http://doi.org/10.1007/s10518-009-9146-1

Iervolino, I., Maddaloni, G., & Cosenza, E. (2008). Eurocode 8 Compliant Real Record Sets for Seismic Analysis of Structures. *Journal of Earthquake Engineering*, *12*(February), 54–90. http://doi.org/10.1080/13632460701457173

INFP. (2006). Seismic Hazard. Retrieved April 4, 2016, from http://www.infp.ro/en/seismic-hazard/

Italian Department of Civil Protection. (2012). Seismic Risk. Retrieved April 5, 2016, from http://www.protezionecivile.gov.it/jcms/en/descrizione_sismico.wp

Kam, W. Y., & Pampanin, S. (2008). Selective Weakening Techniques for Retrofit of Existing Reinforced Concrete Structures. *14th World Conference of Earthquake Engineering*.

Kelly, J. ., Skinner, R. ., & Heine, A. . (1972). Mechanism of Energy Absorption in special devices for use in earthquakes resistant structures. *Bulletin of the New Zealand National Society for Earthquake Engineering*, *5*(3), 63–88.

Kelly, J. M. (1973). Energy absorbption devices for Earthquake resistant structures. In *5th World Conference on Earthquake Engineering, Rome, Italy*.

Liu, H. (1958). Seismic forces on structures. *Chinese Journal of Civil Engineering*, *5*(2), 86–106.

Louie, J. (2011). Plate Tectonics, the cause of Earthquakes. Retrieved April 4, 2016, from http://crack.seismo.unr.edu/ftp/pub/louie/class/100/plate-tectonics.html

Martinez-rueda, J. E., Tsantali, E., Division, G., Rd, L., Bldg, C., Intensity, A., & Velocity, C. A. (2008). Analysis of the correlation between instrumental intensities of strong earthquake ground motion. In *7th European Conference on structural dynamics.*

Masi, A., Vona, M., & Mucciarelli, M. (2011). Selection of Natural and Synthetic Accelerograms for Seismic Vulnerability Studies on Reinforced Concrete Frames, *137*(March), 367–378. http://doi.org/10.1061/(ASCE)ST.1943-541X.0000209.

Mazzolani, F. N., & Tremblay, R. (2000). Buckling-restrained braces as hysteretic dampers. In *Proocedings of the third international conference stessa 2000* (p. 33). Netherlands: A.A. Balkema. Retrieved Febraury 16 2016. From https://books.google.it/

Méndez, F. J. (2007). Prótocolo de la investigación.

MIDAS Information Technology Co. (2015). Midas GEN. Retrieved March 25, 2016, from http://en.midasuser.com/product/gen_overview.asp

National Oceanic and Atmospheric Administration. (2013). Plates Boundaries. Retrieved April 2, 2016, from http://oceanexplorer.noaa.gov/facts/plate-boundaries.html

Nigam, N. C. (1983). *Introduction to Random Vibrations*. (T. M. I. of Technology, Ed.). London: The MIT Press.

Nikulin, M. S. (1973). Chi-square test for continuous distributions with scale and shift parameters. *Theory of Probability and Its Applications*, *18*(3), 559–568.

Pampanin, S., Bolognini, D., & Pavese, A. (2006). Performance-Based Seismic Retrofit Strategy for Existing 2 Reinforced Concrete Frame Systems Using Fiber-Reinforced. *ASCE Journal of Composites in Construction, Special Issue*, (April), 1–16.

Pampanin, S., & Christopoulos, C. (2002). Experimental Validation of a Low-Invasive Seismic Retrofit Solution for Existing Under-Designed Rc Frames. *Response*, 1–8.

Pelà, L., Aprile, A., & Benedetti, A. (2013). Comparison of seismic assessment procedures for masonry arch bridges. *Construction and Building Materials*, *38*, 381–394. http://doi.org/10.1016/j.conbuildmat.2012.08.046

Phocas, M., Brebbia, C. A., & Komodromos, P. (2009). Recent applications of Italian anti-seismic devices. In *Eathquake Resistant Engineering Structure* (1st ed., pp. 336–338). Great Britain: WIT PRESS. Retrieved April 7, 2016, from https://books.google.it/books

Pizzarulli, F. (2015). *Conceptual design di controventi dissipativi per l'adeguamento sismico di un edificio strategico multipiano con struttura mista telaio-pareti in c.a.: il corpo "e" dell'area ex-c.o.o. di Ferrara*. Universti degli study Ferrara.

Powell, G. (2006). Nonlinear dynamic analysis capabilities and limitations. *The Structural Design of Tall and Special Buildings*, *15*(5), 547–552. http://doi.org/10.1002/tal.381

Reitherman, R. (1998). Seismic Design Methodologies for the Next Generation of Codes, Peter Fajfar and Helmut Krawinkler, editors, A. A. Balkema, Brookfield, Vermont, USA, and Rotterdam, The Netherlands, 1997, 411 pages. *Earthquake Engineering & Structural Dynamics*, *27*(12), 1559–1562. http://doi.org/10.1002/(SICI)1096-9845(199812)27:12<1559::AID-EQE800>3.0.CO;2-E

Rock, A. D., Zhang, R., & Wilkinson, D. (2008). *Velocity variations in cross-hole sonic logging surveys: Causes and Impacts in Drilled Shafts*. *Security*.

Sahin, C. (2014). *Seismic Retrofitting of Existing Structures*. Portland State University. Retrieved March 27, 2016, from http://pdxscholar.library.pdx.edu

Shome, N. (1999). *Probabilistic Seismic Demand Analysis of Nonlinear Structures*. Stanford University, Stanford, CA, USA.

Smerzini, C., & Paolucci, R. (2013). *SIMBAD: a database with Selected Input Motions for displacement Based Assessment and Design -3rd release*. Retrieved from http://wpage.unina.it/iuniervo/SIMBAD_Database_Polimi.pdf

Smerzini, C., Paolucci, R., Galasso, C., & Iervolino, I. (2012). Engineering ground motion selection based on displacement-spectrum compatibility. *15th World Conference on Earthquake Engineering*, (2354).

Stafford, P. J. (2012). On the use of Arias Intensity as a lower bound in the hazard integration process of a PSHA. *15th World Conference on Earthquake Engineering (15WCEE)*. Retrieved from http://www.iitk.ac.in/nicee/wcee/article/WCEE2012_1529.pdf

Stafford, P. J., Berrill, J. B., & Pettinga, J. R. (2009). New predictive equations for Arias intensity from crustal earthquakes in New Zealand. *Journal of Seismology*, *13*(1), 31–52. http://doi.org/10.1007/s10950-008-9114-2

Strumento, S., Nazionale, R. A., & Paolucci, R. (2005). Glossario 1, 1–15.

UpSeis. (2007). What are seismic waves? Retrieved April 4, 2016, from http://www.geo.mtu.edu/UPSeis/waves.html

USGS. (2014). Magnitude/Intensity comparison. Retrieved April 7, 2016, from http://earthquake.usgs.gov/learn/topics/mag_vs_int.php

Wald, L. (2012). The science of earthquakes. Retrieved April 4, 2016, from http://www.geo.mtu.edu/UPSeis/waves.html

Yale University Department of Statistics. (1998). Confidence Intervals. Retrieved April 10, 2016, from http://www.stat.yale.edu/Courses/1997-98/101/confint.htm

Ye, L., Ma, Q., Miao, Z., Guan, H., & Zhuge, Y. (2013). Numerical and comparative study of earthquake intensity indices in seismic analysis. *The Structural Design of Tall and Special Buildings*, *22*(4), 362–381. http://doi.org/10.1002/tal.693